UNIVERSITY OF HAWAII
LIBRARY
OCT 16 '60

Journal of MOLECULAR BIOLOGY

EDITOR-IN-CHIEF: J. C. KENDREW

Volume II, Number 1, April 1960

ACADEMIC PRESS LTD., LONDON
ACADEMIC PRESS INC., NEW YORK

JOURNAL OF MOLECULAR BIOLOGY

EDITOR-IN-CHIEF

J. C. KENDREW, Peterhouse, Cambridge, England

EDITORIAL BOARD

P. DOTY, Department of Chemistry, Harvard University, Cambridge, Mass., U.S.A.
A. F. HUXLEY, Physiological Laboratory, University of Cambridge, England.
R. L. SINSHEIMER, Division of Biology, California Institute of Technology, Pasadena, Cal., U.S.A.
J. D. WATSON, Biological Laboratories, Harvard University, Cambridge, Mass., U.S.A.
M. H. F. WILKINS, Physics Department, King's College, London, England.

ADVISORY BOARD

S. BENZER, Purdue University, U.S.A.
M. CALVIN, University of California, Berkeley, U.S.A.
F. H. C. CRICK, University of Cambridge, England.
J. F. DANIELLI, King's College, London, England.
A. ENGSTRÖM, Karolinska Institutet, Stockholm, Sweden.
A. D. HERSHEY, Carnegie Institute, Cold Spring Harbor, U.S.A.
F. JACOB, Pasteur Institute, Paris, France.
A. KORNBERG, Stanford University, Stanford, California, U.S.A.
C. LEVINTHAL, Massachusetts Institute of Technology, Cambridge, Mass., U.S.A.
S. E. LURIA, Massachusetts Institute of Technology, Cambridge, Mass., U.S.A.
D. MAZIA, University of California, Berkeley, U.S.A.
P. B. MEDAWAR, University College, London, England.
L. E. ORGEL, University of Cambridge, England.
M. F. PERUTZ, University of Cambridge, England.
R. D. PRESTON, University of Leeds, England.
G. N. RAMACHANDRAN, University of Madras, India.
A. RICH, Massachusetts Institute of Technology, Cambridge, Mass., U.S.A.
G. SCHRAMM, Max-Planck Institut, Tübingen, Germany.
F. S. SJØSTRAND, Karolinska Institutet, Stockholm, Sweden.
I. WATANABE, University of Tokyo, Japan.
R. C. WILLIAMS, University of California, Berkeley, U.S.A.

Published by Academic Press Inc. (London) Limited

Volume II, 1960: 100*s*. ($14.00)

Subscription orders should be sent to Academic Press Inc. (London) Limited, 17 Old Queen Street, London, S.W.1, with the exception of those originating in the U.S.A., Canada, Central America, and South America; these should be sent to Academic Press Inc., 111 Fifth Avenue, New York 3, N.Y.

Copyright © 1960, by Academic Press Inc. (London) Limited

INSTRUCTIONS TO AUTHORS

1. The *Journal of Molecular Biology* will publish papers on the nature, production and replication of biological structure at the molecular level, and its relation to function. Suitable subjects are sub-cellular organization: molecular genetics: structure and replication of viruses: molecular structure of muscle, nerve and other tissues: structure of proteins, nucleic acids, carbohydrates, lipids, etc., and their synthetic analogues, as investigated by X-rays, light absorption and other methods: problems of inter- and intra-molecular energy transfer.

2. The Journal will also publish Letters to the Editor (averaging 1000 words), and occasional review articles dealing with a more restricted or immediately topical field than those in review journals. (The Editor should be consulted in advance by anyone who considers submitting such a review.)

3. Communications will often describe results obtained by specialized techniques (for example, those of X-ray crystallography and of genetics), and it is most important that technical terms should be avoided or be clearly defined; in any event the actual results obtained and their implications should be described in a way which does not demand from the reader specialized knowledge of a particular technique.

Papers should contain the maximum density of information compatible with clarity, and every sentence should be scrutinized to ensure that its presence is essential. Authors should include enough experimental details to enable others to repeat the work (these may be printed in small type). Careful preparation of manuscript will aid prompt publication; carelessness will cause delay.

4. *Submission of Manuscripts.* Manuscripts should be sent to Dr. J. C. Kendrew, Peterhouse, Cambridge, England, or to any member of the Editorial Board. The submission of manuscript will be taken to imply that the material is original, and that no similar paper has been or will be submitted for publication elsewhere.

Papers will normally be published in English. Manuscripts in French or German will also be accepted, though the use of these languages may cause delay in publication.

5. *Copy.* Papers should be typewritten in double spacing *throughout* (including tables, legends and footnotes), on one side of quarto paper, with a margin of 1 inch all round. The position of tables and illustrations should be indicated in the text; tables and legends for illustrations should be typed separately at the end of the manuscript. All pages should be numbered serially and securely fastened together. Two copies of each manuscript should be submitted, together with three copies of the summary (see § 6) and four copies of the abstract (see § 9).

A short running title of not more than 40 characters (including spaces), suitable for page headings, should be indicated if the full title is longer than this.

The name of the laboratory where the work has been done should be indicated on the title page. All typescript (including the references) should be carefully checked for errors.

6. *Summary.* A summary will be printed at the head of all papers (excluding Letters to the Editor); this should generally not exceed 300 words, and should be intelligible to the general reader without reference to the main text. Abbreviations should be avoided. Summaries of papers to be printed in French or German will be in English, and should be longer (up to 1000 words) for the benefit of readers not familiar with these languages.

7. *Conventions.* The conventions used in current issues of the Journal for headings, references, etc., should be followed in preparing manuscripts. References should be listed alphabetically at the end of the paper, and abbreviated according to the *World List of Scientific Periodicals*, except that for periodicals with English names capital initial letters should be used throughout. Citations in the text should read thus: Smith, Brown & Robinson (1957), or (Smith, Brown & Robinson, 1957). When a citation has more than two authors, the names of all of them should be given at the first citation (except for more than five authors), and on subsequent citations thus: (Smith *et al.*, 1957). The conventions (Brown, 1957*a*), (Brown, 1957*b*) should be used where more than one paper by the same author(s) has appeared in one year. Volume number should be indicated in the typescript thus: **35.**

Footnotes should be avoided whenever possible. Essential footnotes should be indicated by superscript figures in the text and collected on a single page placed at the end of the manuscript.

Customary abbreviations will be used; authors may refer to *Chemical Abstracts*, to the *Biochemical Journal*, **66**, 8 (1957), and to *Notes on the preparation of papers to be communicated to the Royal Society* (1951). Certain non-standard abbreviations of chemical substances are convenient, and those listed in the *Journal of Biological Chemistry* may be used without further definition (e.g. DNA, ATP). Any other abbreviations of this kind should be used sparingly, and must be defined in a footnote at the point in each manuscript where the first such abbreviation occurs.

8. *Illustrations.* It is often convenient to make a *drawing* two or three times larger than it will appear in the Journal, but very large drawings should be avoided and it will be helpful if drawings and illustrations are submitted on quarto (or $8\frac{1}{2}$ by 11 inch) sheets. Drawings should be made in

Indian ink on tracing linen, Bristol board, or faintly blue-lined graph paper; the originals should always be submitted with the manuscript, since photo-prints of drawings often cannot be reproduced satisfactorily. Explanations should, as far as possible, be placed in the legend; the drawing itself should contain a minimum of lettering, and this should be inserted lightly in *blue pencil*, in lower case except for proper names, when a capital should be used. It should be remembered that drawings will be reduced to a size not exceeding 8 by 5 inches, and that the final thickness of the lines should be 0·25 to 0·3 mm. If a curve is given merely for illustrative purposes no cross-lines are needed, but the axes should be graduated at intervals, and the diagram should be boxed in. Where possible, related diagrams should be grouped to form a single figure, and should be prepared uniformly and *on the same scale*. Where appropriate and possible a scale should be included in the illustration itself; the magnification may be noted in the legend and adjusted after reduction by the blockmaker.

Whenever possible *photographs* should be supplied the same size as they are to appear in the Journal. The page area available for a plate is 5 by 7 inches or, at the most, 6 by 8 inches.

Line drawings will be referred to as Figure 1, Figure 2, etc., and half-tone blocks as Plate I, Plate II, etc. The name(s) of the author(s) and the number should be written on all illustrations, together with the indication "Top" if necessary. Besides the original illustrations *one* duplicate set must accompany the second copy of the manuscript; these may be photo-prints, and need not be of the same quality as the originals but must be clear and legible. If *oversize* original drawings are submitted (bigger than 8½ by 11 inches) they must be accompanied by *two* sets of small photo-prints.

9. *Abstracts.* Authors should send with their manuscripts *four copies* (typewritten in double spacing) of an abstract, in about 100 words, suitable for inclusion in biological abstracting journals. This abstract will not appear in the *Journal of Molecular Biology* but will be scrutinized by the Editors before being passed for publication. The abstract should outline as briefly as possible the results and definitive conclusions of the work. Details of methods are generally not required.

The abstract should be headed as follows: title of paper; name(s) of author(s); *J. Mol. Biol.*, followed by space for the year, volume and page references; abbreviated postal address (including country of origin) to which applications for reprints may be sent. For example: The isolation and properties of deoxyribonucleoprotein particles containing single nucleic acid molecules. G. Zubay & P. Doty. J. Mol. Biol. . . . . (Dept. of Chem., Harvard Univ., Cambridge, Mass., U.S.A.). —text of abstract follows.

10. *Reprints.* Fifty reprints of each paper will be supplied free of charge; additional copies may be purchased.

Ultracentrifugation
in Biochemistry

By HOWARD K. SCHACHMAN
Biochemistry and Virus Laboratory, University of California, Berkeley

1959, 272 pp., illus., 70s. 6d.

***From the Foreword by* JOHN T. EDSALL:**

"Over the past decade the use of the ultracentrifuge as a tool in biochemical research has developed in a dramatic fashion. Problems scarcely imagined ten years ago can now be investigated with brilliant success and with techniques only recently developed. There remains a need for a moderately extended discussion of these more recent developments, combined with a statement of the basic and indispensable theory and a general description of the old and new experimental techniques. I believe that these needs are admirably met by the present book.

"It is likely to become an indispensable companion to the laboratory worker who is planning and conducting an ultracentrifuge run for almost any purpose. It should also be of fundamental value to the thoughtful student or investigator who wants to know the present state of our knowledge in the field, both experimental and theoretical.

" Dr. Schachman has, I believe, performed a major service by portraying the broad range of experimental techniques in sedimentation experiments and by providing a rigorous discussion of the underlying principles."

CONTENTS:

Introduction
General Considerations
Experimental Aspects
Sedimentation Velocity
The Transient States during the Approach to Sedimentation Equilibrium
Sedimentation Equilibrium
Interpretation of Sedimentation Data
References
Glossary

AUTHOR INDEX—SUBJECT INDEX

ACADEMIC PRESS, New York and London

111 Fifth Avenue, New York 3, New York
17 Old Queen Street, London, S.W.1

The first authoritative, integrated account **in 2 volumes**

The Plasma Proteins

Edited by FRANK W. PUTNAM

College of Medicine, The J. Hillis Miller Health Center, University of Florida

"PLASMA, the viscous medium through which the red cells are transported and the tissues nourished, reflects and guards the internal milieu. Through its myriad protein components the plasma contributes to nitrogen needs, to defense against invasion and injury, to maintenance of body pH and osmotic balance, and to regulation of cellular activity and function. As components of a metabolically dynamic system, the plasma proteins fluctuate in disease, usually nonspecifically, and their determination and fractionation have been the subject of thousands of papers in the past century.

"Heretofore, no book has been available in English or other languages that treats broadly and collectively of the many types and manifold functions of the plasma proteins. It will be the objective of this collectively written treatise to describe from the modern, experimental point of view the purification and characterization of plasma proteins, their metabolic function and activity, and their derangement and dysfunction in disease."

—From the Editor's Introduction

VOLUME 1—Isolation, Characterization, and Function

April 1960, 420 pp., illus., 96s. 6d.

Introduction
By FRANK W. PUTNAM

Fractionation and Isolation of Purified Components by Precipitation Methods
By ROBERT B. PENNELL

Electrophoretic and Ultracentrifugal Analysis of Normal Human Serum
By GERALD R. COOPER

Chromatography of the Plasma Proteins
By ELBERT A. PETERSON and HERBERT A. SOBER

Chemical Composition and Molecular Parameters of Purified Plasma Proteins
By ROBERT A. PHELPS and FRANK W. PUTNAM

Plasma Albumin
By JOSEPH F. FOSTER

γ-Globulin and Antibodies
By R. R. PORTER

Macroglobulins and High Molecular Weight Antibodies
By HENRY G. KUNKEL

Glycoproteins
By RICHARD H. WINZLER

Metal-Binding Plasma Proteins and Cation Transport
By C. B. LAURELL

AUTHOR INDEX—SUBJECT INDEX

VOLUME 2—Biosynthesis, Metabolism, Alterations in Disease

June 1960, 518 pp., illus., 103s. 6d.

Structure and Function of Human Serum Lipoproteins
By FRANK T. LINDGREN and ALEX V. NICHOLS

Plasma Enzymes
By WILLIAM H. FISHMAN

Circulating Hormones
By HARRY N. ANTONIADES

The Blood Coagulation System
By R. G. MACFARLANE

Comparative Biochemistry and Embryology
By RALPH L. ENGLE, JR. and KENNETH R. WOODS

The Biosynthesis of Plasma Proteins
By H. S. ANKER

Alterations in Plasma Protein Patterns in Disease
By MARY L. PETERMANN

Abnormal Serum Globulins
By FRANK W. PUTNAM

Genetic Alterations in Plasma Proteins of Man
By DAVID GITLIN and CHARLES A. JANEWAY

AUTHOR INDEX—SUBJECT INDEX

ACADEMIC PRESS, New York and London

111 Fifth Avenue, New York 3 · 17 Old Queen Street, London, S.W.1

Journal of MOLECULAR BIOLOGY

EDITOR-IN-CHIEF
J. C. KENDREW

ASSISTANT EDITOR
S. BRENNER

EDITORIAL BOARD
P. Doty
H. E. Huxley
M. Meselson
R. L. Sinsheimer
J. D. Watson
M. H. F. Wilkins

VOLUME 5
July to December 1962

ACADEMIC PRESS
LONDON and NEW YORK

Copyright © 1962, by Academic Press Inc. (London) Ltd.
ALL RIGHTS RESERVED
No part of this volume may be reproduced in any
form, by photostat, microfilm, or any other means,
without written permission from the publishers.

Printed in Great Britain

CONTENTS OF VOLUME 5

Number 1, July 1962

R. R. Rueckert and W. Zillig. Biosynthesis of Virus Protein in *Escherichia coli* C *in vivo* Following Infection with Bacteriophage ϕX174 . . . 1

R. R. Rueckert, W. Zillig and W. Doerfler. Incorporation of [^{14}C]Leucine into Bacteriophage Proteins in Cell-free Extracts of *Escherichia coli* . . 10

W. Arber and D. Dussoix. Host Specificity of DNA Produced by *Escherichia coli*. I. Host Controlled Modification of Bacteriophage λ . . . 18

D. Dussoix and W. Arber. Host Specificity of DNA Produced by *Escherichia coli*. II. Control over Acceptance of DNA from Infecting Phage λ . . 37

D. J. Cummings and L. M. Kozloff. Various Properties of the Head Protein of T2 Bacteriophage 50

M. Riley and A. B. Pardee. β-Galactosidase Formation Following Decay of ^{32}P in *Escherichia coli* Zygotes 63

I. Bendet, E. Schachter and M. A. Lauffer. The Size of T3 DNA . . 76

K. S. McCully and G. L. Cantoni. Non-random Base Sequence of S-RNA and an Hypothesis for S-RNA Biosynthesis 80

S. W. Bowne, Jr. and P. Rogers. Ultraviolet Light and Enzyme Synthesis . 90

H. Lamfrom and E. R. Glowacki. Controlled Dissociation of Rabbit Reticulocyte Ribosomes and its Effect on Hemoglobin Synthesis 97

J. Marmur and P. Doty. Determination of the Base Composition of Deoxyribonucleic Acid from its Thermal Denaturation Temperature . . . 109

S. Lacks. Molecular Fate of DNA in Genetic Transformation of *Pneumococcus* . 119

Letter to the Editor

J. Brahms and C. M. Kay. Molecular and Enzymatic Studies of Cardiac Myosin 132

Number 2, August 1962

U. Lagerkvist and P. Berg. The Enzymic Synthesis of Amino Acyl Derivatives of Ribonucleic Acid. V. Nucleotide Sequences Adjacent to the . . pCpCpA End Groups 139

P. Berg, U. Lagerkvist and M. Dieckmann. The Enzymic Synthesis of Amino Acyl Derivatives of Ribonucleic Acid. VI. Nucleotide Sequences Adjacent to the ..pCpCpA End Groups of Isoleucine- and Leucine-Specific Chains 159

R. B. Inman and R. L. Baldwin. Helix–Random Coil Transitions in Synthetic DNAs of Alternating Sequence 172

R. B. Inman and R. L. Baldwin. Formation of Hybrid Molecules from Two Alternating DNA Copolymers 185

R. G. Wake and R. L. Baldwin. Physical Studies on the Replication of DNA *in vitro* 201

H. H. Hiatt. A Rapidly Labeled RNA in Rat Liver Nuclei 217

E. M. Bradbury, L. Brown, the late A. R. Downie, A. Elliott, R. D. B. Fraser and W. E. Hanby. The Structure of the ω-Form of Poly-β-benzyl-L-aspartate 230

Letter to the Editor

R. G. Kallen, M. Simon and J. Marmur. The Occurrence of a New Pyrimidine Base Replacing Thymine in a Bacteriophage DNA: 5-Hydroxymethyl Uracil 248

Number 3, September 1962

A. Ishihama, N. Mizuno, M. Takai, E. Otaka and S. Osawa. Molecular and Metabolic Properties of Messenger RNA from Normal and T2-infected *Escherichia coli* 251

W. K. Joklik. Some Properties of Poxvirus Deoxyribonucleic Acid . . 265

S. McGavin. The Structure of Elastoidin in Relation to that of Tendon Collagen 275

A. Tsugita. The Proteins of Mutants of TMV: Composition and Structure of Chemically Evoked Mutants of TMV RNA 284

A. Tsugita. The Proteins of Mutants of TMV: Classification of Spontaneous and Chemically Evoked Strains 293

L. Broman, Bo G. Malmström, R. Aasa and T. Vänngård. Quantitative Electron Spin Resonance Studies on Native and Denatured Ceruloplasmin and Laccase 301

R. Monier, S. Naono, D. Hayes, F. Hayes and F. Gros. Studies on the Heterogeneity of Messenger RNA from *E. coli* 311

H. R. Mahler and A. da S. Pereira. Properties of the DNA Associated with Crystalline Yeast Lactic Dehydrogenase 325

L. Alföldi, G. S. Stent and R. C. Clowes. The Chromosomal Site of the RNA Control (*RC*) Locus in *Escherichia coli* 348

C. A. Thomas, Jr. and T. C. Pinkerton. Sedimentation Equilibrium Studies on Intact and Fragmented Bacteriophage DNA 356

Letter to the Editor

R. Thomas and L. Lambert. On the Occurrence of Bacterial Mutations Permitting Lysogenization by Clear Variants of Temperate Bacteriophages 373

Number 4, October 1962

V. Luzzati, D. Luzzati and F. Masson. La Structure des Acides Désoxyribonucléiques Bactériens en Solution 375

V. N. Schumaker and C. Bennett. A study of the Viscosity of T4*r* DNA Using a Rotating Cylinder Viscometer 384

J. Drenth, J. N. Jansonius, R. Koekoek, J. Marrink, J. Munnik and B. G. Wolthers. The Crystal Structure of Papain C. I. Two-dimensional Fourier Syntheses 398

W. Fiers and R. L. Sinsheimer. The Structure of the DNA of Bacteriophage ϕX174. I. The Action of Exopolynucleotidases 408

W. Fiers and R. L. Sinsheimer. The Structure of the DNA of Bacteriophage ϕX174. II. Thermal Inactivation 420

W. Fiers and R. L. Sinsheimer. The Structure of the DNA of Bacteriophage ϕX174. III. Ultracentrifugal Evidence for a Ring Structure . . . 424

M. Mandel. The Interaction of Spermine and Native Deoxyribonucleic Acid . 435

I. Tessman. The Induction of Large Deletions by Nitrous Acid . . . 442

Letters to the Editor

J. H. Fessler and A. J. Hodge. Ultracentrifugal Observation of Phase Transitions in Density Gradients. I. The Collagen System . . 446

A. Ehrenberg, B. G. Malmström, L. Broman and R. Mosbach. A Magnetic Susceptibility Study of Copper Valence in Ceruloplasmin and Laccase 450

A. I. Aronson. Sequence Differences Between Ribonucleic Acids Isolated from 30 s and 50 s Ribosomes 453

R. D. B. Fraser and T. P. MacRae. An Investigation of the Structure of β-Keratin 457

W. F. Dove and N. Davidson. Cation Effects on the Denaturation of DNA . 467

W. F. Dove and N. Davidson. The Thermal Inactivation of Transforming Activity at Low Ionic Strength 479

E. M. Bradbury, A. Elliott and W. E. Hanby. Optical Rotatory Dispersion and Infrared Studies of β-Structures of Poly-O-benzyl-L-serine in Solution . 487

K. S. McCully and G. L. Cantoni. Studies on Soluble Ribonucleic Acid (S-RNA) of Rabbit Liver. VII. A Base Sequence Model of S-RNA . . 497

K. Ebisuzaki. Functional Interdependence of Genes in Bacteriophage T2 . 506

E. R. Huehns, N. Dance, E. M. Shooter and G. H. Beaven. The Preparation and Properties of Haemoglobin α^A, a Haemoglobin consisting of α^A-Polypeptide Chains 511

A. M. Liquori, B. De Lerma, F. Ascoli, C. Botré and M. Trasciatti. Interaction between DNA and Polycyclic Aromatic Hydrocarbons . . 521

K. Okamoto, Y. Sugino and M. Nomura. Synthesis and Turnover of Phage Messenger RNA in *E. coli* Infected with Bacteriophage T4 in the Presence of Chloromycetin 527

M. Nomura, K. Matsubara, K. Okamoto and R. Fujimura. Inhibition of Host Nucleic Acid and Protein Synthesis by Bacteriophage T4: Its Relation to the Physical and Functional Integrity of Host Chromosome . 535

A. R. Peacocke and I. O. Walker. The Thermal Denaturation of Sodium Deoxyribonucleate. I. The Limits 550

A. R. Peacocke and I. O. Walker. The Thermal Denaturation of Sodium Deoxyribonucleate. II. Kinetics 560

A. R. Peacocke and I. O. Walker. The Thermal Denaturation of Sodium Deoxyribonucleate. III. Light-scattering Studies 564

Letters to the Editor

Y. Mukohata, S. Ikeda and T. Isemura. The Electric-streaming Birefringence of Poly-γ-benzyl-L-glutamate in *m*-Cresol . . . 570

A. Elliott and E. M. Bradbury. Infrared Spectra of Proteins and Polypeptides and their Conformations 574

K. Suzuki, H. Yamagami and N. Rebeyrotte. Quantitative Estimation of the Transforming Activity of Hybrid DNA 577

D. Shugar and W. Szer. Secondary Structure in Poly-ribothymidylic Acid 580

B. Strandberg, B. Tilander, K. Fridborg, S. Lindskog and P. O. Nyman. The Crystallization and X-ray Investigation of One Form of Human Carbonic Anhydrase 583

Number 6, December 1962

G. Felsenfeld and G. Sandeen. The Dispersion of the Hyperchromic Effect in Thermally Induced Transitions of Nucleic Acids 587

R. Langridge and K. C. Holmes. X-ray Diffraction Studies of Concentrated Gels of Ribosomes from *E. coli* 611

J. R. Beckwith, A. B. Pardee, R. Austrian and F. Jacob. Coordination of the Synthesis of the Enzymes in the Pyrimidine Pathway of *E. coli* . . . 618

P. F. Davison and D. Freifelder. The Physical Properties of T7 Bacteriophage 635

P. F. Davison and D. Freifelder. The Physical Properties of the Deoxyribonucleic Acid from T7 Bacteriophage 643

C. Ning and A. Stevens. Studies of the Effect of T2 RNA Formed with Purified RNA Polymerase on Amino Acid Incorporation into Protein . 650

A. B. Edmundson and C. H. W. Hirs. On the Structure of Sperm Whale Myoglobin. I. The Amino Acid Composition and Terminal Groups of the Chromatographically Purified Protein 663

A. B. Edmundson and C. H. W. Hirs. On the Structure of Sperm Whale Myoglobin. II. The Tryptic Hydrolysis of the Denatured Protein . . 683

A. B. Edmundson and C. H. W. Hirs. On the Structure of Sperm Whale Myoglobin. III. Amino Acid Sequences of the Smaller Tryptic Peptides Containing Aromatic Residues 706

P. B. Sigler, D. R. Davies and H. T. Miles. A Displacement Reaction Between a Polynucleotide Helix and a Random Coil 709

Index 719

J. Mol. Biol. (1960) **2**, 1-4

Calculation of the Rate of Uncoiling of the DNA Molecule

H. C. Longuet-Higgins

The University Chemical Laboratory, Cambridge, England

AND

Bruno H. Zimm

General Electric Research Laboratory, Schenectady, New York, U.S.A.

(*Received 18 November 1959*)

A roughly quantitative calculation is attempted for the rate of separation of the two strands of the deoxyribonucleic acid (DNA) molecule when the helical structure is suddenly made unstable by the addition of some agent that weakens the cross bonding between the bases. Reasons are given for believing that the rate-controlling process is the unwinding of the ends driven by the increase of entropy on unwinding and hindered by the viscous resistance of the surrounding medium. The entropy increase is estimated roughly from the number of freely rotating bonds in the chain backbone, while the resistance coefficient can be related to the known relation between intrinsic viscosity and molecular weight of denatured DNA. As a result it is calculated that the time needed for the two strands of a long DNA molecule to dissociate is of the order of a few seconds, the time increasing with the 5/2 power of the molecular weight.

It is commonly believed that the two strands of the DNA molecule separate when a cell divides, one strand going to each daughter cell. There is, indeed, some direct evidence in one case (Meselson & Stahl, 1958). Since in the Watson-Crick (Watson & Crick, 1953*a*, 1954) helical structure two strands of the molecule are wound around each other several hundred times, the separation of the two must require a large amount of relative motion, and it is a matter of interest to consider where the force that causes the motion might originate, and how much time might be required.

This problem has already been discussed by Watson & Crick (1953*b*), and reviewed again by Delbrück & Stent (1957), who quote an unpublished calculation by Levinthal & Crane. The latter authors assumed that the growth of new replica chains along the separating strands of the old DNA molecule provided the driving force for the unwinding, while the resistance thereto was the rotational viscous drag on the unwinding helix. They concluded that there was ample energy available in the energy-rich triphosphate bonds of the presumed precursors of the new DNA chains to drive the unwinding at a reasonable rate. However an obvious weakness of this discussion is the lack of a detailed mechanism for the conversion of the energy potentially available in a phosphate bond into a torque tending to rotate the helix. This remark is not intended as a criticism of the authors of the above discussion; indeed, in the present imperfect state of our knowledge it would be presumptuous to propose a detailed mechanism.

We are therefore led to consider the simplest possible scheme for the replication of DNA. In our view, this is one in which the two strands of the old molecule separate spontaneously when the double helix becomes unstable as a result of some change in its environment. We assume that the synthesis of the new chains occurs at some other

stage. In this communication we show that the time required for the separation step can be estimated, and that its magnitude appears to be reasonable.

In general, problems of this kind must be treated by solving a diffusion equation in the multidimensional space of the coordinates of the chain. However, in this case we believe that a substantial simplification is possible, since the process of unwinding the ends should on the one hand be slower than the diffusion of the free ends into their randomly coiling forms, and on the other it should be faster than any other competing kind of unwinding (e.g. untwisting in the middle). In consequence, we can assume with good accuracy that the overall rate is determined by the rate of unwinding of the ends. In what follows we attempt to justify these statements.

As our model we take the Watson & Crick (1954) structure, a double-stranded helix of two polynucleotide chains, held together and made rigid by interactions between the purine and pyrimidine bases, with a twist of 36° for every pair of bases. We consider that the separation process is initiated by a sudden change in the surroundings, such as the appearance of an agent that hydrogen-bonds to the bases, with the result that the rigid structure becomes thermodynamically unstable. *In vitro*, a moderate increase in temperature or reduction in pH would have this effect, but some more subtle change *in vivo* seems more reasonable.

In order to separate, however, the chains must unwind. At the base pairs at the ends of the double helix a torque is created; this is the free energy gained by the dissociation of the last base-pair divided by the rotation needed to unwind this base-pair, or (36/57·3) radians. This torque tends to rotate the free ends with respect to the rest of the helix. Torques arising from the same cause appear at each base-pair in the middle of the double helix also, but these are smaller, because the gain of free energy on dissociating a base-pair that is tied at both ends of both chains is smaller than the free energy gained by dissociating a pair that is tied at one end of each chain only, the final configurations of the latter pair being much less restricted. Since all the torques are opposed to each other, the strongest prevails, with the result that the ends unwind, while at a point in the middle the strands must usually stay twisted until the unwinding of the ends progresses to that point.

This is not to deny that occasional fluctuations may occur in which untwisting in the middle may proceed for a while. In fact, since the free energy changes are of the order of kT (see below), some such fluctuations should be expected. However, the occurrence of occasional untwisting in the middle should not increase the rate of separation of the chains for the following reason: the sum of the rates of such medial untwisting plus unwinding at the ends cannot be greater than the rate of unwinding unaccompanied by medial untwisting, since the net free energy gain per base-pair separated is less in the former case, while the frictional resistance is about the same. Hence, we feel justified in ignoring medial untwisting in the following simple calculation.

The actual magnitude of the torque is not known with certainty, but we can make some rough estimates. The maximum value of the torque would appear in the circumstance that the initial separation of the bases and their binding to the extraneous agent took place with no net change in free energy. The free energy gain on untwisting the helix would then result entirely from the increase in freedom of the chains in going from the rigid structure to the randomly coiling form. The latter can be estimated, since there are five valence bonds per base in each chain that are held fixed in the helix but can twist freely in the randomly coiling form. Unfortunately, four of these bonds involve the phosphate group, and very little is known about their twisting

character, except that they must have some freedom for twisting, since separated DNA chains are highly flexible. We assume therefore that on the average each of the five twisting bonds in the DNA chain has n rotational positions of minimum potential energy, where n is a small number in the range 2 to 4. In the double helix the bonds can occupy only one of their minima, but in the random coil they can occupy any of them. The entropy gain on taking one base-pair and its associated chains from the helical to the random forms is then $(2\times5)k(\ln n)$, and since we have already assumed that the free energy of separating the base-pair is zero, the torque becomes

$$10\times(57{\cdot}3/36)kT(\ln n).$$

If n is taken to be 3, this is $7{\cdot}18\times10^{-13}$ dyne-cm at 25°C.

We suggest that this figure is a maximum value, because if the separation of the base-pair consumes free energy, the total gained on unwinding must be less than the above value, while, on the other hand, if the separation proceeds spontaneously, the rigid structure will loosen *before* unwinding, so that what would otherwise be an additional free energy gain is lost.

At this point it is appropriate to mention a pioneering attempt by Kuhn (1957) to calculate the rate of unwinding. Kuhn concluded that the time needed to unwind the ends would be very long, about 150 days, and hence he rejected it as a possible mechanism. We feel that this conclusion is the result of two assumptions that are inappropriate to the present problem. The first of these assumptions is that the individual chains after being unwound are equivalent hydrodynamically to rigid cylinders. This leads to a very low value for the diffusion coefficient, which leads in turn to a very slow rate of unwinding. The second assumption, which has an even more serious effect, is that the unwinding is to be treated as a simple diffusion process unbiased by an appreciable free energy decrease. The unwinding of each turn of the helix is then reversible, and the time for the unwinding of many successive turns then increases as the square of the sum of the square roots of the unwinding times of the individual turns. For many turns the total time then becomes exceedingly long. We are treating here, on the other hand, a case in which there is a substantial free energy decrease with unwinding. Hence the unwinding is not reversible, and the time for the whole molecule to unwind is the sum of the times needed for the unwinding of each turn. A general and complete discussion of the unwinding problem would probably include Kuhn's method and ours as two special cases, the one appropriate when the free energy decrease is small compared to kT, the other when it is large; we are dealing with the latter case in this paper.

The unwinding torque is opposed by the frictional resistance of the motion of the free ends through the viscous medium. Since equal and opposite torques act at each end of the helix, the helix itself will not move; only the strands that have already separated, and which we presume to form random coils, rotate. It is easy to calculate, by the method of normal coordinates (Zimm, 1956), the frictional resistance coefficient for a random coil of given size rotated about a given axis. However, since the procedure is rather technical, we omit the details here, but quote two relevant results. For a chain rotated about its middle segment, the resistance coefficient is

$$4{\cdot}6M\eta[\eta]/N$$

where M is the molecular weight, η the viscosity of the medium, $[\eta]$ the intrinsic viscosity, and N is Avogadro's number. Likewise, for a chain rotated about its terminal segment, the resistance coefficient is

$$6{\cdot}5M\eta[\eta]/N.$$

The intrinsic viscosity of denatured (single-strand) DNA has been studied by Thomas & Doty (1956); they find that

$$[\eta] = 0{\cdot}06\, M^{\frac{1}{2}}.$$

However, Geiduschek & Holtzer (1958) in their review quote a value of 400 ml./g for the intrinsic viscosity of a sample of molecular weight $7{\cdot}7\times10^6$; this is a little more than twice that given by the Thomas-Doty formula. Faced with this unresolved discrepancy, we choose, for purposes of illustration, the value that gives the maximum rate of unwinding, i.e. that of Thomas & Doty.

Now, if we assume that the two strands in each free end of the unwinding DNA molecule are together equivalent hydrodynamically to a single chain of molecular weight equal to their combined total and rotated about its middle segment, we find that the rate of unwinding of each end, which is the torque over the resistance coefficient, is

$$3{\cdot}9\times10^{13}\ M^{-\frac{3}{2}} \text{ radians/sec.}$$

Here we have assumed, along with Levinthal & Crane (quoted in Delbrück & Stent, 1957), that the viscosity has a value of four centipoises, a rough approximation to the imperfectly known value in the interior of a cell nucleus. The mass of chain unwound per unit time at each end is this rate times $(57{\cdot}3/36)\times660$, 660 being the average molecular weight of a base-pair. The final relation between the time, t, and the amount unwound, M, obtained by integrating the above rate and doubling the result to account for the fact that the unwinding proceeds at both ends at once, is

$$t = 4{\cdot}6\times10^{-18}M^{\frac{5}{2}}.$$

If M is 10×10^6, for example, t is 1·4 sec.

If we assume that only one strand at each end rotates, the other remaining attached to some fixed structure, such as a part of the chromosome, the second resistance coefficient quoted above is applicable, and the result is a value of t of 1·0 sec.

The above values of t are minima, since we have used the maximum value of the torque and the minimum values of $[\eta]$ in our estimates.

These times are interesting in view of the fact that the time actually needed for the complete separation and replication process, in some organisms at least, is no more than a few minutes. It would appear that there is enough time available for the DNA to divide by the method proposed, though there does not appear to be much more than enough. Our calculation also shows that DNA molecules with weights much in excess of 10×10^6 would require inconveniently long times for division, of the order of minutes or even hours; perhaps it is noteworthy that such molecules have not yet been found in nature.

REFERENCES

Delbrück, M. & Stent, G. (1957). In *The Chemical Basis of Heredity*, ed. by W. D. McElroy & B. Glass, p. 699. Baltimore: Johns Hopkins Press.
Geiduschek, P. & Holtzer, A. (1958). *Advanc. Biol. Med. Phys.* **6**, 490.
Kuhn, W. (1957). *Experientia*, **13**, 307.
Meselson, M. & Stahl, F. W. (1958). *Proc. Nat. Acad. Sci., Wash.* **44**, 671.
Thomas, C. A., Jr. & Doty, P. (1956). *J. Amer. Chem. Soc.* **78**, 1854.
Watson, J. D. & Crick, F. H. C. (1953*a*). *Nature*, **171**, 964.
Watson, J. D. & Crick, F. H. C. (1953*b*). *Cold Spr. Harb. Symp. Quant. Biol.* **18**, 123.
Watson, J. D. & Crick, F. H. C. (1954). *Proc. Roy. Soc.* A, **223**, 80.
Zimm, B. H. (1956). *J. Chem. Phys.* **24**, 269.

J. Mol. Biol. (1960) **2**, 5-9

The Intrinsic Viscosity of ^{32}P-Labelled Phage DNA

C. A. Thomas, Jr. and A. T. Matheson

Biophysics Department, Johns Hopkins University, Baltimore, U.S.A.

(*Received 6 November, 1959 and in revised form 25 November 1959*)

The intrinsic viscosity (at zero gradient, zero concentration) of osmotically disrupted T4 bacteriophage has been measured. For a variety of reasons it seems likely that there is very little DNA-protein aggregation in dilute solutions and the measurable viscosity is due to the DNA molecules alone. The magnitude of the intrinsic viscosity is unaltered by changing the growth conditions, or exposing the infected bacteria to moderate doses of X-rays or added ^{32}P β-decay irradiation. This would mean that the DNA molecules are neither stuck together nor broken down by these treatments.

Therefore, if these conclusions are correct, the large subunit as seen by autoradiography of the same material is not a consequence of the labelling process.

1. Introduction

At the present time the most convincing evidence for the existence of a large subunit of DNA (LSU) in T2 and T4 bacteriophage comes from the autoradiography of disrupted phage (Thomas, 1959; Levinthal & Thomas, 1957). The LSU is found in the reaction products following different kinds of disruptive treatments (Thomas, 1959), and does not appear to be the result of attachment of DNA molecules to the protein coat of the phage (Thomas & Knight, 1959).

The logical possibility exists, however, that the ^{32}P-labelling process, which requires quite high total radioactivities during the growth period, results in some radiation-induced artifact. The total energy dissipated in a solution containing 200 μc of ^{32}P is approximately 1000 r (840 rad.) over a three hour period and the question arises whether the LSU is a consequence of this dose.

To answer this question, T4 phage were grown in a medium which contained ^{32}P at the appropriate level, or alternatively they were exposed to an equivalent dose of hard X-rays during growth. The phage were collected and their DNA released by osmotic shock. The intrinsic viscosity of this DNA was measured at low gradients.

2. Methods and Procedures

(a) *Growth and purification of phage*

T4D wild type phage were grown in *E. coli* strain BB, which is lysis-inhibited for rapidly lysing phage. Log-phase cultures in 3XD† were inoculated with young plaques and 12 hr allowed for complete lysis. Chloroform was added to lyse any remaining cells. DNase was added to 5 μg/ml. and allowed to act 30 to 60 min at 37°C. The lysate was filtered through a Millipore HA-type filter. Additional $CHCl_3$ was added and the lysate was stored in the cold. The titers (usually 2×10^{11}/ml.) were stable over a period of months. In the ^{32}P experiments the medium was 800 ml. of tris-glucose (Hershey, 1955) with

† The glycerol medium of Fraser & Jerrel (1953).

approximately 3·7 μg of inorganic phosphate per ml. To rapidly growing cells, an appropriate amount of neutralized ^{32}P (200 to 300 μc/ml.) was added and growth was allowed to continue for three or more generations before infection. Multiplicity of infection ranged from 3 to 8. Growth, lysis and purification were the same.

In preparation for a viscosity measurement, the lysate was promptly centrifuged at 15,000 rev/min in the Spinco rotor No. 30 for 20 min (high speed spin) and the pellets gently resuspended at room temperature in 0·10 M-NaCl, 0·032 M-phosphate pH 7. This was followed by a sequence of low (5,000 rev/min, 5 min), high, and low spins. The "*E*-value" (the OD^{260} per plaque forming unit) (Adams, 1959) was determined and no unlabelled stock was considered acceptable unless this value lay in a range of 0·7 to $1{\cdot}1 \times 10^{-11}$. The highly ^{32}P-labelled stocks have values of 1·4, 2·1 and $3{\cdot}9 \times 10^{-11}$ indicating that the higher the specific activity of the growth medium the larger the fraction of dead phage (see entries 9, 10, and 11 in Table 1). The phage were then shocked from 4·0 M-NaCl, resulting in the death of at least 99·9% of the phage. The solvent was adjusted to the composition shown in Table 1, checked by refractive index, and clarified by a low speed spin. In a typical experiment the viscosity of this solution was then measured.

(b) *Viscosity measurements*

A special low gradient, multibulbed, capillary type viscometer was constructed. The capillary length was 2·7 m, the radius 0·739 mm and the average gradient was 51, 98, 160 sec^{-1} for each bulb for water. In 4·0 M-NaCl these values decreased to 35, 68, 115; this results from the increased solvent viscosity. A special washing procedure was adopted and certain checks were made to verify that no DNA had adsorbed onto the glass. The liquids were drawn up slowly to avoid any excessive shear which might break DNA molecules. The flow times measured were constant and reproducible.

The concentration is expressed in g DNA per 100 ml. of solution and was determined by measuring the optical density at 260 mμ assuming an extinction coefficient of 213.

3. Intrinsic Viscosity of Phage DNA

Deproteinization procedures such as phenol extraction, shaking with $CHCl_3$, or the use of detergents, involve some mechanical shaking. It is almost sure that DNA molecules are mechanically broken. This will be discussed in more detail later. Therefore, most of the measurements reported here have been made on the unseparated reaction products of osmotic shock. While under these conditions DNA molecules have probably not been mechanically broken, there is the other possibility that impromptu aggregates form between molecules perhaps *via* protein connections.

(a) *Absence of DNA-protein aggregates*

There are a number of reasons that lead us to believe that DNA-protein aggregation occurs only to a very small extent either in low salt (0·10 M-NaCl, 0·032 M-phosphate) or in high salt (4M-NaCl, 0·032 M-phosphate) both at pH 7.

Firstly, the sedimentation velocity distributions measured on the shock product show that more than 95% of the u.v.-absorbing material sediments with s values below 70 when the concentration of DNA is about 20 μg/ml. Thus it would appear unlikely that much of the DNA is associated with the more rapidly moving (211 s) ghost particles (Thomas, 1960).

Secondly, DNase free phage antisera fails to precipitate 85 to 90% of ^{32}P from the shocked products, irrespective of carrier phage concentration.

Phenol extraction of whole phage, a procedure which results in the removal of 99·5% of the ^{35}S label from the aqueous phase (Mandel, personal communication), while removing less than 0·1% of the ^{32}P (Thomas, unpublished experiments), results in a decrease in the intrinsic viscosity to about 65% of its former value (Table 1; 1, 3).

The same decrease in intrinsic viscosity can be brought about by the same shaking treatment with no phenol (Table 1; 16, 17). Thus removal of protein plays no obvious role in the high value of the viscosity which is observed.

TABLE 1

Intrinsic viscosity of T4 DNA (100 ml/g.)

The intrinsic viscosity of T4 DNA was measured at low gradients and extrapolated to zero gradient by either the best straight line or by drawing a gentle curve through the 3 points. These procedures result in the first and second values quoted in each entry. Equivalent experiments were performed at 3 or 4 lower concentration values and extrapolations made to zero concentration. The η_{sp}/c values displayed little or no concentration dependence at any gradient. The T4B *r* (deletion) phage (Nos. 13, 14) appear to have a 25% higher intrinsic viscosity in 4·0 M-NaCl. This is somewhat more than the experimental error. It is not inconsistant to suppose that this DNA (which is known to contain a genetic deletion) has a slightly altered configuration.

No.	Sample	0·032 M-phosphate 0·10 M-NaCl	0·032 M-phosphate 4·0 M-NaCl
1	T4D wild shockate grown in 3XD	140–160	100–120
2	T4D wild shockate + 0·01 M-pyrophosphate		105–125
3 A	Phenol extracted T4D phage	96–110	
B	Same as A	114–126	87–<150‡
4	T4D shockate grown in tris-glucose	165–200	107–115
			110–120
5	Same as No. 4 but 5·3 r/min X-ray‖ during phage growth (3 hr)	150–190 160–200	145–155
6	Same as No. 5 but 10·8 r/min		105–110
7	Same as No. 5 but 30 r/min		90–105
8	Chalk River juice† (^{32}P control)		95–110
9	^{32}P $\alpha N_0 = 3{\cdot}07$ $E = 1{\cdot}4\times10^{-11}$		110–135
10	^{32}P $\alpha N_0 = 9{\cdot}42$ $E = 2{\cdot}1\times10^{-11}$		105–110
11	^{32}P $\alpha N_0 = 14{\cdot}23$ $E = 3{\cdot}9\times10^{-11}$		95–110
12	T4BH grown in 3XD (shockate)		135–155
13	T4B *r* 240 grown in 3XD (shockate)	175–200¶	150–175
			125–145
14	Sample 13 after treatment with trypsin and chymotrypsin	150–170¶	
15	T4 wild (shockate)	165–175¶	
16	Sample 15 after treatment with trypsin and chymotrypsin	150–160¶	
17	Sample 16 shaken gently 500 times	90–95¶	

† Phosphate solution after decay of ^{32}P.

‡ Low gradient point aberrantly high and should be rejected.

¶ 0·036 M-tris pH 7·8
0·14 M-NaCl
0·005 M-Ca

‖ The X-rays were generated by a G.E. Maxitron operated at 250 Kv with a Cu-Al filter. The dosage was determined by a standard Victoreen meter introduced into the empty growth vessel. The shielding due to the medium was taken into account, and the dose rates quoted are the mean dose rate received by the culture.

We note there is a decrease in the intrinsic viscosity on passing from 0·10 to 4·0 M-NaCl. This might be interpreted either as dissociation of protein or some residual polyelectrolyte effect. The gently phenol-extracted DNA displays the same (almost 30%) reduction in 4·0 M-NaCl. This conclusion is based on the reduction of intrinsic

viscosity determinations at 73 and 120 sec^{-1} and the straight line extrapolation to zero gradient. (Table 1; 3B). Since the phenol-DNA contains very little protein the observed reduction is probably not due to the loss of protein interconnections.

The direct action of chymotrypsin and trypsin result in a 10 to 15% reduction, a marginal yet observable decrease in the intrinsic viscosity. This possibly represents some tendency toward aggregation which may play a larger role at higher DNA concentrations. It is important to note that the LSU-autoradiograph ("star") is not affected by 2 days' exposure to these enzymes (Thomas, 1959).

(b) *Intrinsic viscosity of T4 shock products*

In Table 1 are listed the intrinsic viscosity values for a number of T4 shockates in 0·10 M-NaCl, 0·032 M-phosphate or in 4·0 M-NaCl, 0·032 M-phosphate. These values have been obtained by measuring the η_{sp}/c values at a number of concentrations usually between 11 and 22 μg/ml. and at three average gradients usually 35, 68, and 115 sec^{-1}. At any gradient, the η_{sp}/c values were independent of concentration. When η_{sp}/c was plotted against the average gradient, the three experimental points did not lie precisely on a straight line. Extrapolation to zero gradient was performed in two ways, first by the best straight line, and secondly by a gentle curve fitting the three points. The two resulting intercepts are quoted consecutively in Table 1. The difference between these values gives a qualitative estimate of the curvature.

An examination of Table 1 leads to the following conclusions. Apparently growth conditions (Nos. 1, 4, 5, 6, 7, 8, 9, 10, 11, 15, 16), continual X-radiation during growth (Nos. 4, 5, 6, 7), or the presence of 200 μC/ml. ^{32}P (Nos. 8, 9, 10, 11) do not result in more than 15% change in the intrinsic viscosity. This strongly argues that within the reproducibility of our measurements there is no radiation effect, and that in particular, radiation at these levels is not causing DNA molecules to stick together, or to be broken down.

The conclusions from these experiments are that the intrinsic viscosity of T4 shockates is a reproducibly measured value whose magnitude reflects the presence of large DNA molecules in solution and is not a consequence of casual attachments of such molecules with each other *via* protein. Further, there is no growth medium effect or any alteration resulting from irradiation during growth. These conclusions are supported by sedimentation equilibrium experiments on the same material (Thomas, 1960). This means that the LSU as seen by autoradiography is *not* a consequence of the labelling process.

It is important to note that the absolute magnitudes of the intrinsic viscosity values shown in Table 1 fall considerably below the value expected from the empirical work of Doty, McGill & Rice (1958) on calf thymus DNA. The autoradiographic experiments indicated the presence in T4 of one large subunit (LSU) and 6 small units (SMU). The predicted intrinsic viscosity for such a mixture is about 272. For a uniform collection of molecules of 12×10^6 mol wt the expected value is 125, which accidentally is in excellent agreement with our measurements. We do not take this agreement as evidence against the LSU, because calf thymus DNA is different from phage DNA. Hermans' studies (Hermans, 1959) have revealed that different sources of DNA, and indeed different preparations of DNA from the same source, display different relationships between $[\eta]$ and M. It is possible that the proportionately lower values of $[\eta]$ shown by phage shockates results from the persistance of some residual "kinks" or folds that were necessary to pack this DNA in the small phage head.

It is a pleasure to acknowledge that this work was supported by an Atomic Energy Commission Contract AT(30–1)–2119. We would like to express our appreciation to Dr. Timothy Merz for his help with the X-ray experiments.

REFERENCES

Adams, M. (1959). *The Bacteriophages*, New York: Interscience.
Doty, P., McGill, B. B. & Rice, S. A. (1958). *Proc. Nat. Acad. Sci., Wash.* **44**, 432.
Fraser, D. & Jerrel, E. A. (1953). *J. Biol. Chem.* **205**, 291.
Hermans, J. (1959). *J. Phys. Chem.* **63**, 170.
Hershey, A. D. (1955). *Virology*, **1**, 108.
Levinthal, C. & Thomas, C. A., Jr. (1957). *Biochim. biophys. Acta*, **23**, 453.
Thomas, C. A., Jr. (1959). *J. Gen. Physiol.* **42**, 503.
Thomas, C. A., Jr. (1960). *J. Gen. Physiol.* in the press.
Thomas, C. A., Jr. & Knight, J. (1959). *Proc. Nat. Acad. Sci., Wash.* **45**, 332.

J. Mol. Biol. (1960) **2**, 10-18

Electron Microscope Observations on the Structure of Microsomal Particles from *Escherichia Coli*

H. E. Huxley

Medical Research Council, Department of Biophysics, University College, London, England

AND

G. Zubay†

Medical Research Council Biophysics Research Unit, King's College, London, and Department of Biophysics, University College, London, England

(*Received 18 January 1960*)

Microsomal particles from *E. coli* are known to exist in a number of different stable forms, depending foremost on the concentration of free magnesium ions, and characterized by sedimentation coefficients of 100 s, 70 s, 50 s and 30 s. These different forms, identified in each case by sedimentation analysis, have been investigated by electron microscopy, using both negative and positive staining. Using negative staining it was found that the 100 s particles consisted of two 70 s particles joined together as a dimer. The 70 s particles could be seen to contain two subunits of unequal size with a well-marked cleft between them, and in the 100 s particles the smaller subunits of the two 70 s particles were apposed. 50 s and 30 s particles were found to resemble closely the larger and the smaller subunits of the 70 s particles. In addition, it was found that purified 50 s particles, when transferred to a medium in which 100 s particles were stable, formed dimers with a sedimentation coefficient of about 81 s.

The particles were not found to have a regular polyhedral form, in contrast to some small spherical viruses. The 50 s particles appeared to be very approximately dome-shaped. The 30 s particles had a flatter form with a rather irregular outline. In the 70 s particles, the smaller subunit was seen to fit like an overlapping cap on the flattened face of the larger one.

When microsomal particles were stained with uranyl acetate (which in many situations appears to act as a preferential stain for nucleic acids) they showed a complex internal structure, but no indication of the cleft between the subunits in 70 s particles. No evidence was found for the existence of a protein shell around a nucleic acid core in the particles, again in contrast to some small spherical viruses.

1. Introduction

Microsomal particles (ribosomes) from *Escherichia coli* have been characterized by Tissières & Watson (1958). These authors have shown that the ribosomes exist in a number of different stable forms, depending foremost on the concentration of free magnesium ions. At the higher magnesium concentrations (0·005 M-magnesium acetate in presence of 0·5 mM-tris (2-amino-2-hydroxymethylpropane-1:3-diol) buffer pH 7·4) particles having a sedimentation coefficient of approximately 100 s are the predominant species; in lower concentrations of magnesium (0·002 M-magnesium acetate in dilute tris) these appear to split into smaller units with a sedimentation coefficient of 70 s, and at lower effective magnesium concentrations

† Now at The Rockefeller Institute, New York 21, New York, U.S.A.

still (0·001 M-magnesium acetate in 0·01 M-phosphate buffer pH 7·0) these appear to subdivide again into particles having sedimentation coefficients of 50 s and 30 s. These changes are all reversible. All the different species (referred to as 100 s, 70 s, 50 s and 30 s particles) are similar in chemical composition and contain approximately 60% RNA and 40% protein. In addition to the components already mentioned, we have found that a purified preparation of 50 s ribosomes, when transferred to the 100 s solvent, shows in the ultracentrifuge a peak with a sedimentation coefficient of 81 s. Ribonucleoprotein particles having sedimentation coefficients rather similar to some of those mentioned above have been prepared from a variety of animal and plant tissues and from yeast (e.g. Schachman, Pardee & Stanier, 1952; Chao & Schachman, 1956; T'so, Bonner & Vinograd, 1956; Palade & Siekevitz, 1956; Petermann & Hamilton, 1957; Chao, 1957; McQuillen, Roberts & Britten, 1959); in several instances, these ribosomes too appear to be capable of splitting into discrete subunits.

We have investigated these different forms of the microsomal particles from *E. coli* by electron microscopy, particularly by the method of negative staining (Hall, 1955; Huxley, 1957; Brenner & Horne, 1959) and by positive staining with uranyl acetate.†

2. Methods

(a) *Preparation of ribosomes*

Bacteria (*E. coli*) were kindly supplied to us by Dr. Geoffrey Brown; they were grown in a continuous culture apparatus. Ribosomes from them were prepared in the manner described by Tissières & Watson (1958). As these authors state, the character of the preparation varies with the particular salt solution used. When the purification is done in 0·005 M-magnesium acetate plus 0·5 mM-tris buffer pH 7·4, one usually obtains a mixture of two components, having sedimentation coefficients of 70 s and 100 s. When this system is dialysed against 0·002 M-magnesium acetate-tris buffer, the 100 s component mostly disappears, leaving a 70 s peak. The 50 s and 30 s components may be prepared by dialysing the 70 s preparation against 0·001 M-magnesium acetate plus 0·01 M-phosphate buffer pH 7·0. We too have found that the areas under the peaks in the schlieren sedimentation diagrams of the 50 s and 30 s components are always very nearly in the ratio of 2 : 1 when they are prepared from pure 70 s component. The 50 s and 30 s particles may be separated from one another by fractional centrifugation in 0·01 M-phosphate plus 0·001 M-magnesium acetate solvent. We have observed that when the purified 50 s component is dialysed against the 0·005 M-magnesium acetate-tris solvent (where one would normally obtain a mixture of 70 and 100 s particles) one obtains a single peak with a sedimentation coefficient of about 81 s. The conversion between 50 and 81 s particles is reversible. On the other hand when the purified 30 s particles are dialysed against the 0·005 M-magnesium acetate-tris solvent they do not give rise to any new component visible in the ultracentrifuge but gradually precipitate.

In most of our preparations we obtain 70 and 100 s particles when the preparation is made in 0·002 M-magnesium acetate-tris, pH 7·4. However, on occasions a preparation made under these conditions gives rise to a mixture of 50 and 81 s particles. The latter system differs fundamentally from the first in the total absence of 30 s particles. Since the method of preparation is identical we believe that this difference has its origin in the somewhat variable conditions of growth of the bacteria. Two possibilities exist: (1) that the bacteria are capable of growing without the 30 s particle, or (2) that at some late stage in the growth cycle of the bacteria the 30 s particles disintegrate perhaps because of the deficit of some salt or buffer in the growth medium.

† Note inserted in proof: since this paper went to press a study of the same material using the shadow-casting technique has been published by C. E. Hall & H. S. Slayter (*J. Mol. Biol.* **1**, 329 (1959)).

(b) *Fixation of ribosomes*

Preliminary results showed that the negative staining technique, which involves treating the preparation with 1% phosphotungstic acid (PTA), could not be applied satisfactorily to unfixed ribosomes. Electron microscope observations showed considerable evidence that degradation had taken place, preparations of different particle species failed to show characteristically different appearances, and the particles which were still visible showed up with rather poor contrast. The situation was not improved by treating the preparations with buffered 1% osmium tetroxide solution (a popular fixative used in electron microscopy) prior to negative staining. However, we eventually found that if the preparations were treated with 10% formalin (4% formaldehyde), in the medium in which the particular species in question was stable, for one hour at pH 6·0, and if the negative staining was carried out at pH 5·3 with 1% PTA in the presence of 5 to 7×10^{-3} Mg^{2+}, then the appearance of the particles was much more satisfactory, and characteristic features of the different molecular species were visible. As a further check, we carried out parallel experiments in the ultracentrifuge.

If formalin is added as described to a ribosome preparation, the general pattern of peaks seen in the ultracentrifuge is unchanged, though there is a small drop (of about 10%) in the absolute values of the sedimentation coefficients observed. If now 1% PTA plus 0·005 M-Mg^{2+} is added, the pattern of peaks is still undisturbed, though the absolute values of the sedimentation coefficients now increase again, returning virtually to those of the untreated preparation, presumably as a consequence of small uptake of PTA. The relative areas under the different peaks in a mixed preparation are not affected by the formalin-PTA treatment. In contrast, if 1% PTA is added to a preparation of *unfixed* particles which originally showed, say, both 100 S and 70 S peaks in the ultracentrifuge, then both these peaks disappear and a peak corresponding to particles with a sedimentation coefficient of about 47 S is seen. There is no sign of anything corresponding to a 30 S component.

The procedure adopted, then, was as follows. The ribosomes were in each case prepared as a concentrated suspension, containing approximately 0·2% by weight of ribonucleoprotein, in the media specified above for the particular species required. The stock fixing solutions contained 1 part of "40% formaldehyde" to 4 parts of the media used, the pH being adjusted to around pH 6. For fixation, equal volumes of ribosome suspension and stock fixative were mixed, and at least 1 hr allowed to elapse before staining. More prolonged fixation times (e.g. up to 8 hr) appeared to be without detriment to the particles, so that one such preparation could be used all day. The fixed preparation was usually diluted 5 to 20 times before use, media containing 10% formalin being used for the purpose.

(c) *Electron microscopy*

(i) *Negative staining.* In the course of these studies, we have developed a technique for negative staining which, both on ribosomes and on other macromolecules which we have studied, appears to be considerably superior to previous variations of this method; we will therefore discuss it in some detail.

The basic requirement in negative staining is to produce a thin sheet of phosphotungstic acid in which the particles under examination are embedded; the particles will then show up in the electron microscope by negative contrast, for they will be less dense than their surroundings. The effect seems to have been first reported by Farrant (1954), then by Hall (1955) and then observed again and used to investigate the form of tobacco mosaic virus by one of us (Huxley, 1957), all independently. More recently, Brenner & Horne have made extensive and elegant use of the same principle, and have described (Brenner & Horne, 1959) a procedure in which the sample, mixed with neutralized PTA, is sprayed onto carbon-filmed grids, made unusually hydrophilic by manufacture in a special evaporating unit with a "trapped" vacuum system.

We have not found that the employment of specially prepared grids is an essential requirement, even when the preparation is sprayed on. Indeed, grids made extremely hydrophilic (by ion bombardment) were found to be unsuitable, for the negative staining solution then spreads out so thinly and evenly as to give very low contrast around the particles. Satisfactory results were obtained using grids filmed with carbon in a conven-

tional evaporating unit; the spreading of the spray droplets can be improved, if required, by increasing the concentration of particles in the preparation, or by soaking the grids for a few minutes in carbon tetrachloride. If the particle suspension is applied directly to the grid (e.g. from a dropper) either before or at the same time as the PTA solution, then no difficulty is usually encountered in obtaining satisfactory spreading, and negative staining takes place equally well. The excess staining solution is removed by applying a fine glass capillary to the edge of the grid.

We have found, however, that the best results are obtained when the supporting film is done away with altogether! We have commonly employed carbon films with small holes in them (made by breathing gently on the initial collodion film as it is being prepared by evaporation of the solution in amyl acetate on a slide), as an aid to focusing and astigmatism correction. We observed by chance that the PTA in some places dries in a thin film *across* these holes, and that where particles are present in this film, they show up with superior clarity and contrast. Judging from their dimensions, such particles are less flattened than ones which have dried down onto a supporting film, and they show surface detail much more clearly. The absence of supporting film in itself no doubt aids clarity. The tungstate films often pull away from the supporting film on one side of the hole, and so the edge can still be used for focusing. Care must be taken to choose areas which are free from drift and blurring due to instability of the film. The sample under observation can either be sprayed on ready mixed with the phosphotungstate solution, or it can be applied directly to the grid, which is then rinsed before applying the staining solution. In the latter instance, it is rather surprising that so many particles are still found over the holes, but such is the case; presumably they remain there in a surface film, even during rinsing. They are not found if the grid is rinsed on both sides.

We have experimented with PTA solution adjusted to various pH's by addition of NaOH, and find that optimum results in terms of contrast and lack of granularity in the stain are obtained at pH 5·3; the concentration of the PTA in the final solution on the grid was made 1%, and 5 to 7×10^{-3} M-Mg^{2+} was also present.

(ii) *Positive staining by uranyl acetate.* The use of aqueous uranyl acetate as a staining and stabilizing solution for electron microscopy has already been reported (Watson, 1958; Kellenberger, Ryter & Sechaud, 1958), and the former author has shown that microsomal particles in sections of pancreas are heavily stained by it. We have found (Huxley & Zubay, in preparation) that 2% uranyl acetate in water with the pH adjusted to around 5·0 by addition of NaOH acts as a strongly preferential stain for nucleic acids in a number of different situations, and that very fine detail is revealed by its use. Accordingly, we have employed it here. A drop of the ribosome preparation, fixed in formalin and diluted with appropriate solvent so that the particle concentration was approximately 0·005%, was placed on a carbon-filmed grid and then rinsed several times with pure solvent. The grid was then immersed in the uranyl acetate solution for 4 to 8 hr at room temperature. After rinsing in distilled water and either air- or freeze-drying, the grid was ready for examination.

(iii) *Aids to high-resolution microscopy.* Both the techniques described above yield preparations which show fine detail limited only by the resolution of the microscope and the degree of fatigue in the operator. The limiting factors are:

(1) The accuracy with which the astigmatism is corrected

(2) The accuracy with which the objective current is set for optimum focal position.

Using a Siemens Elmiskop I (high tension 80 kv, double condenser (200μ aperture), 50μ objective aperture, final magnification $\times$80,000), we have found that the biggest gains in the quality and resolution of the pictures come only when both astigmatism correction and focusing are accurate to better than $\Delta f \cong 1{,}000$ Å (1 click of the fine focus control). This is particularly noticeable in the case of micrographs of preparations stained with uranyl acetate, in which the internal fine detail becomes almost totally obscured by electron-optical artifacts if this degree of defocusing is exceeded; and there are visible imperfections in even the best images we have obtained.

Correction of the astigmatism to the required degree is more conveniently done with the objective aperture in place, rather than by making the correction on the objective lens

alone and relying on finding an aperture which introduces zero astigmatism. Even so, apertures remain usable for only a short time before the correction setting begins to vary slightly with the position and nature of the specimen. The presence of small holes all over the supporting film makes it possible to keep a continuous check on the condition of the instrument and on any local instabilities in the specimen.

A further factor of importance in the case of positively stained specimens is the thickness of the supporting film. A great gain in clarity is obtained when exceptionally thin carbon films are employed (about 10 Å in thickness). Such films are very fragile and can only be used if the grids are first coated with a carbon film of conventional thickness, containing large holes, and then the specially thin film (with small holes in it) laid down on top of this.

(d) *Ultracentrifuge examination*

All preparations were examined in the Spinco model E ultracentrifuge using schlieren optics, and the presence of the required type of ribosomes confirmed before the preparation was studied in the electron microscope.

3. Results

(a) *Negative staining*

When a preparation containing a mixture of 100 s and 70 s ribosomes, and characterized in the ultracentrifuge (see Plate I(a)) by the two appropriate peaks, was examined by the negative staining technique, the images seen in the electron microscope always had the very characteristic features illustrated in Plates II and VI(a). Two different types of particle are readily visible. The smaller type has a diameter of 140 to 180 Å and a rather irregular outline, and appears to be built up of two unequal subunits; the larger subunit is somewhat flattened on the side which faces the smaller one, and the smaller one often appears slightly concave on the side which faces the larger one so that it gives the impression of fitting onto it like an overlapping cap. There is a distinctive cleft in the composite particle between these two subunits, and in many instances one can see considerable local variation in the size of this cleft.

The larger type of particle very clearly consists of two of the smaller particles joined together, their smaller subunits being apposed. The apposed subunits may be seen to have a crescent or a triangular form; and the area of contact between them is displaced to one side of the long axis of the particle, so that a wedge-shaped space is often visible between the two halves. The composite particle has a length of 350 to 400 Å and a width of about 140 Å.

The relative numbers of the large and small particles seen in the electron microscope were approximately the same as the relative numbers of 100 s and 70 s ribosomes found by ultracentrifugal analysis of the same preparations (assuming that the 100 s particles were twice as heavy as the 70 s ones). When a preparation consisting virtually of 70 s particles alone was examined (see typical ultracentrifuge pattern in Plate I(b)) only the smaller type of particle, with its two unequal subunits, was found to be present in significant amounts (Plate III). We feel justified at this stage in identifying this smaller particle as the 70 s component, and in identifying the larger "dimeric" particle, consisting of a pair of 70 s particles, as the 100 s component.

If a preparation of 70 s ribosomes is transferred to a medium containing 0·001 M-Mg^{2+}, 0·01 M-phosphate buffer pH 7·0, then components with sedimentation coefficients of 50 s and 30 s replace the 70 s component seen in the ultracentrifuge (see Plate I(c)). Such a preparation, fixed and negatively stained, has the appearance shown in Plates IV and VI(b). Again, two types of particle seem to be present. The larger one, having a diameter of 140 to 160 Å, and sometimes appearing very

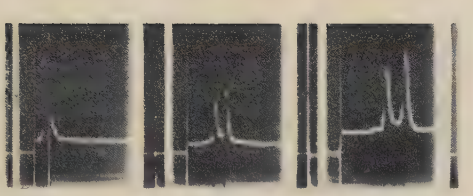

PLATE I. (a) Ultracentrifuge sedimentation pattern of 70 s and 100 s particles. Pictures taken every 8 min at 29,500 rev/min.

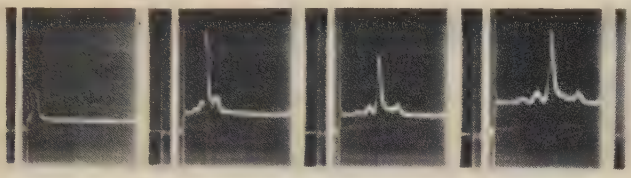

(b) Ultracentrifuge sedimentation pattern of 70 s particles. Pictures taken every 8 min at 29,500 rev/min. The one faster and two slower minor components represent small amounts of the 100 s, 50 s and 30 s particles respectively.

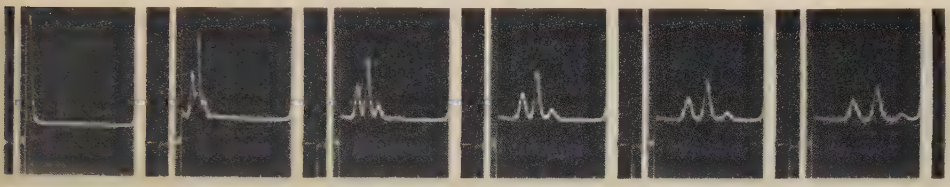

(c) Ultracentrifuge sedimentation pattern of 30 s and 50 s particles. Pictures taken every 8 min at 29,500 rev/min. The faster component represents a small amount of 70 s particles.

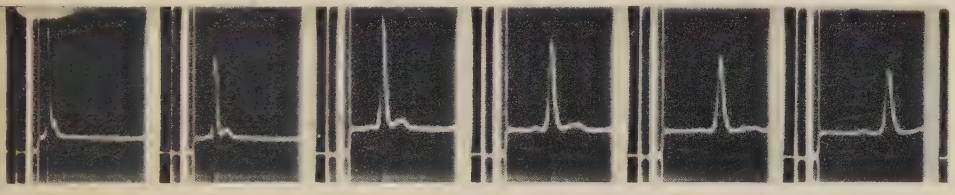

(d) Ultracentrifuge sedimentation pattern of 50 s particles. Pictures taken every 8 min at 29,500 rev/min.

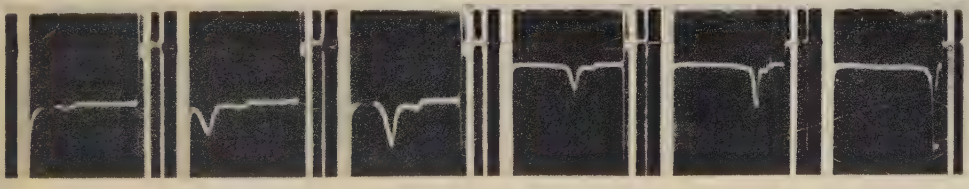

(e) Ultracentrifuge sedimentation pattern of 81 s particles. Pictures taken every 8 min at 29,500 rev/min. The slower minor component represents 50 s particles.

[*To face page* 14

ERRATUM

Owing to a printer's error Plate I (e) facing page 14 of Volume II no. 1, April 1960, is upside down: the other parts of Plate I are correctly printed.

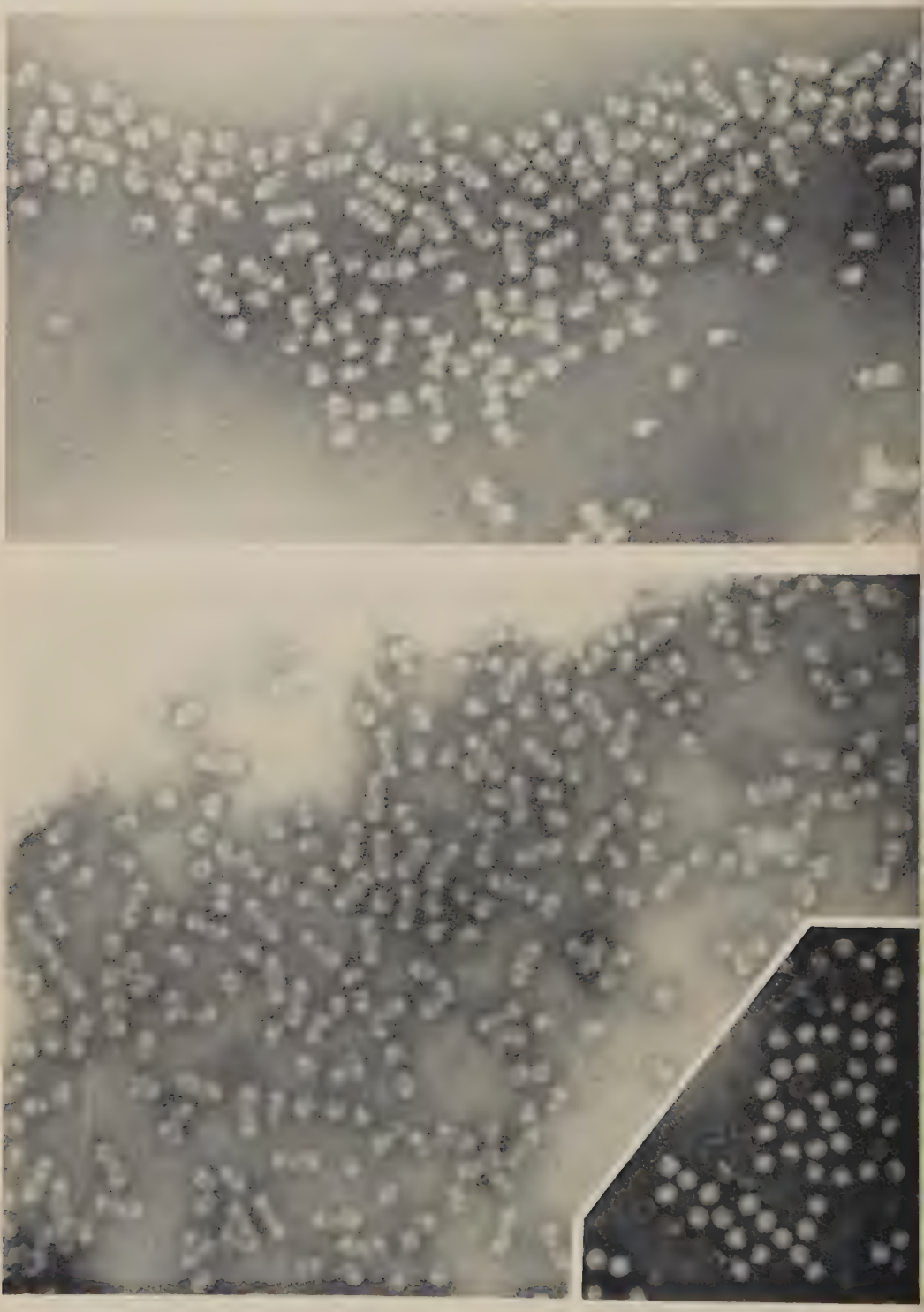

PLATE II. (a) and (b) Preparation containing a mixture of 100 S and 70 S particles, negatively stained with PTA. Two types of particle are visible, (1) monomers, containing two unequal subunits, (2) dimers, consisting of two of the monomers joined together at their smaller subunits.

Inset. A comparison micrograph of turnip yellow mosaic virus, negatively stained with PTA under identical conditions. Note the much more regular and clearly defined form of the virus particles, and the presence of some "empty" shells. The surface structure of the virus (which appears to us (Huxley & Zubay, in preparation) to resemble a rhombic triacontahedron, with 32 subunits) is readily visible. (Magnifications: (a) × 200,000, (b) × 160,000, (*Inset*) × 160,000.)

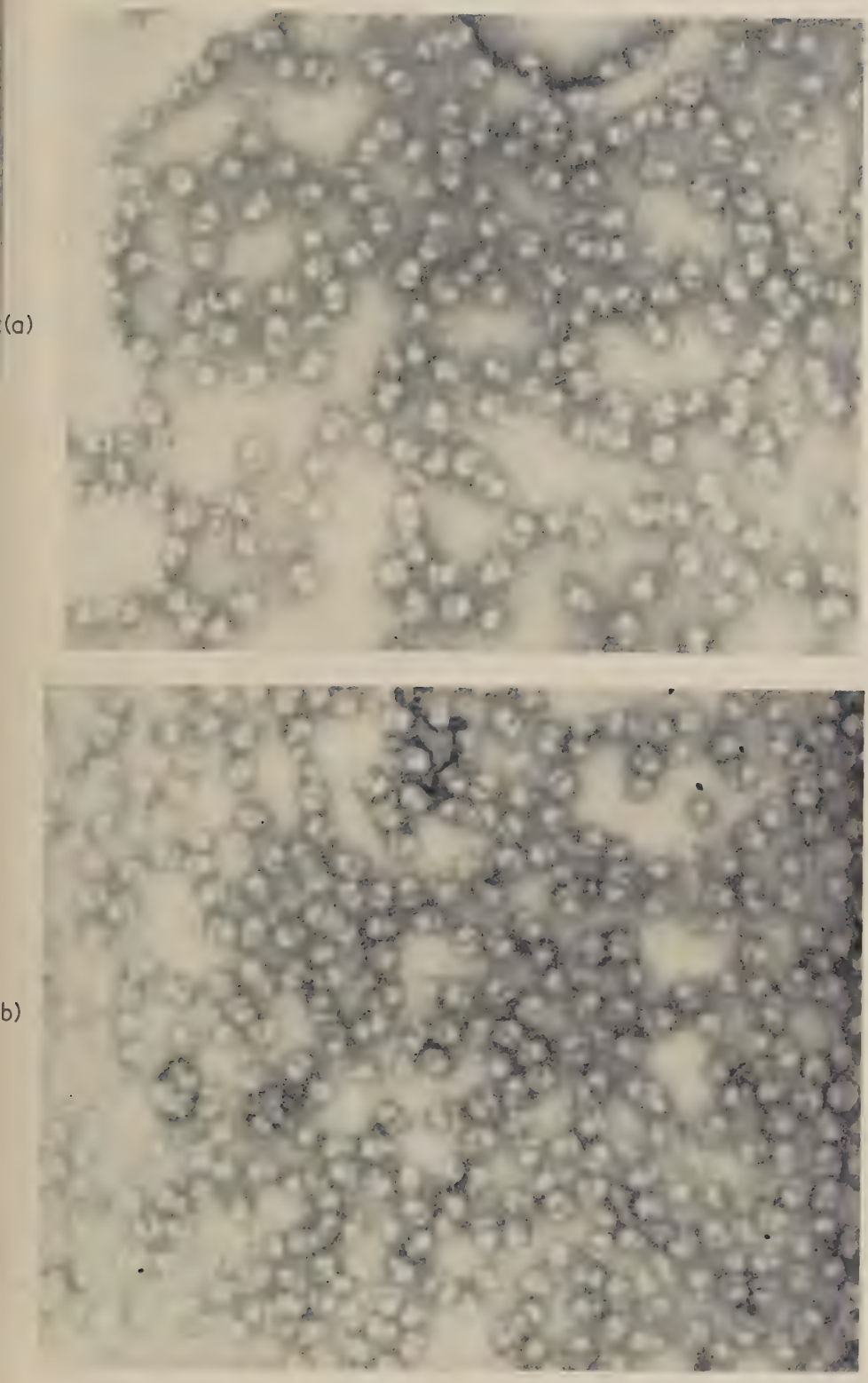

PLATE III. (a) and (b) Preparation of 70 S particles, negatively stained with PTA. Most of the particles present show two unequal subunits. In some places, the subunits may be seen separated (e.g. Plate III (a), left hand side). A few dimeric particles (100 S) are also visible. A supporting film was present, and, the particles appear slightly larger than when dried down over holes. (Magnification × 200,000.)

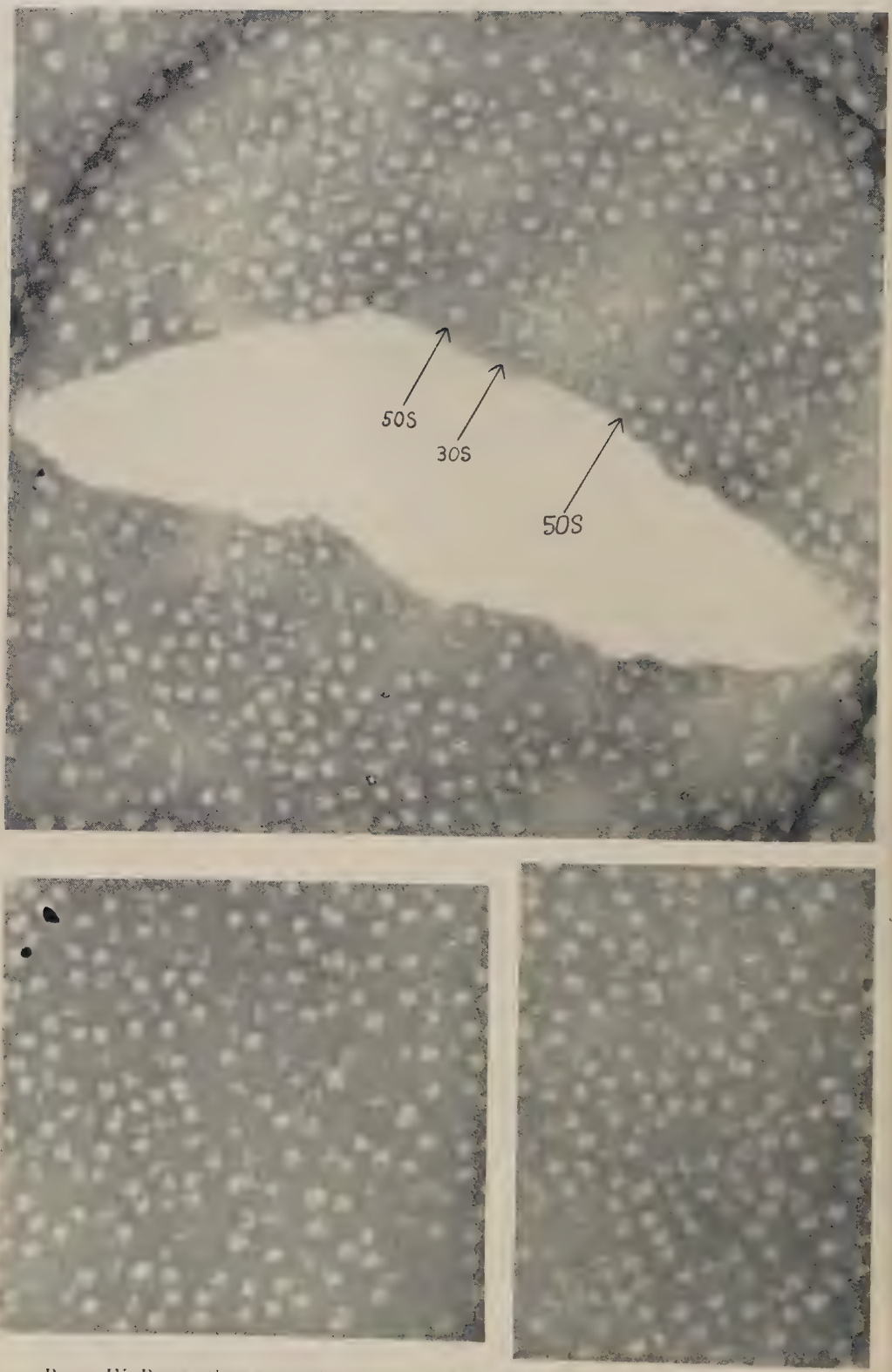

PLATE IV. Preparations containing mixture of 50 s and 30 s particles, negatively stained with PTA. A variety of different forms are visible, particularly prominent being (1) larger particles, showing up with good contrast, and often with suggestions of polygonal outline. (2) Smaller particles, often showing up with much lower contrast, having more irregular and variable outlines and frequently somewhat elongated. Suggestions of surface structure are occasionally visible. The larger particles probably represent the 50 s species, the smaller, 30 s. (Magnification × 200,000.)

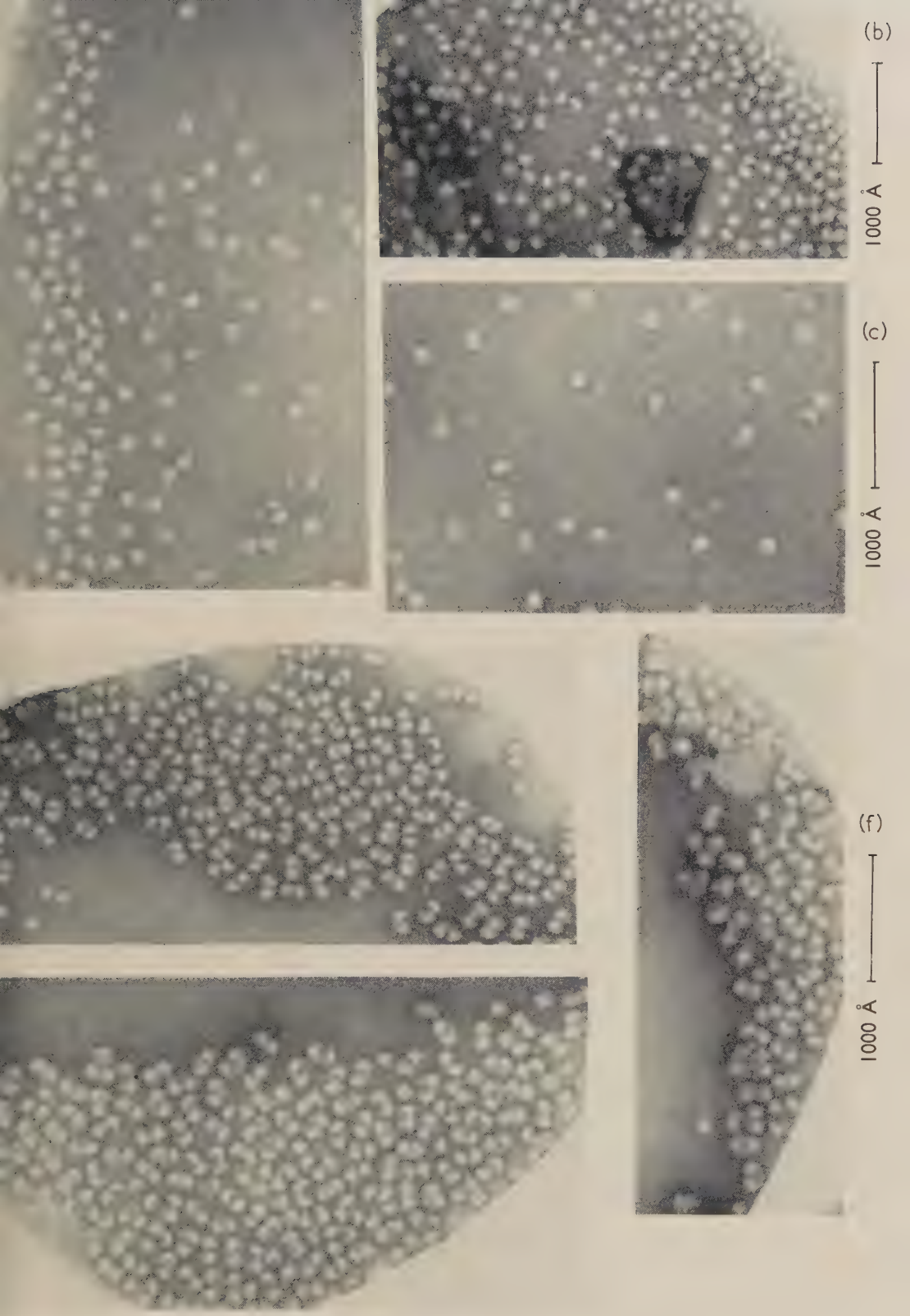

PLATE V. (a), (b) and (c) Purified preparation of 50 s particles, negatively stained with PTA. Almost all the particles visible are of the same species, and appear identical to the larger particles seen in (50 s + 30 s) preparations.

(d), (e) and (f) Preparations of 50 s particles, transferred to 100 s solvent (0·005 M-magnesium acetate + tris), and negatively stained with PTA. Virtually all the particles visible are dimers, formed by the association of two 50 s particles with flattened faces apposed. In Plate V (f), a phage with its banded tail may be seen. (Magnifications: (a) × 200,000, (b) × 160,000, (c) × 200,000, (d) × 160,000, (e) × 200,000, (f) × 200,000.)

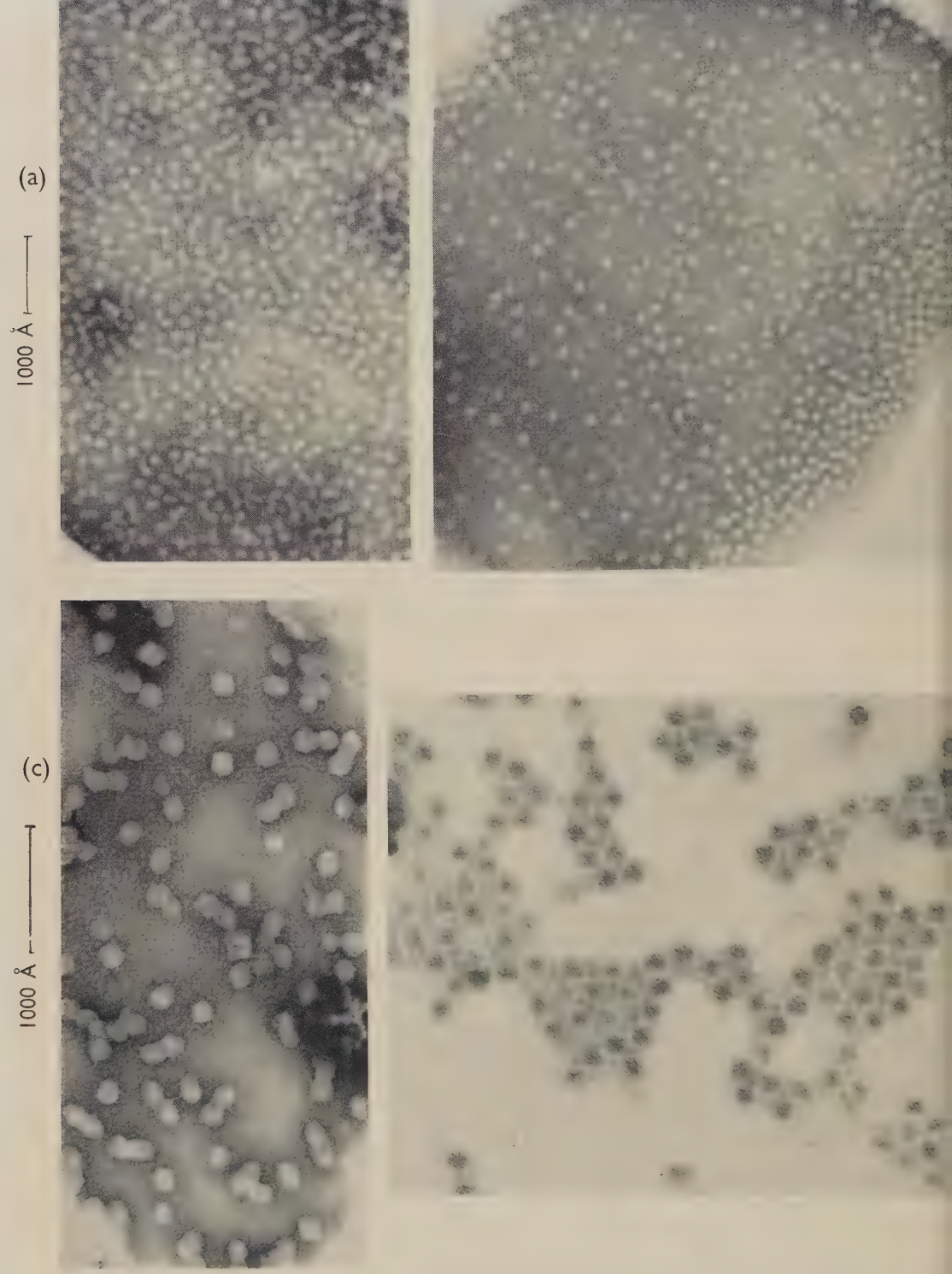

PLATE VI. (a) Preparation of 100 s + 70 s particles, showing typical appearance after negative staining. (Magnification × 120,000.)

(b) Comparison micrograph of 50 s + 30 s preparation (obtained by dialysing 100 s preparation against 0·01 M-phosphate buffer + 0·001 M-Mg^{2+}) illustrating the splitting up of the larger particles into their component subunits. (Magnification × 120,000.)

(c) Microsomal particles, positively stained with uranyl acetate and then negatively stained with same salt. No differential staining of the periphery of the particles is apparent. (Magnification × 200,000.)

(d) Comparison micrograph showing TYMV particles treated in identical manner, i.e. positive and negative staining combined. The virus particles appear to have a shell of material at their surface, which is inaccessible to the negative stain, and which is not positively stained by uranyl acetate. (Magnification × 200,000.)

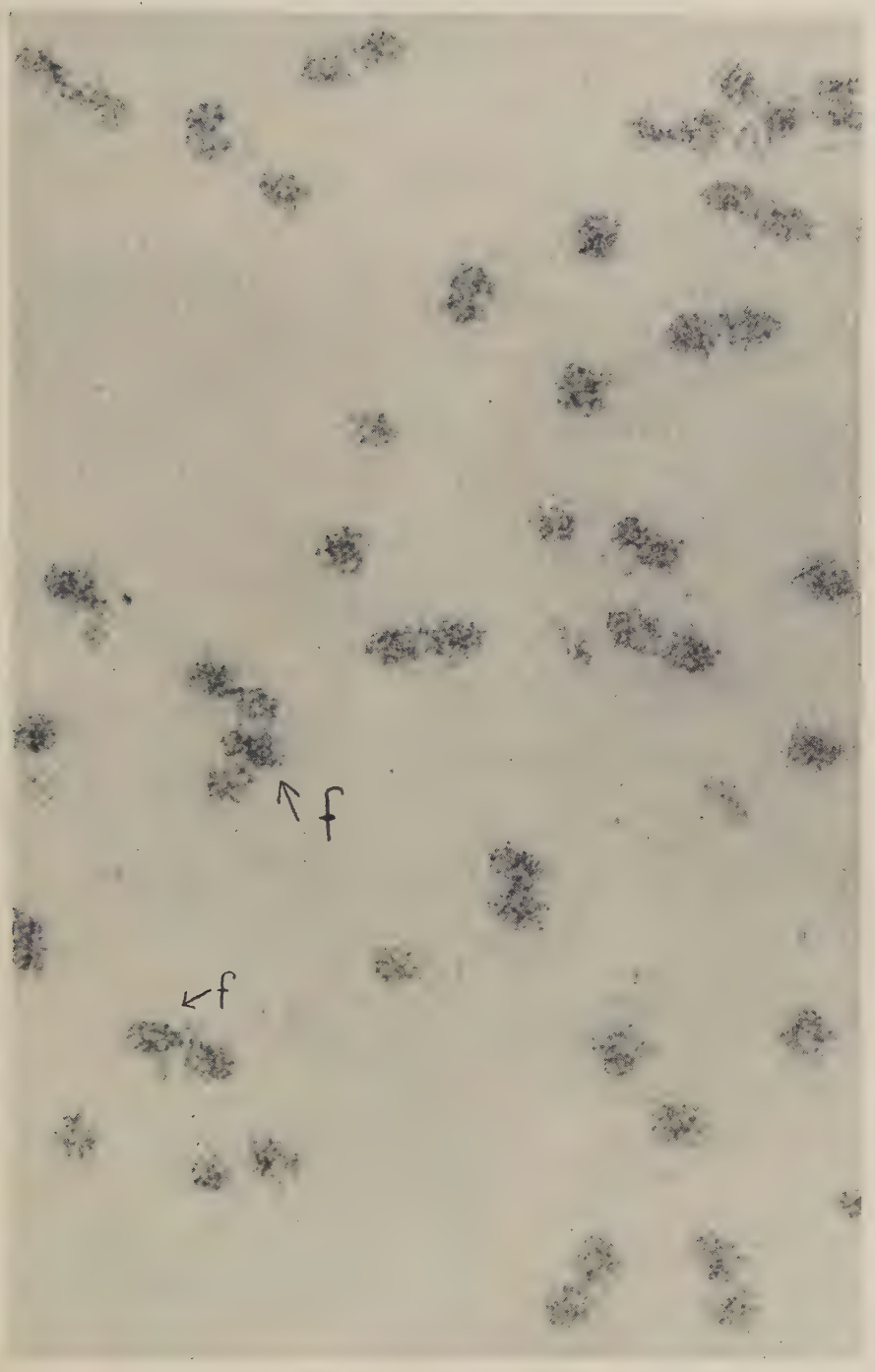

PLATE VII. Preparation containing a mixture of 100 s and 70 s particles, positively stained with aqueous uranyl acetate, pH 5, for 6 hr. The two species of particle are easily recognized, but no division of the 70 s particles into two subunits is shown up by this staining method. Many of the particles show internal structure; a fenestrated appearance is visible in those marked "f". (Magnification × 415,000.)

1000 Å

(a)

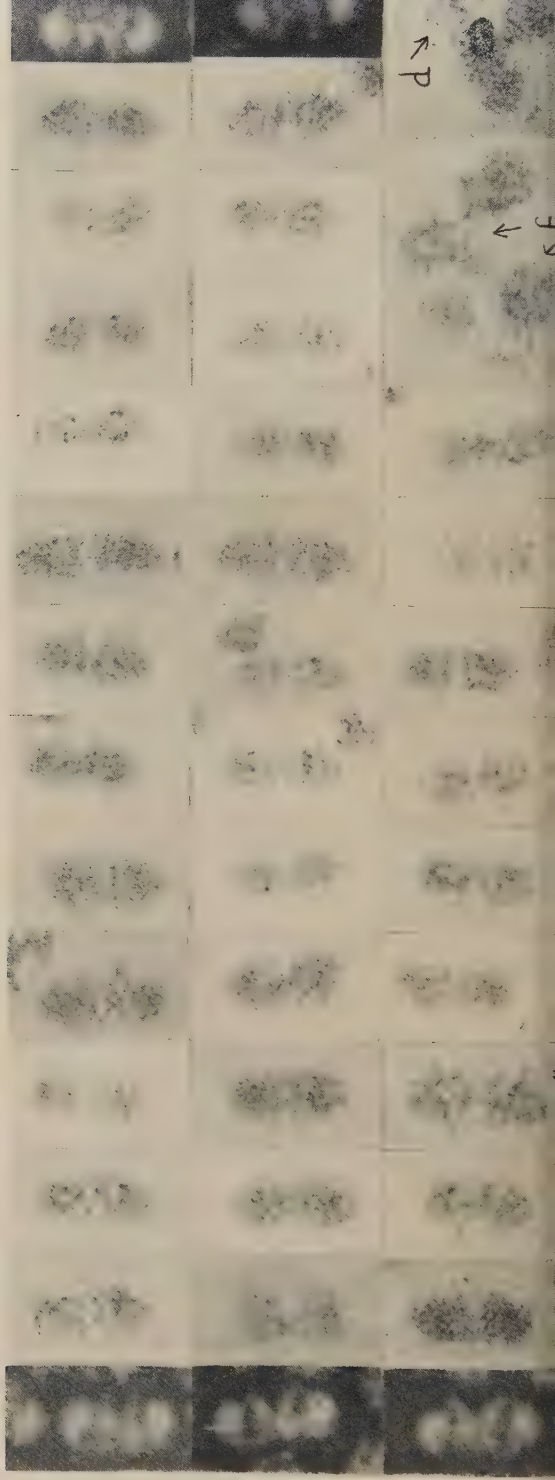

1000 Å

(b)

Plate VIII. (a) Another preparation containing a mixture of 100 s and 70 s particles, positively stained with aqueous uranyl acetate. (Magnification × 300,000.)

(b) A number of 100 s particles, stained with uranyl acetate, taken from different micrographs and, for comparison (at top and bottom) some 100 s particles, negatively stained with PTA, photographed at same magnification. The variation in the apparent size of the positively stained particles is most probably to be accounted for by varying degrees of flattening during drying. The failure of uranyl acetate staining to show the subunits within the two halves of the 100 s particles is well-marked. A structure which is seen from time to time, and is suggestive of a a disintegrating particle, is shown in the micrograph marked "d". At "f", more particles having a fenestrated appearance are shown. (Magnification × 415,000.)

approximately pentagonal, bears a considerable resemblance to the larger subunit seen in the intact particle in the 70 s preparations. The smaller particles are more elongated and often show up with much less contrast than the larger ones, as though they were much thinner and were lying flat in the stain. Their shape is somewhat variable, and a variety of different forms, including triangles, trapezia and more irregular forms, can usually be found. The appearance is consistent with their being identical to the smaller subunit visible in the particles in the 70 s preparations.

The 50 s and 30 s components may be separated by differential centrifugation. Electron microscope examination of purified 50 s component showed that it consists of the larger subunits described in the previous paragraph. Typical fields are shown in Plate V(a), (b), (c). If the purified 50 s component is suspended in 0·005 M-magnesium acetate plus 0·5 mM-tris buffer pH 7·4, then a new peak, with a sedimentation coefficient of 81 s, appears in the ultracentrifuge diagram (see Plate I(d) and (e)). Such a preparation, negatively stained, may readily be seen in the electron microscope to contain dimeric particles, closely resembling the larger subunits of the 70 s particles (or the particles in the 50 s preparations) associated together in pairs with flattened faces apposed (Plate V(d), (e), (f)).

The edges of the various particles almost always appear considerably less sharply defined than those seen in negatively stained preparations of the small viruses, such as turnip yellow mosaic virus (TYMV). For comparison, a preparation of the latter is shown in the inset on Plate II. The general contrast in the ribosomes is somewhat lower too, as though some penetration of the negative stain into the structure takes place. When they are dried with a supporting film, rather than over a hole, the ribosomes show particularly poor contrast and their apparent dimensions indicate considerable flattening. Some surface detail is often visible on the particles, but we have so far recognized very little regularity in it; occasionally, 50 s particles show some suggestion of a pentagonal, or incomplete hexagonal, arrangement of subunits about 70 Å apart. Particles are sometimes seen which show one or more relatively straight edges, whilst others have irregular shapes and short irregularly disposed projections on them. It is not possible to decide at present whether this represents a genuine variability in the surface of the particles, or whether it is a consequence of extraneous factors, either in the orientation of the particles or in the negative staining. The particles of any particular species do appear, however, to be very similar to each other. Nevertheless, even in very concentrated preparations, the particles never showed any tendency to order themselves in regular arrays on the electron microscope grid, again in contrast to the small spherical viruses.

(b) *Positive staining in uranyl acetate*

The appearance of a preparation of 100 s and 70 s ribosomes stained in 2% uranyl acetate for 6 hr is shown in Plates VII and VIII. The 100 s particles again appear elongated, and built up by the end-to-end association of two of the smaller (70 s) particles. However, the two subunits in the 70 s particles are not shown up by this method, although the overall dimensions are very similar to those observed by negative staining. It appears that there is a cleft between the two subunits in the 70 s particle, into which the negative stain can penetrate, and that structures in the ribosome which stain with uranyl acetate extend across this cleft. It is also noticeable that there is no gap visible in these structures where the two 70 s particles join to form the 100 s particle.

A certain amount of structure within the microsomes is shown up by staining with uranium. In some instances, this has a fenestrated or honeycombed appearance; the diameter of the holes visible is about 30 Å, and the diameter of the densely staining regions framing them, about 10 to 20 Å. In other instances, one can only see a number of lines 10 to 20 Å in width, together with dense spots of similar diameter. One must remember that the thickness of the particles is about 150 Å, and that within this depth a great number of overlapping structures can be present, whose resultant appearance will depend critically on their relative positions and on the orientation of the particle. Occasionally, there are visible what seem to be particles in process of disintegration, and in these, longer threads, again 10 to 20 Å in diameter, may be seen.

We have looked for indications of a shell of protein around a nucleic acid core by using a combination of negative and positive staining. In the case of a number of small spherical viruses, we have found that there is a very obvious annular region at the periphery of the particle into which the "negative" stain does not penetrate and which is not positively stained by uranyl acetate. Plate VI(d) shows this effect in the case of TYMV, and it seems very likely that this shell represents the protein of the virus. The shell measures 20 to 30 Å in thickness. If all the ribosomal protein were in a uniform shell, its thickness would be about 15 Å. We have observed no such clear indication of a protein shell in the case of the ribosomes; the boundaries of the negatively and positively staining regions are much less clear-cut than in the viruses, but, for what the observation is worth, we have seen no obvious and consistent annular space between them. Nor have we seen anything that might correspond to an "empty" microsomal particle (i.e. one lacking its RNA), whereas such images (i.e. empty shells without cores) are common in the case of the spherical viruses.

4. Discussion

The electron microscope observations are in full agreement with the current view that the different types of microsomal particle from *E. coli* represent different stages of association of the common subunits. Thus, a 30 s particle and a 50 s particle can associate to form a 70 s particle, and two 70 s particles can associate to give a 100 s particle. Two 50 s particles can also associate to give an 81 s particle. The observations show that the outlines of the individual subunits is easily visible, in each case, in the intact particle, and that the shape of the subunits is not noticeably affected by the combination. They further show that the association of the two 70 s particles takes place by the apposition of the exposed faces of their 30 s subunits and that the association of two 50 s particles takes place by the apposition of the same faces of each that are apposed to the 30 s particle in the 70 s species. There seems to be an "active" end to the 50 s particles.

The sizes of the particles as measured by this technique are somewhat uncertain, for one does not know how much shrinkage or flattening has taken place during drying. However, the particles found embedded in sheets of PTA over holes in the film always have smaller diameters and higher contrast than those lying on the intact film, so the former are certainly less flattened; also, such particles have dimensions which are very similar to those measured on ribosomes which have been positively stained with unbuffered PTA and then frozen-dried.

The 50 s particles have diameters of 140 to 160 Å when seen individually; the larger subunits in the 70 s particles are slightly asymmetrical and have dimensions

of about 160×130 Å, the shorter dimension lying in the direction of the axis joining the large and small subunits together. As the large subunit appears to be somewhat flattened on the side where it faces the small one, it seems likely that the 50 s particle is somewhat dome-shaped, and that one usually sees an overhead view of it when looking at a 50 s particle, and a side-view in 70 s and 100 s particles. Such a particle would have a volume of $1{\cdot}95 \times 10^6$ Å^3. Alternatively an oblate ellipsoid of dimensions $160 \times 160 \times 130$ Å would have a volume of $1{\cdot}75 \times 10^6$ Å^3. If the partial specific volume of the particles is 0·66 (Tissières & Watson, 1958), and if we ignore any internal hydration, then the molecular weights in the two examples considered would be $1{\cdot}8 \times 10^6$ and $1{\cdot}6 \times 10^6$ respectively. These are of course only very approximate values and we have calculated them merely to show that they are compatible with the value $1{\cdot}85 \times 10^6$ obtained from sedimentation-diffusion measurements by Tissières & Watson (1958). This agreement, however, is only obtained if one assumes that the particles are built up of solidly-packed nucleoprotein, so that the mean density of the nucleoprotein in the whole particle is $1/0{\cdot}66 = 1{\cdot}52$. The fact that the outlines of the ribosomes are less sharply defined by negative stain than those of the small spherical viruses indicates that some penetration of the stain is taking place and suggests that the structure of the ribosomes is less tightly packed at the surface.

The shape of the 30 s particles is more uncertain. When seen uncombined (see Plate IV) they appear as approximate triangles, trapezia or polygons, with a long dimension of 150 to 180 Å; they often have considerably lower contrast than the 50 s particles lying amongst them, and are presumably much thinner. The smaller subunit in the 70 s particle has a width of about 70 Å and a length of 160 to 180 Å, and it seems plausible that this corresponds to an edge-on view of disc-shaped 30 s particles which are seen face-on when they are uncombined. The 30 s particles do however appear more variable in form when they are uncombined than do the other species; perhaps they are less stable, on their own, during the drying process. (The observation that in the absence of formalin fixation the 30 s particles appear to be destroyed by 1% PTA, whereas the 50 s particles are mostly intact, also suggests that the 30 s particles are less stable.) If one approximates to their shape by an oblate ellipsoid $180 \times 180 \times 70$ Å, then their molecular weight, on the same basis as before, would be $\sim 6 \times 10^5$. This is rather low compared with the molecular weight of 9×10^5 found from sedimentation-diffusion measurements by Tissières & Watson (1958). As before, there are considerable uncertainties in the calculation.

As we have already mentioned, there are indications that uranyl acetate often acts as a preferential stain for nucleic acids. If this is also the case in ribosomes, then the observation that there is no cleft visible in the uranyl acetate stained structures in the region of junction of the subunits in the 70 s particle is rather significant. The simplest interpretation would be that the RNA in the two subunits is in close, if not molecular, contact when the two subunits are united, and that there is a lower concentration of protein in the junctional region than elsewhere in the particle, allowing the "negative" stain to penetrate. However, we would not conclude necessarily that it is the RNA which is solely responsible for the affinity between subunits.

Finally, there is the question whether the ribosomes resemble the small spherical viruses in having a nucleic acid core surrounded by a protein shell—perhaps an incomplete one. Such a shell is so easy to demonstrate in the small viruses that we feel that the difficulty of seeing any analogous structure in the ribosomes is significant. If such a shell exists, then it does not provide an effective and clearly defined barrier to the negative stain. In several of the small viruses, the protein shell is built up of

similar subunits arranged in a regular manner, thus giving rise to the very characteristic regular polyhedral form of the virus particles. The microsomal particles appear to be characterized by their much more irregular shape.

We wish to thank Professor B. Katz for the encouragement he has given us. We are indebted to Miss Pamela Dyer for her expert technical assistance at many points of this work, and we are very grateful for the help we received from Mr. A. W. Cooper in the growing of bacteria and preparation of microsomal particles. One of us (G.Z.) acknowledges with appreciation the support of a postdoctoral fellowship from the National Institutes of Health of the United States.

REFERENCES

Brenner, S. & Horne, R. W. (1959). *Biochim. biophys. Acta*, **34**, 103.
Chao, Fu-Chuan (1957). *Arch. Biochem. Biophys.* **70**, 426.
Chao, F. C. & Schachman, H. K. (1956). *Arch. Biochem. Biophys.* **61**, 220.
Farrant, J. L. (1954). *Biochim. biophys. Acta*, **13**, 569.
Hall, C. E. (1955). *J. Biophys. Biochem. Cytol.* **1**, 1.
Huxley, H. E. (1957). *Proc. Stockholm Conference on Electron Microscopy*, 1956, p. 260. Stockholm: Almqvist & Wiksell.
Kellenberger, E., Ryter, A. & Sechaud, J. (1958). *J. Biophys. Biochem. Cytol.* **4**, 671.
McQuillen, K., Roberts, R. B. & Britten, R. J. (1959). *Proc. Nat. Acad. Sci., Wash.* **45**, 1437.
Palade, G. & Siekevitz, P. (1956). *J. Biophys. Biochem. Cytol.* **2**, 171, 671.
Petermann, M. L. & Hamilton, M. G. (1957). *J. Biol. Chem.* **224**, 725.
Schachman, H. K., Pardee, A. B. & Stanier, R. Y. (1952). *Arch. Biochem. Biophys.* **38**, 245.
Tissières, A. & Watson, J. D. (1958). *Nature*, **182**, 778.
T'so, P. O. P., Bonner, J. & Vinograd, J. (1956). *J. Biophys. Biochem. Cytol.* **2**, 451.
Watson, M. L. (1958). *J. Biophys. Biochem. Cytol.* **4**, 475.

J. Mol. Biol. (1960), **2**, 19-37

The Molecular Configuration of Deoxyribonucleic Acid

I. X-ray Diffraction Study of a Crystalline Form of the Lithium Salt

R. Langridge and H. R. Wilson

Wheatstone Laboratory, King's College, London, England

C. W. Hooper and M. H. F. Wilkins

Medical Research Council Biophysics Research Unit, King's College, London, England

L. D. Hamilton

Sloan-Kettering Institute, New York, U.S.A.

(*Received 26 January 1960*)

Fibres of the alkali metal salts of deoxyribonucleic acid (DNA) give a variety of X-ray diffraction patterns. The type of pattern is largely determined by the metal and the relative humidity around the fibre. An analysis has been made of the oriented crystalline pattern given by fibres of the lithium salt (LiDNA) at 66% relative humidity. The general form of the pattern is the same as that given by the sodium salt (NaDNA) at 92% relative humidity. From this form it may be deduced that the DNA molecule is helical with pitch 34 Å, probably contains two polynucleotide chains, and that each chain contains 10 nucleotides per turn. This configuration is known as the *B* type and exists in unfixed cell nuclei. The crystal lattice of LiDNA is orthorhombic and each unit cell contains one repeat unit of two DNA molecules. With the aid of a well-collimated X-ray beam, overlap of X-ray reflections has been minimised and 3-dimensional diffraction intensity data (90 reflections) have been obtained. Details are given of experimental technique, e.g. making DNA fibres, X-ray camera design, measurement of position and intensity of X-ray reflections, and preparation of LiDNA.

1. Introduction

Many recent findings show that deoxyribonucleic acid (DNA) transmits hereditary characteristics, and many studies have been made of its properties and structure with a view to understanding how it performs its biological function. These investigations culminated in the derivation of the chemical structure and molecular configuration of DNA, and the complementary nature of the configuration led Watson & Crick (1953) to their idea of how DNA replicates. This idea, now fairly well established (Meselson & Stahl, 1958; Levinthal & Thomas, 1957; Bessman *et al.*, 1958), is the first major contribution of three-dimensional structural chemistry to the understanding of biological phenomena. The present papers (Parts I and II) describe an X-ray diffraction study of the DNA molecule. As an introduction we shall briefly recount how ideas about the structure of DNA developed and describe the contribution of X-ray diffraction.

Chemical research showed that DNA consists of nucleotides joined together in a polymer chain, and the high viscosity and flow birefringence of solutions of DNA (Signer, Caspersson & Hammersten, 1938) indicated that the molecule was long and thin. Ultraviolet dichroism (Caspersson, 1940) and birefringence of DNA showed the

planes of the nitrogen bases were roughly at right angles to the length of the molecule, and X-ray diffraction photographs of fibres of DNA led Astbury (1947) to suggest that the bases were stacked 3·4 Å apart like a "pile of pennies." It was also clear from the photographs that the molecule had longer periodicities along its length. The idea that the bases in DNA were joined by hydrogen bonds between the NH_2 and C=O groups was derived by Gulland & Jordan (1947) from electrometric titration data; and, combining these results with viscosity data, they suggested that DNA consisted of polynucleotide chains joined in groups by the hydrogen bonds between bases (Gulland, 1947). Improved preparations of DNA were made by Signer & Schwander (1949); and Riley & Oster (1951) took X-ray diffraction photographs of this material unoriented and observed that when the water content of the specimen was varied there was a transition between a crystalline and a semi-crystalline form. Using fibres of this material in a moist atmosphere, Wilkins, Gosling & Seeds (1951) obtained well-oriented and sharp diffraction patterns. The form of this two-dimensional pattern suggested that the DNA molecule had a helical configuration; this led A. R. Stokes (unpublished) to calculate the diffraction pattern given by helical structures. The solution was also derived by Cochran, Crick & Vand (1952) for the study of helical polypeptides.

Molecular model building of DNA was stimulated by the success of the technique in elucidating the structure of proteins, by the defining of the covalent bonds in the polynucleotide chain (Brown & Todd, 1952), and by the derivation of the configuration of a nucleoside (Furberg, 1950). Pauling & Corey (1953) and R. D. B. Fraser (unpublished) built 3-chain helical models of DNA but these did not agree with the X-ray data. In Fraser's model, which represented the state of thought in our laboratory at that time, right-handed helical chains were intertwined and linked by hydrogen-bonded bases 3·4 Å apart lying perpendicular to the helix axis; the phosphate groups were on the outside of the molecule as suggested by Franklin & Gosling (1953*a*). The hydrogen-bonding scheme was incompletely defined and but vaguely foreshadowed the specific pairing scheme of Watson & Crick. It was clear that the regular structure observed in DNA was due to regular arrangement of the sugar and phosphate parts of the molecule; but the problem of how to fit the bases of various sizes in a complicated sequence and in varying proportions inside the structure was unsolved. Meanwhile, improved X-ray data were obtained by Franklin & Gosling (1953*a*) from Signer DNA. By varying the humidity around DNA fibres they observed the transition between a well defined and oriented crystalline pattern and a semi-crystalline pattern. The two patterns corresponded to different configurations of the DNA molecule, one called *A*, the other *B*. Franklin & Gosling derived the lattice for the crystalline *A* structure and obtained 3-dimensional diffraction data. They attempted a direct solution of the structure by Patterson methods (Franklin & Gosling, 1955). An apparent lack of symmetry in the 3-dimensional data led them to believe the DNA molecule might not be helical, and, as a result of this uncertainty about the basic structural hypothesis, our model-building was postponed. The *B* configuration was also observed in DNA of varying composition, prepared from widely different sources (Wilkins, Stokes & Wilson, 1953). The structure was found to exist in cells (Wilkins & Randall, 1953) and was therefore of direct biological interest.

Chemical analyses (Chargaff, 1950) then provided an important clue in deriving the structure. Although the base composition of DNA varied widely in different species, certain bases were always present in equal numbers. This suggested some kind of pairing (Wyatt & Cohen, 1953).

The general nature of our results had been made known to Drs. Watson & Crick. They believed, in spite of the confusion concerning the interpretation of the X-ray data, that the molecule was helical and made molecular models with the general form and dimensions suggested by the X-ray data (Crick & Watson, 1954). They arrived at a model in which two polynucleotide chains were joined by hydrogen bonds between pairs of bases and which was therefore in agreement with the chemical data. This model, built independently of the Fraser model, was a great advance on it because different pairs of bases were the same size and it was possible therefore to fit bases of various sizes, in pairs, into a regular structure. The key features of the model were the two chains with atomic sequences in opposite directions and the specific pairing of bases and, since the latter was precisely defined, it became possible to attempt detailed correlation of X-ray data and molecular models. It was shown that there was no inconsistency between a helical hypothesis and the 3-dimensional data of the *A* pattern (Wilkins, Stokes, Wilson & Seeds, 1953; Franklin & Gosling, 1953*b*). Promising agreement was then obtained between the model and the 2-dimensional data of the *B* pattern after the model had been suitably adjusted (Feughelman *et al.*, 1955; Wyckoff, 1955). We then found that the lithium salt of DNA (LiDNA) in the *B* configuration gave a crystalline pattern with 3-dimensional data. We decided to concentrate on this structure rather than on the *A*, because the *B* configuration existed *in vivo* and the *A* did not, and because the sodium ions in the *A* structure complicated the analysis—they scattered X-rays appreciably and their position was uncertain whereas lithium ions scattered more weakly and could be ignored.

A preliminary account of the correlation of molecular models of the *B* and *A* configuration with X-ray data has been given (Langridge *et al.*, 1957). More sharply defined X-ray photographs are now being obtained and will enable the correlation of model and X-ray data to be extended quantitatively in three dimensions. Since work is slow, it seems worth publishing our results at the present stage; and since little detail has been published on the production of high resolution fibre diagrams and their quantitative analysis, we give our account in some detail. We describe our experimental results in Part I and the correlation of these results with molecular models in Part II.

This work establishes fairly precisely the configuration of the DNA molecule. The information on the *B* configuration is detailed and, even if we study it alone, it does not seem likely that agreement between data and model is fortuitous, i.e. that a structure of some other kind might also correlate with the data. Moreover we can correlate models and data for the *A* configuration (Langridge *et. al.*, 1957) and the *C* configuration (Marvin, Spencer, Wilkins & Hamilton, 1958) as well as for *B*, and this greatly reduces the possibility that suitable molecular models might be built embodying a stereochemical hypothesis (e.g. Donohue, 1956) other than the base-pairing scheme of Watson & Crick.

Important evidence in favour of the Watson-Crick pairing is also given by observations (Bessman *et al.*, 1958) on the synthesis of DNA. These results are not compatible with the base-pairing hypothesis of Donohue (1956). Evidence for the pairing is also given by the observation that a DNA-like structure is produced by combining poly-ribo-uridylic and -adenylic acids (Rich & Davies, 1956).

2. The General Nature of X-Ray Diffraction from DNA Fibres

A variety of diffraction patterns may be obtained from fibres of DNA. These show that the helical DNA molecule may extend or twist in various ways, and that several different crystalline and semi-crystalline forms exist (Table 1).

TABLE 1

Various structures of DNA in fibres

Configuration of molecule	Number of nucleotide pairs per turn of helix	Inclination of base pairs in molecule	Salt	Relative humidity and condition necessary	Lattice	Crystallinity	Equivalent positions	Unit cell dimensions			
								a	*b*	*c*	*β*
A	11·0	20°	Na, K, Rb	75%	monoclinic	crystalline	0, 0, 0 $\frac{1}{2}$, $\frac{1}{2}$, 0	22·07 Å	40·4 Å.	28·1 Å	97·1°
B	10	0°	Li	66%	orthorhombic	crystalline	0, 0, $\frac{1}{6}$ $\frac{1}{2}$, $\frac{1}{2}$, $-\frac{1}{6}$	22·7	31·2	33·7	
			Li	75 to 90%	orthorhombic	semi-crystalline	0, 0, $\frac{1}{8}$ $\frac{1}{2}$, $\frac{1}{2}$, $-\frac{1}{8}$	24·4	38·5	33·6	
			Li, Na, K, Rb	92%	hexagonal	semi-crystalline	0, 0, 0 $\frac{1}{3}$, $\frac{2}{3}$, $\frac{1}{6}$ $\frac{2}{3}$, $\frac{1}{3}$, $-\frac{1}{8}$	46		34·6	
B_2	9·9	0°?	Na	75% under tension	tetragonal	semi-crystalline	0, 0, 0 $\frac{1}{2}$, $\frac{1}{2}$, $\frac{1}{4}$	27·4		33·8	
C	9·3	− 5°	Li	44%	orthorhombic	semi-crystalline	0, 0, $\frac{1}{8}$ $\frac{1}{2}$, $\frac{1}{2}$, $-\frac{1}{8}$	20·1	31·9	30·9	
			Li	44% in some specimens only	hexagonal	semi-crystalline	0, 0, 0 or $\frac{1}{2}$ $\frac{1}{3}$, $\frac{2}{3}$, $\frac{1}{6}$ or $-\frac{1}{3}$ $\frac{2}{3}$, $\frac{1}{3}$, $-\frac{1}{6}$ or $\frac{1}{3}$	35·0		30·9	

PLATE I. X-ray diffraction patterns given by different salts of DNA at 92% relative humidity. One quarter of each pattern is shown: (a) is lithium salt; (b) sodium; (c) potassium; (d) rubidium.

[*To face page* 22

In the present work we are concerned with the crystalline form of the lithium salt of DNA (LiDNA) (Langridge *et al.*, 1957).

The diffraction pattern given by LiDNA changes with humidity, but in many specimens the molecules remain in the *B* configuration (Franklin & Gosling, 1953*a*; Feughelman *et al.*, 1955) and change little between 92% and 60% relative humidity, although their position in relation to one another in the crystallites alters. At lower humidities the molecules adopt the *C* configuration (Marvin *et al.*, 1958). In no case has the *A* configuration (Franklin & Gosling, 1953*a*; Wilkins, Seeds, Stokes & Wilson, 1953) been observed for LiDNA. With all specimens the diffraction pattern (Plate I) at 92% relative humidity is indistinguishable from that given by NaDNA. Most good preparations of LiDNA give a well defined crystalline diffraction pattern (Plate II) at humidities from about 47 to 75%; the sharpest pictures are obtained in the region of 66%.

The diffuse photographs (Plate I) obtained from semi-crystalline DNA give a clear impression of the scattering factor of the DNA molecule in the *B* configuration and enable us to deduce the general form of the molecule (Wilkins *et al.*, 1953; Franklin & Gosling, 1953*c*). It resembles a double spiral staircase with each step a nucleotide. On the photograph there is a large meridional region free of strong diffraction; this is so because a helix has uniform density when projected on its axis. The strong intensity near the meridian on the 10th layer line reveals the step-like structure of the helix and shows that the nucleotides are 3·4 Å apart along the axis. Regions of strong intensity form a cross pattern at the centre of the picture (see Plate I); this pattern is not a marked characteristic of all helical structures but occurs when the repeat unit is rod-shaped and, like a step on the spiral staircase, lies perpendicular to the axis and in a plane with it. If the steps merge into each other they form a continuous surface, and reflection of X-rays from this surface concentrates diffraction into the cross pattern. The arms of the cross make an angle with the axis equal to the average angle of ascent of the helix.

The whole pattern is divided into layer lines, the spacing of which corresponds to the pitch of the helix. This length, 34 Å, is ten times the internucleotide spacing; therefore, we know that there are ten nucleotides per turn of each helical chain. The general intensities of the various layer lines differ considerably. A marked alternation—weak, strong, weak—occurs on the first, second and third layer lines and on the seventh, eighth and ninth; this suggests there are two helical chains in the molecule, intertwined about the axis and displaced relative to one another about half a pitch length along the axis. A rough estimate of the diameter of the molecule may be obtained from the equatorial spacings and also from the pitch length and angle of ascent of the helix.

The pattern shown in Plate II consists of sharp spots corresponding to spacings from about 20 to 3 Å. The crystallites are quite well aligned in the fibre and possess a fair degree of internal regularity. We have not been able to obtain single crystals, and double orientation has only been found in fibres containing the *A* structure. Many reflections in the fibre diagram overlap and to try to separate them we can do no more than use a well-collimated X-ray beam and seek specimens that give sharp reflections.

3. Experimental Method

(a) *Preparation of specimens for the X-ray camera*

The original DNA preparation was a solid lump or a mass of tangled fibres a few μ in diameter. These fibres gave poorly-oriented X-ray pictures. In most of our work we used

fibres 50 to 100 μ in diameter (Wilkins *et al.*, 1951), made by wetting with a droplet of glass-distilled water a few mg of DNA on a glass slide, dipping a pointed glass rod into the sticky and very stiff mass, and slowly withdrawing it. The coarse focusing adjustment on a microscope gave a good motion for drawing fibres, and during drawing the fibres were observed through a $\times 5$ magnifier. Quick withdrawal from wet gel gave thin fibres; less wet gel and slower motion gave thicker fibres. Some specimens of DNA gave fibres of almost unlimited length, others of only a few centimetres, and degraded samples gave fibres only with much difficulty. Some fibres were of uniform diameter and gave good extinction when viewed between crossed nicols in a polarising microscope. Such optical homogeneity in a fibre often correlated with a high degree of orientation of the molecules parallel to the fibre length. However, this need not be so; any degree of orientation of molecules or submicroscopic crystallites, provided it is uniform, will give a fibre with good extinction. Poor extinction shows that regions of the fibre of size comparable with or greater than the wavelength of light have extinction directions inclined to one another. Use of fibres with non-uniform diameter or poor extinction was avoided.

It is almost certain that parallelism of the molecules in a fibre is produced by shearing in the material during fibre-drawing. Some specimens of DNA swell in water but do not dissolve quickly, presumably because of cross-linking or tangling of molecules. Such material may be drawn into fibres that stretch like rubber while moist, and which give poor X-ray pictures, presumably because the molecules could not slide freely past one another during fibre drawing and thus arrange themselves regularly.

When a micro-camera was used, a single fibre of diameter 50 to 100 μ was cemented with quick-drying Le Page's number 29 cement to a small holder or to the collimator itself. In larger cameras, fibres were mounted on a holder (see Fig. 1) and kept in tension by a phosphor-bronze spring designed so that the fibre did not move at right angles to its length when stretching. Several fibres (even 10 or more of about 50 μ diameter) could be mounted parallel under a binocular dissecting microscope, with the aid of watchmaker's tweezers and slow-setting cement (Hooper, 1957) containing xylene as a solvent. To set the axis of the fibres at a known angle to the X-ray beam, the holder was arranged to rotate about an axis at right angles to the fibre axis. The fibres were then viewed in a polarising microscope and, with the eyepiece crosswire and rotating stage, the angle was set within 1°.

Absorption of X-rays in the specimen did not create difficulty in obtaining diffracted intensities. The reciprocals of the absorption coefficients for LiDNA at 66 and 91% relative humidity are about 600 and 800 μ. To obtain well exposed photographs, specimens consisting of several fibres and of 200 to 400 μ thickness were used, but intensities from such photographs were checked against those obtained from a single fibre of diameter 100 μ or less and for which the effects of absorption were negligible (Bradley, 1935).

When a series of photographs was taken of a specimen we sometimes found that after a total of 2 or 3 weeks' exposure to X-rays the photograph then taken was little inferior to that first taken. However, when a very long exposure was used to obtain a specially well-defined photograph, the specimen was moved along its length once a week so that a new portion of the specimen was brought into the beam and possibility of the specimen deteriorating was reduced.

(b) *X-ray set and its operation*

To obtain sharply defined X-ray photographs we used small pinholes in the cameras, and as a result the X-ray beam was weak and exposure times inconveniently long. The maximum electron current per unit area of anode increases as the area of the focus decreases (Ehrenberg & Spear, 1951) and therefore flux through the collimator is a maximum when the area of anode from which X-rays may pass to the specimen is about equal to that of the electron focus. Our requirements were well met by the Hilger & Watts semi-micro focus X-ray unit based on the design of Ehrenberg & Spear (1951). With filament horizontal, our measurements gave 0·075 mm for the vertical half-width of the focal spot; and for the beam direction inclined 5° to the anode surface, the horizontal width was about 0·10 mm. The voltage reading on the set corresponded to about 40 kv (direct current) across the tube. We did not use higher voltage because the ratio of white radiation of wavelength about 0·05 Å to the Cu Kα became too high. The anode was cleaned once a

week because "cracking" of diffusion-pump oil produced a deposit on the anode and this deposit increased the proportion of white radiation. The deposit was reduced when we changed from Edwards 703 silicone oil to Apiezon C. Filament life was about three weeks: to obtain such a life it was necessary to ensure that the vacuum was good and the filament heater current was kept low so that the tube current was $\sim 0{\cdot}05$ mA below the saturation value. Sets were operated continuously day and night.

(c) *The X-ray cameras*

For preliminary study of a DNA preparation, microcameras similar to those designed by Chesley (1947) were used, with lead-glass capillaries (kindly supplied by Dr. H. P. Rooksby) about 100 μ diameter and 10 to 13 mm long to collimate the X-ray beam. Specimen-to-film distance was 15 to 25 mm, and single-coated Kodak "Fluordak blue sensitive" film was used.

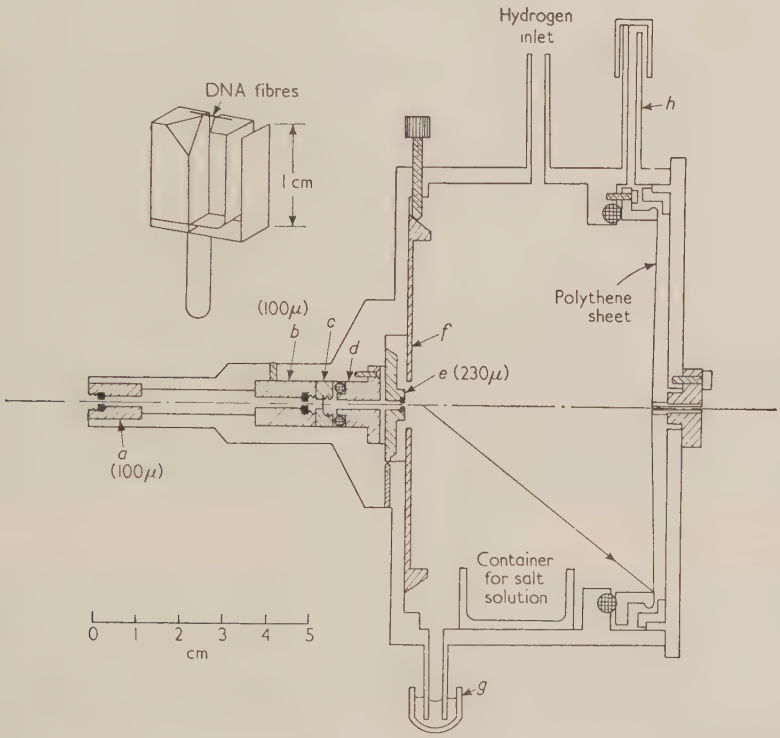

FIG. 1. Scale drawing of X-ray camera for spacings up to 100Å. The parts *a*, *b* and *c* carry the first collimating pinhole, second pinhole, and mica sheet, and are threaded so that they can be extracted with a screw. There is an O ring seal between *c* and *d*. Phosphor-bronze springs secure *e* (which holds the guard pinhole) and the specimen holder *f*. Liquid paraffin is placed in the glass tube *g* and enables one to check that there is a small excess pressure in the camera. *h* is one of two tubes allowing hydrogen which might leak into the film-containing compartment to escape. The inset shows the holder for DNA fibres.

Our main interest was to obtain photographs of the highest resolution. To do this we used cameras in which the X-rays were collimated by two pinholes 70 to 120 μ diameter drilled in lead and 4 to 6 cm apart. Specimen-to-film distance was 5 to 8 cm and large compared with specimen thickness ($\sim 0{\cdot}2$ mm). A guard pinhole was placed between specimen and collimator to intercept X-rays scattered at low angles from the second collimating pinhole and diffracted from the crystalline lead. For a given degree of collimation the specimen received maximum irradiation when the specimen and guard pinhole were placed as close as possible to the collimator. If the second collimating pinhole and the

guard were mounted together 6 mm apart in a brass tube, they could be drilled in-line in a collet in a watchmaker's lathe. With care the guard pinhole could be made sufficiently small to cut off scattered radiation from the whole DNA pattern, i.e. up to 30 Å spacing. To study spacings up to $\sim$ 100 Å it was necessary to place the guard $\sim$ 2 cm from the second pinhole. The guard pinhole was about 30 μ greater in diameter than the X-ray beam passing through it and was centred in relation to the beam by adjusting screws. This design of camera is shown in Fig. 1.

Pinholes were drilled in lead (1 mm thick for the collimator and 0·5 mm for the guard) on a watchmaker's lathe with a twist or spade-type drill mounted in the tail stock. Frequently a 100 μ drill (Muller & Co., Cleobury Mortimer, Kidderminster) was used, but the 100 μ part was only 0·7 mm long joined by a conical part to a 1 mm shank. The cone was pressed through the lead until the drill emerged on the other side and the hole was inspected with a microscope to check that it was free of lead shavings. Quite thin lead would absorb Cu Kα radiation, but 1 mm thickness was used in the collimator to prevent traces of short-wavelength white radiation penetrating the camera during very long exposures.

Sometimes pinholes became clogged with crystals, presumably from droplets of salt solution carried over in the moist hydrogen used to fill the camera. To avoid this, we placed a mica sheet about 5 μ thick between the collimator and the guard pinhole so that gas could not escape through the collimator. Diffraction from the mica was intercepted by the guard. The specimen was aligned by viewing it with a low-power microscope and shining light through the collimator. Fogging of the film was noticeable for exposures of more than one week with relative humidity 75% or above, and at 98% relative humidity the black paper covering the film often stuck to it. To avoid this we used polythene sheet (30 μ thick) to separate the film from the part of the camera containing the specimen. The polythene was sealed with a rubber band and Bostik 252 adhesive to a brass ring fitted to the camera by an O ring seal. Diffraction from the polythene was prevented from falling on the photographic film by a brass tube that fitted into a hole punched in the film and pressed against the polythene sheet.

The direct X-ray beam passed through the hole in the film, and measurement of the beam with a Geiger counter was most useful in aligning the cameras with the X-ray tube and for testing the focus and output of the tube. To bring the cameras into alignment with the small area on the anode emitting X-rays, they were mounted on kinematic slides on a steel girder firmly bolted to the vacuum connection supporting the X-ray tube.

(d) *Humidity control*

Hydrogen was passed through the camera to prevent the centre of the X-ray photograph being darkened by X-rays scattered by air. The water content of the specimen was controlled by bubbling the hydrogen through a sintered-glass filter immersed in a saturated salt solution. The dry hydrogen from the cylinder was passed through water to avoid clogging the filter with crystals, and a small trap caught drops of liquid that might be blown into the camera. We placed in the camera a vessel containing a large area of saturated salt solution. The humidity-controlling apparatus was suspended close to the X-ray camera in order that the difference of temperature between the salt solution and specimen was a minimum. We chose salts for which the relative humidity changed little with temperature. We were more concerned with obtaining constant and reproducible humidity conditions than with the reliability of the humidity value for a given salt. We used potassium carbonate, sodium nitrite, chlorate and tartrate for 44, 66, 75 and 92% relative humidities respectively.

(e) *Photographic technique*

In most work with the larger cameras we used Ilford Industrial G film. Later we changed to Ilfex film, because it was the custom of the manufacturer to coat the film only a few weeks before delivery and as a result it gave a minimum of chemical fog. Photographic processing was designed to minimize distortion of the film, shrinkage or swelling of the DNA picture relative to the calibration photograph of the calcite 3·029 Å ring, and variation in the relation between optical density of film and exposure to X-rays. Film was processed throughout at constant temperatures ($\sim$ 20°C). It was presoaked in water, developed for

7 min in Kodak D19 B developer with agitation, rinsed, fixed for 15 min, and washed in several changes of water for only 30 min to reduce uptake of water by the film base.

We measured the optical density of the photographic film for a range of exposures to Cu Kα X-rays monochromatised by reflection from a lithium fluoride crystal. The relation between optical density and exposure agreed with that published later by the Commission on Crystallographic Apparatus (1956). For Ilfex & Industrial G film the ratio of density to exposure is constant for density up to 1·0 but appears to decrease gradually for higher values. The densitometer traces across strong spots on our X-ray pictures sometimes record peak values of density as high as 2, but if we make the approximation that X-ray intensity is proportional to optical density, our results for integrated intensity should not have been more than 10% low. We also used two films, one over the other, in the X-ray cameras and by measuring the ratio (about 3 : 1) of the densities of the two films reduced our errors.

(f) *Measurement of the lattice and indexing of spots*

When we had taken a photograph and wished to calibrate it, we left the specimen in place in the camera, lightly dusted it with calcite powder, and then took another photograph using the same batch of film. The two films were allowed to dry slowly at room temperature for 24 hr, and then photographic enlargements (about 4 times) were made on 12×15 in plates with a cold-cathode lamp and a Taylor, Taylor & Hobson Aviar Series II lens. A Hilger glass graticule of equally spaced lines at right angles, accurate to 1 part in 15,000, was used to measure enlargement and check distortion. By adjusting the enlarger easel, enlargement was made uniform to about 0·3 parts in 1000; shrinkage of the film is, according to the makers, about the same.

The diffraction photograph was taken on flat film. Positions of spots near the centre of the pattern were used to fix the centre. The distance of all spots from the centre was then measured. When spots in opposite quadrants were almost diametrically opposite each other, the distance between them was measured. If the film was not perpendicular to the X-ray beam, the centre of the pattern with respect to spots at different radii was different, and the measurements needed correction. Graininess of the X-ray film restricts accuracy of measurements, but this approaches 0·1% for outer spots and was sufficient to enable all spots to be indexed unambiguously (see Fig. 2), except for some spots on the 10th, 11th and 13th layer lines, and where spots overlapped very completely.

(g) *Measurement of intensities*

The diffraction photograph of the fibre resembles a single-crystal rotation photograph except that disorientation of the crystallites causes the spots to be drawn into arcs of circles with centre at the centre of the photograph. The angular length of the arcs is constant after allowance is made for lack of collimation of the X-ray beam and oblique intersection of the reflecting sphere. We used a recording densitometer (Walker, 1955) and measured the variation of optical density on the photograph along a radius passing through the centre of each spot. On these traces (see Fig. 3) the half-widths of the spots increases with diffraction angle partly because specimen thickness was appreciable compared with specimen-to-film distance. The size of the spots was also due in part to the crystallites in the fibre being imperfect or of a size comparable with the wavelength of the X-rays. The area under the trace across each spot, measured with a planimeter, was taken as a measure of the intensity of reflection, after correction (Franklin & Gosling, 1953*d*) had been made.

One of the greatest difficulties in measuring intensities accurately is the uncertain position of the base-line that limits the area to be measured under the trace across a spot (see Fig. 3). However, in photographs with fairly sharp spots, the base-line may be determined fairly accurately by measuring the background density between spots where they are clearly separated. The background density increases steadily towards the centre of the picture. The other important factor limiting accuracy is overlap of spots; this is much more noticeable on densitometer traces than on the picture itself.

Allowance can be made for overlap if the distance between spots is measured and if the shape of the trace for each spot separately is assumed (see Fig. 3). This shape can be measured on adjacent spots where overlap does not occur, and in many photographs

appears to be the same for all spots, except that the half-width increases with diffraction angle. We checked the position of the base-line by taking traces along a layer line and along lines half-way between the layer lines. When the length of the arc forming the spot is inclined to the layer line by an angle ϕ, the trace can be adjusted to pass

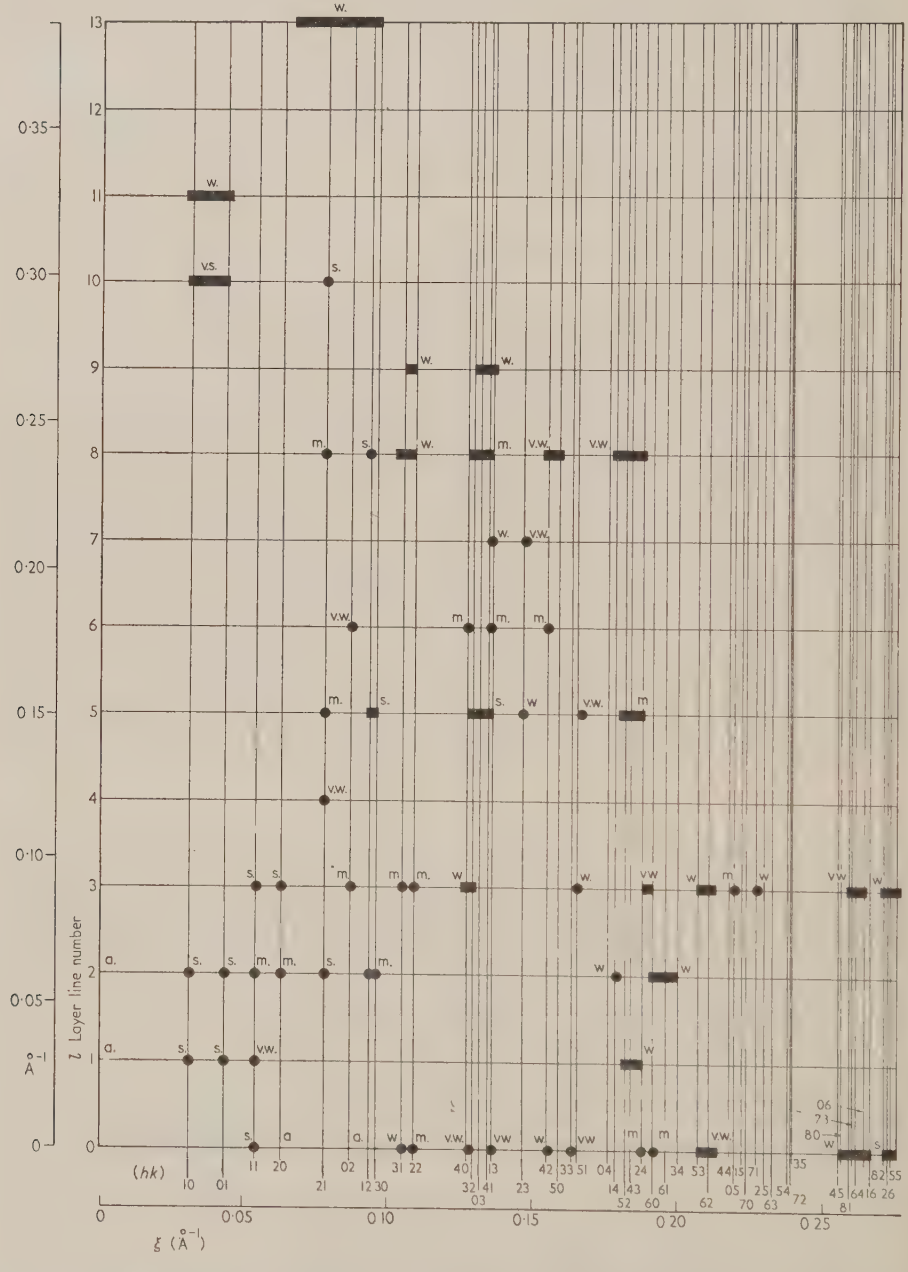

FIG. 2. Diagram in reciprocal space of the diffraction pattern obtained from fibres of LiDNA. Spots labelled s., strong; m., medium; w., weak; v.w., very weak; a., absent.

through the maximum density of the spot. If the width s of the spot is small compared with the arc length l, the area under the trace should be $1/\sin\phi$ times that obtained from a radial trace. When s is comparable with l the ratio of the areas is less than $1/\sin\phi$,

and the maximum heights of the radial and layer line traces may be compared but not the areas.

Graininess of the film makes the densitometer traces irregular but the curve can be made smoother by passing light into the instrument through as large an area of the film as possible. On the other hand, this area must not be so large that the density in different parts of it is very different, for if this is so the trace may not give a reasonably accurate measure of how the optical density varies across the film. In practice, an image of a slit

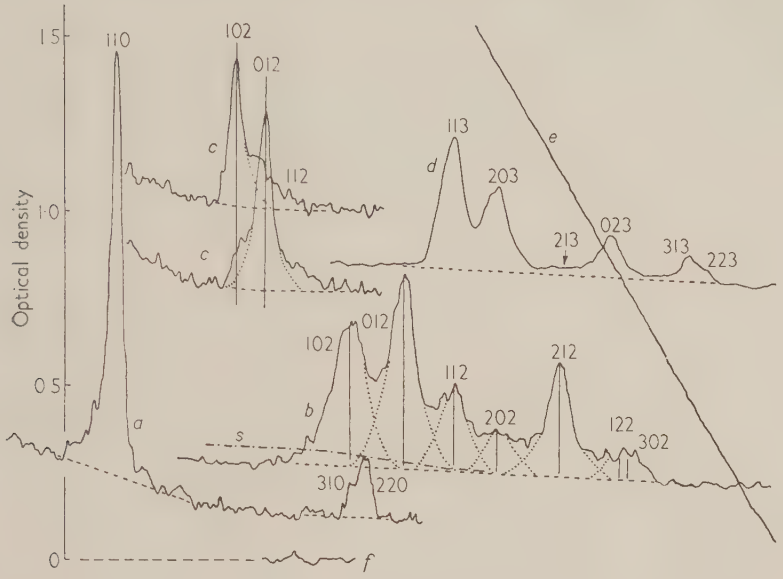

Fig. 3. Examples of densitometer traces.

(a) Central part of the equator showing the strongest spot 110 (peak density 1·5), and the background intensity increasing towards the centre of the photograph. The optical density scale is correct for curves *a* and *e*; the other curves are displaced relative to the scale.

(b) Trace along the second layer line with length of slit parallel to spot 012. The overlap between spots is greater than for most parts of the photograph. The observed intensity can be accounted for in terms of the spots, and the estimated contours of these are shown. There is therefore little sign that a streak (see Plate III) exists along the layer line and is superimposed on the spots. The trace halfway between the 2nd and 3rd layer lines coincides with the base-line shown, but, towards the centre of the picture (on the left), increasing background intensity causes the trace *s* halfway between the 1st and 2nd layer lines to rise above the base line.

(c) Radial traces across the maxima of the spots 102 and 012 on the 2nd layer line. Overlap of the spots is allowed for by marking the positions of the spots and estimating the contribution of each spot individually. It is assumed that the contour of a given spot has the same form but a different height on both traces.

(d) Trace along the third layer line. The intensity of the 213 spot, which may be present at the position indicated by the arrow, is not more than one-tenth that of the adjacent 203 spot.

(e) Calibration trace along a linear density wedge.

(f) Trace along clear film.

as traversed across the spots, the length of the slit lying along the arc length. The length and width of the slit were such that if they were increased by about 50% the shape of the trace was only slightly distorted. Larger slits were used for the outer part of the X-ray picture, and all four quadrants of the photograph were measured. Inaccuracy was greatest in the central part of the picture where background density was varying fairly rapidly; where faint spots were measured adjacent to strong ones; and where spots were so faint as not to be clearly defined against the background of fluctuating density due to graininess. The intensity of very faint spots was in most cases estimated by eye by comparing the appearance of the spot on the top film with that of spots of known intensity which had the same appearance on the under film.

(h) *Measurement of density and water content of DNA*

The density of DNA was measured by flotation in liquids similar to those used for protein crystals (Low & Richards, 1952). A concentrated gel of DNA in water was centrifuged to remove air bubbles and divided into parts so that, after drying, roughly spherical lumps of about 1 mm diameter were obtained. The lumps were equilibrated at the required relative humidity at 22°C in open weighing bottles for 1 to 2 weeks. The bottles were then closed in the humidity chamber and afterwards inverted and reopened in the laboratory atmosphere so that a lump dropped, in an instant, from the bottle into a mixture of benzyl chloride and bromide. The proportions of the mixture were then adjusted until the lump neither floated nor sank. Rapid and final adjustment of the mixture was made using a fresh DNA lump, and as a result errors in the density measurement, due to dehydration of the DNA or chemical reaction with the liquid, were minimised. Water contents of DNA lumps were measured in parallel experiments. To obtain dry weights, the DNA was kept over P_2O_5 for a week or more at room temperature and then dried at 110°C for 12 hr *in vacuo*.

(i) *Extraction of DNA*

In early work we used sodium dodecyl sulphate (SDS) to remove protein from DNA (Marko & Butler, 1951; Kay, Simmons & Dounce, 1952). The method of Kay *et al.* was modified as follows:

Calf thymus glands are frozen in solid CO_2 within 10 min of slaughtering, stored at − 75°C for not more than 2 weeks, and processed throughout at 4°C. LiCl replaces NaCl. The volume of 0·15 M-LiCl and of SDS in which the first deproteinization is done is halved. The protein-detergent complex is removed at 20,000 rev/min for 1 hr in the 21 rotor (40,000 *g*) in the Spinco model L ultracentrifuge, and by filtering through several layers of gauze or suction-filtering through "Super-Cel" previously sedimented several times from large volumes of water in order to remove very fine particles. To avoid denaturation impure DNA is redissolved in 5/7 of the recommended volume of 0·01 M-salt solution, and not in water. A correspondingly reduced amount of detergent is added. The centrifugation at 20,000 rev/min and filtration are repeated.

The DNA is given two extra repurifications by dissolving in 0·01 M-LiCl (2 mg DNA/ml.), adding LiCl to make 0·14 M, centrifuging in Spinco model L for 30 min at 17,500 rev/min in the 30 rotor (26,000 *g*), adding LiCl to supernatant until 1 M and precipitating.

For most LiDNA preparations, protein was removed from the DNA by sodium xylene sulphonate as suggested by Simmons, Chevas & Orbach (1952) but in a somewhat modified way.

The process used for calf thymus was carried out at 4°C in containers covered to exclude dust.

Chop 50 g frozen thymus into cm cubes, remove obvious connective tissue and fat, and extract 5 times with 200 ml. ice-cold solution of 0·15 M-LiCl, 0·1 M-lithium citrate and 0·01 M-Li ethylenediaminetetra-acetate (EDTA) by homogenizing in a Waring blender for 3 min. centrifuging for 20 min at 0°C at 2000 rev/min in a Servall refrigerated centrifuge and discarding supernatant.

Homogenize nuclear sediment for 1 min in 250 ml. ice-cold solution of 1·5 M-LiCl—0·01 M-lithium citrate and stir in flask for 1 hr. Add 500 ml. 15% (w/v) solution of sodium xylene sulphonate and stir for $\frac{1}{2}$ hr.

Remove protein-detergent complex at 20,000 rev/min for 2 hr in 21 rotor in Spinco model L ultracentrifuge and by repeated suction-filtration through sedimented Celite on M-porosity sintered glass funnels until clear in strong light beam.

Precipitate lithium nucleate in flask by adding, while vigorously stirring, up to 0·5 vol of cold 98 to 99% redistilled *iso*propyl alcohol. Collect precipitate with stirrer or by centrifuging for 20 min at 2000 rev/min in Servall refrigerated centrifuge. Homogenize nucleate in 250 ml. 0·01 M-LiCl for 30 sec in blender, transfer to flask, and allow to dissolve. Add lithium acetate until 0·3 M and precipitate DNA by adding between 0·5 and 1·0 vol of *iso*propyl alcohol. Reprecipitate 3 times as above.

Dissolve DNA in 0·01 M-LiCl (approximately 1 to 2 mg DNA/ml.) in flask. Add sodium xylene sulphonate until 10% (w/v) and stir for 1 hr. Filter through sedimented Celite on

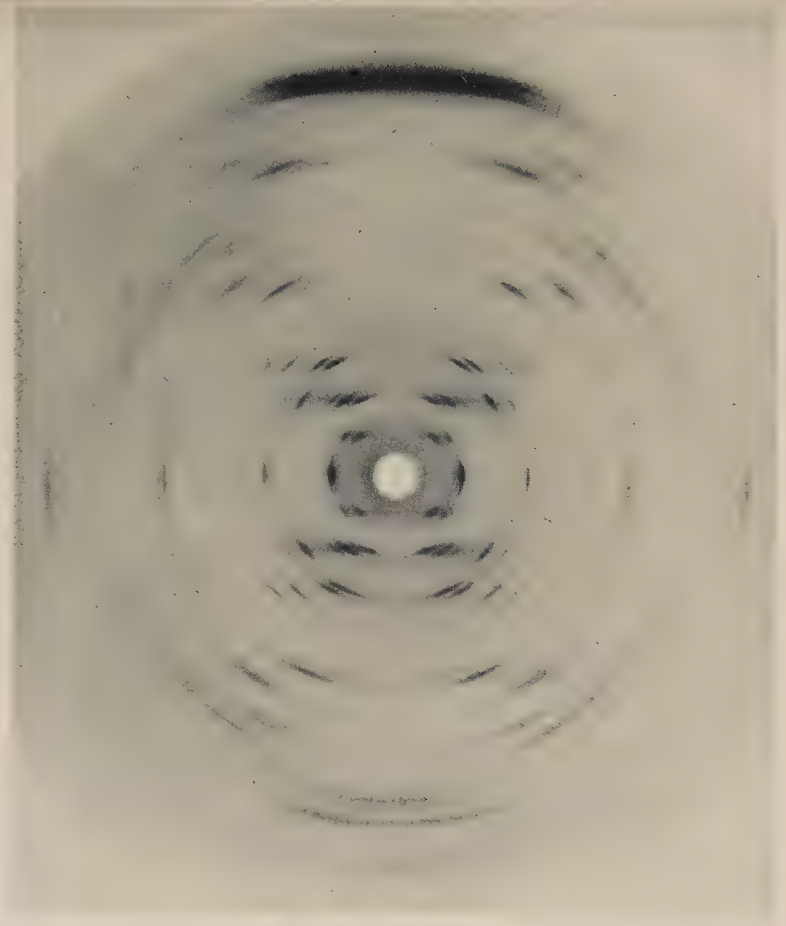

PLATE II. X-ray diffraction pattern given by LiDNA at 66% relative humidity and showing sharp spots.

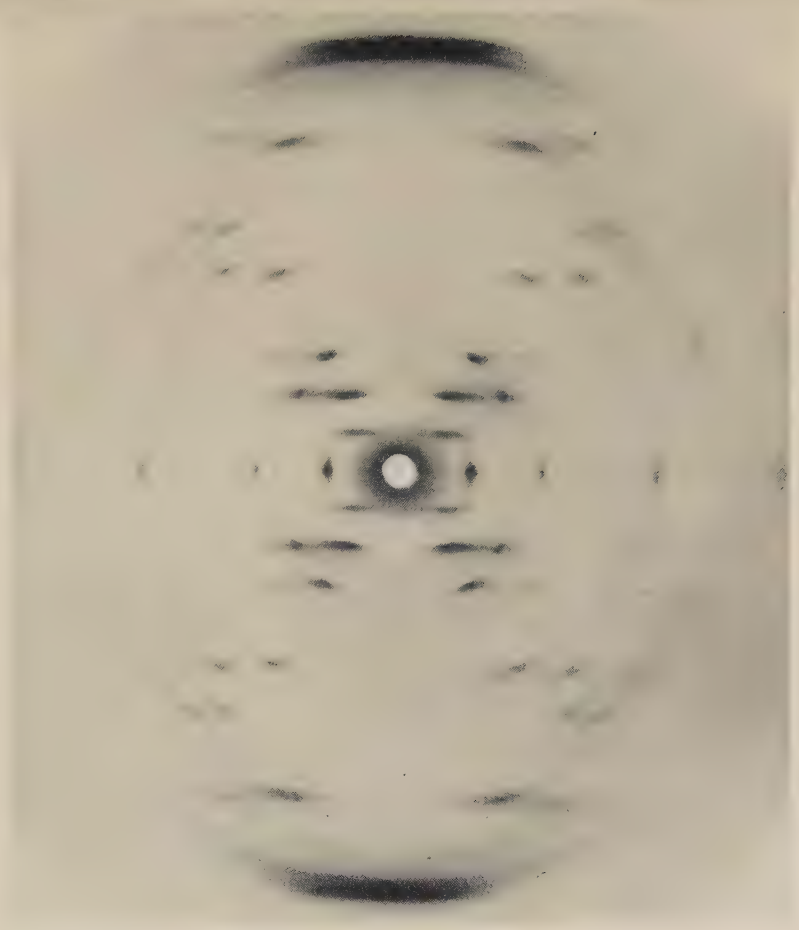

PLATE III. X-ray diffraction pattern given by LiDNA at 66% relative humidity and showing streaks and spots.

[*To face page* 30

PLATE IV. X-ray diffraction pattern given by LiDNA at 66% relative humidity. This photograph (obtained with D. A. Marvin) is similiar to Plate II but contains more data and has not yet been analysed fully.

M porosity sintered glass funnels until filtrate is clear. Precipitate DNA as above with *iso*propyl alcohol and reprecipitate 4 times from 0·3 M-lithium acetate. Before final precipitation centrifuge in Spinco model L for 30 min at 17,500 rev/min in the 30 rotor and filter through a C porosity sintered glass funnel.

Dissolve DNA in 0·01 M-LiCl (2 mg/ml.), add LiCl until 0·14 M, centrifuge in Spinco model L for 30 min at 17,500 rev/min in the 30 rotor, add LiCl until 1 M and precipitate with *iso*propyl alcohol. Repeat and precipitate while stirring by hand with a glass rod to wrap DNA around the rod. Wash the DNA on the rod successively in 50, then 70, 90 and 100% ethyl alcohol (redistilled), and then rapidly with redistilled acetone. Roll the DNA down off the rod, rewash in acetone and press between watch-glasses. Let acetone evaporate at room temperature. Store DNA preparations in sealed containers at — 75°C.

In later preparations 0·01 M-Na EDTA buffer and subsequently Li EDTA buffer were added to the saline-citrate solution used to extract the thymus initially. To reduce the sodium content of the final product lithium xylene sulphonate was used in place of the sodium salt.

4. Experimental Results

(a) *The X-ray photographs*

The most clearly defined photograph we obtained is shown in Plate II. Relative humidity was 66%; distance from specimen to film was 61 mm; the specimen was a double fibre about 120 μ thick and 80 μ wide; exposure time was 68 hr. The fibre was tilted 18° from perpendicular to the X-ray beam in order that reflection might take place, near the meridian, from reciprocal lattice points on the 10th and adjacent layer planes. The photograph was under-exposed but attempts to obtain a better photograph failed because, on re-exposing, the fibres broke and all other specimens of LiDNA we tested gave less well defined photographs, e.g. Plate III.

Recently LiDNA preparations have been made which (with D. A. Marvin) give sharper X-ray patterns. We have used these photographs (Plate IV) to check a number of uncertain points in the data given here.

The X-ray diffraction patterns obtained from different specimens sometimes showed variations from the usual form. A second, somewhat different, lattice has been observed (with D. A. Marvin) but its nature has not been elucidated. Many photographs show streaks (Plate III) on layer lines other than the equator; this shows that the DNA molecules are displaced in an irregular way parallel to their length. These observations suggest that the forces determining the arrangement of the molecules are delicately balanced, and that small differences in the nature of the DNA preparation cause differences of molecular packing in the fibres. The streaky patterns are of interest because the crystalline patterns give information about the scattering factor of the DNA molecule only in the direction of crystalline reflections, whereas the streaks give information for other directions.

(b) *The crystal lattice*

The lattice derived from the X-ray photograph in Plate II is orthogonal with $a = 31{\cdot}22 \pm 0{\cdot}1$ Å, $b = 22{\cdot}72 \pm 0{\cdot}1$ Å, and $c = 33{\cdot}70 \pm 0{\cdot}1$ Å; c is roughly parallel to the fibre axis.

The a and b values were obtained primarily by measuring the positions of the 240 and 600 reflections and by least squares reduction; the c value was fixed mainly by spots 218, the close 128 + 308 doublet, 426 and 2,1,10. On the 10th layer line there is some uncertainty about the indices of the very strong spot. Measurement gives $\xi = 0{\cdot}038$ Å^{-1}, whereas the values for the first two row lines are 0·032 and

0·044 Å^{-1}. It appears very likely that both 1,0,10 and 0,1,10 are reflecting and this would be so for most structures we have considered. On the 11th layer line the one spot observed gives $\xi = 0{\cdot}04$ Å^{-1}; this suggests 1,0,11 is reflecting and 0,1,11 not, but errors may be larger than they appear and probably both planes are reflecting. Indexing on the 13th layer line is very uncertain.

(c) *Arrangement of the molecules in the unit cell*

All spots on the equator are missing when $h + k$ is odd. In other words, the projection of the structure down the c axis fits a simpler lattice. The repeat units in this lattice are about 20 Å apart and, because the diameter of the DNA molecule is about 20 Å, must correspond to single molecules of DNA. The lattice that accounts for all spots on the photograph has a repeat unit corresponding to two molecules, one (m_1, Fig. 4) displaced distance dc in the c direction relative to the other (m_2). The $h + k$ odd spots are also absent on the third and sixth layer line (see Fig. 3) and hence d is about $\frac{1}{3}$. Difference of orientation about the c axis of the two molecules in the unit cell would cause $h + k$ odd reflections to appear on the outer part of the equator and 3rd layer line and on the 6th layer line, but there is no sign of these.

If f_m is the scattering factor for one DNA molecule, the structure factor F^2 of the two molecules in the unit cell is given by

$$F^2(hkl) = 2f_m^2\left(1 + \cos 2\pi\left(\frac{h+k}{2} + ld\right)\right) \qquad (1)$$

If $d = \frac{1}{3}$ and $l = 3n$ (where n is an integer), $F^2(hkl)$ is zero when $h + k$ is odd. When $l \neq 3n$, $F^2(hkl)$ is $3f_m^2$ when $h + k$ is odd and f_m^2 when $h + k$ is even. In agreement with this, it is observed that when $l \neq 3n$ the $h + k$ even reflections are weaker than adjacent ($h + k$) odd reflections on the same layer line. By comparing these intensities, we may fix limits for the value of d. If the molecule is helical, f_m^2 will be symmetrical about c^* in regions of reciprocal space close to c^*. When f_m^2 (hkl) is calculated by (1) from the observed $F^2(hkl)$, the correct value of d will give values of f_m^2 (hkl) that correspond with a symmetrical and continuous distribution of F^2 in reciprocal space. For example, comparison of F^2 values for the adjacent 112 and 012 reflections shows that d lies between 0·33 and 0·32; comparison of the doublets 128 + 308 and 318 + 228 gives $0{\cdot}329 \pm 0{\cdot}003$. On the 3rd layer line 213 is not visible and the intensity of the spot cannot be greater than 10% that of 203; this shows that d is $0{\cdot}333 \pm 0{\cdot}022$. These considerations suggest d is about 0·328 and enable us to deduce a value for the relative displacement (11 Å) of the molecules probably to within 0·02 Å.

Fig. 4 shows the arrangement of the molecules in the unit cell. Molecules m_1 are displaced in the c direction 11·0 Å relative to the molecules m_2. Adjacent m_2 molecules are at the same height in the unit cell and are 22·7 Å apart. The 11·0 Å difference in height of m_1 and m_2 enable them to approach each other more closely, and they are 19·3 Å apart. It will be shown in Part II that the arrangement of the molecules in the unit cell is consistent with the molecular structure.

It is frequently found that patterns (e.g. Plate IV) have streaks and spots on the 1st and 2nd layer lines but no streaks on the equator and 3rd layer line. This effect is explained by the idea that a sheet of contiguous molecules with its plane parallel to the bc plane is displaced randomly either $c/3$ or $-c/3$ in the c direction relative to the neighbouring sheet. One might expect this type of crystalline disorder to occur because the distance between neighbouring molecules in a sheet parallel to the

ac plane is large (31·22 Å) and hence the interaction between the molecules is small and less than in a sheet in the *bc* plane.

Measurement of the positions of the spots in the fibre diagram shows that within close limits the *a*, *b* and *c* axes are at right an; therefore it is reasonable to assume that the lattice is orthorhombic. This implies that there are elements of symmetry

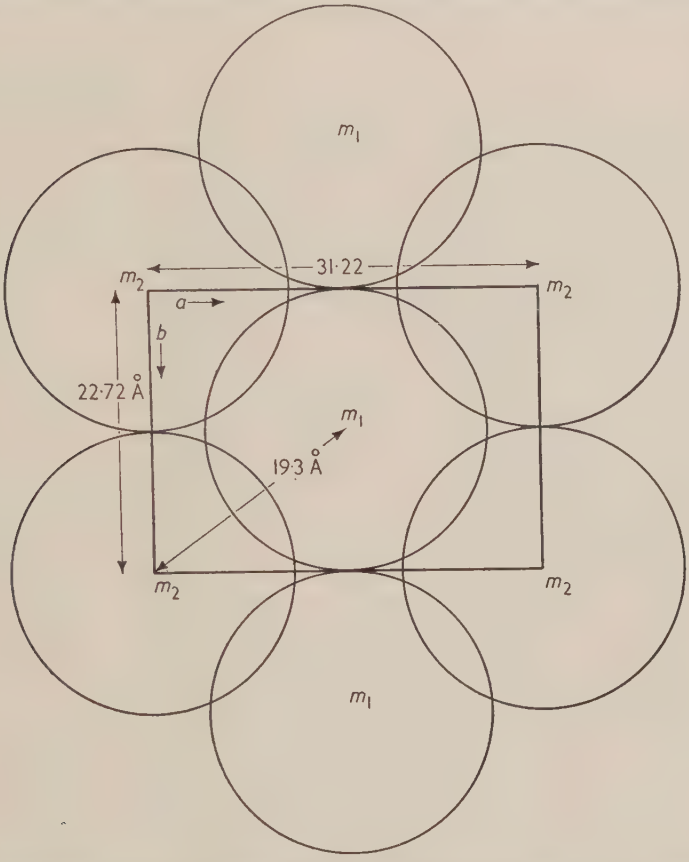

FIG. 4. Arrangement of DNA molecules in the unit cell. Molecules m_1 are displaced in the *c* direction 11Å relative to molecules m_2.

in the space group. The relation of these elements to the system of dyad axes (Crick & Watson, 1954) in the molecule is discussed in Part II. We may note that the ratio a/b is tan 36° 2′. We have not, however, been able to relate this ratio to the tenfold symmetry of the DNA molecule.

(d) *Intensities of reflections*

The data in Table 2 have been obtained from the photograph shown in Plate II. A is the area under the radial densitometer trace across a spot in the fibre diagram; I is the corresponding average value of f_m^2 calculated by equation (1), with $d = \frac{1}{3}$ (for simplicity), from the values of F^2.

$$F^2 = \frac{A\xi l}{n} \tag{2}$$

where ξ is the distance of the reciprocal lattice point from c^*,

l is the arc length on the photograph,

n is the number of reciprocal lattice points contributing to the spot.

We have tabulated f_m^2 in preference to F^2 because the f_m^2 values should correspond with T^2, the calculated square of the Fourier transform of a molecule of DNA (see Part II). Intensities of strong spots were measured with the densitometer and are probably accurate to about 20% are marked in Table 2 with an asterisk. Other intensities may be in error by 40%; very weak intensities are more uncertain and are

TABLE 2

Intensities of the X-ray

hkl	*A*	*I*	T^2	*hkl*	*A*	*I*	T^2	*hkl*	*A*	*I*	T^2
110	560	22*	34	321, 031, 411, 401, 131	< 10	< 1	1	142, 522, 432	~ 20	~ 5	6
020	0	0	7								
200	0	0	1·5					612, 342	~ 15	~ 3	3
310	30	4*	10								
220	60	9*	13					252, 632, 542, 722, 352	~ 15	~ 4	6
400	~ 10	~ 4	7	501, 421, 331, 511	~ 5	~ 1	6·5				
130	~ 10	~ 2	3								
420	~ 15	~ 4	7								
330, 510	~ 10	~ 2	0·5	141							
040	0	0	1·5	521, 431	~ 10	~ 3	3	113	150	10·5*	18
240	55	25*	25					203	110	20*	30
600	38	36*	21	611, 341	~ 5	~ 1	0·5	023	56	15*	24
530	~ 15	~ 8	3								
440	~ 7	~ 4	1	631, 251, 541, 721, 351	< 5	< 1	7	313, 223	50	5*	5
620	0	0	1					403	~ 10	~ 5	4
150	0	0	0					333, 513	~ 20	~ 4	7
710	0	0	0								
350	0	0	7					243, 603	~ 10	~ 3	4
800	~ 12	~ 20	11·5	102	208	15*	18	533	~ 20	~ 13	9
730	~ 12	~ 10	7	012	320	34*	38	623	~ 20	~ 13	18
640	~ 12	~ 10	3·5	112	140	31	51	443, 153	55	18	20
060	~ 12	~ 20	26	202	68	37	51				
820, 260, 550	86	28*	21	212	185	23*	29	713, 803, 733, 643, 063	20	14	14
				122, 302	48	6*	5				
101	203	10*	11	312, 222	< 10	< 1	0·5		~ 10	~ 3	1·5
011	140	12*	9								
111	~ 20	~ 3·5	5	322, 032, 412, 402, 132	< 10	< 1	0·5	823, 263, 553	~ 10	~ 3	7
201	0	0	1								
211	0	0	0								
121, 301	~ 7	~ 1	2								

marked ~. The intensity of the 13th layer line was obtained from a micro-camera photograph.

Equation (2) cannot be used for 00*l* reflections. However, this was not a difficulty because the intensities of these reflections were small and they were ignored. Even on the 10th layer line the intensity of 0,0,10 is small compared to neighbouring reflections, because of interference between radiation scattered from the two molecules in the unit cell. The disorientation of crystallites in the fibre was not sufficient to cause much overlap of the two very strong arcs on the 10th layer line and, as a result, equation (2) could be applied without much error to these reflections. Because the orientation was not very good it was not necessary to incline the fibre at a different angle to the beam in order to observe the various 00*l* reflections.

(e) *Density and water content of specimens*

Measurements of density and water content of various specimens of LiDNA are given in Table 3. The specific volume of LiDNA is about the same in all specimens and at all humidities, except for the high value of 0·61 obtained from a specimen which

reflections shown in Plate II

hkl	*A*	*I*	T^2	*hkl*	*A*	*I*	T^2	*hkl*	*A*	*I*	T^2
214	~ 10	~ 2	1	406	35	25*	20	0 0 10			
124, 304	< 10	< 1	2	136	55	22*	25	1 0 10, 0 1 10, 1 1 10	2100	300*	210
034, 324, 414, 404, 134	< 10	0	1	426	80	38*	37	2 0 10, 2 1 10	500	170*	120
434, 524, 144	< 10	< 1	2	336, 516	< 10	< 2	4	0 2 10, 1 2 10, 3 0 10	~ 100	~ 32	32
215	45	10*	15	246, 606	< 10	< 3	3	0 1 11, 1 0 11	40	9	10
125	135	24*	37	217	< 10	< 2	7	0 2 13, 1 2 13, 3 0 13	~ 25	~ 10	1
305, 315, 225	~ 20	~ 10	9	127, 307	< 10	< 1	6				
405, 325, 035, 415, 135	140	21*	13	407, 327, 037, 417, 137	~ 20	~ 4	1				
235	~ 20	~ 11	2	237	~ 10	~ 7	1				
515	~ 10	~ 10	2	108	< 10	0	3				
335, 045, 145, 525, 435	90	21*	7	018	< 10	0	5				
615, 345	< 20	< 7	1	218	75	25*	5				
116	~ 10	~ 1	1·5	128, 308	147	37*	33				
206	~ 10	~ 2	2	318, 228, 408, 328, 038, 418, 138	~ 40	29	44				
026	~ 10	~ 4	8	119, 209	< 20	< 3	3				
316, 226	~ 10	~ 1	4	029	~ 10	~ 6	4				
				319, 229	~ 20	~ 4	4				
				409, 139	~ 20	~ 7	0				

had not been centrifuged during preparation and which might therefore have contained air bubbles which could give rise to an apparently high value. The water content of various specimens at the same relative humidity varies considerably. The calculated number of nucleotides per unit cell (N) also varies and is always greater than the value of 40 corresponding to a two-chain molecule. However, the observed values are closer to 40 than to 60 which would correspond to a three-chain molecule. These variations and discrepancies are almost certainly associated with the presence of

non-crystalline material in the fibre. Apparently the amorphous regions are less hydrated than the crystalline and the fraction of amorphous material is different in various specimens. The fraction of crystalline material is reduced at 44% and absent at 92% relative humidity and N has not been calculated. At 75% relative humidity crystallinity is not always reproducible and much weight should not be attached to the value of N calculated. There is little reason to expect that the specific volume of the DNA is different in amorphous and crystalline regions and we do in fact find the observed values are markedly constant. The value for NaDNA in dilute solution is

Table 3

Relative humidity %	Density	Water content: gm water/ 100 gm DNA	Preparation number	Number of nucleotides per unit cell N	Temperature °C	Specific volume of LiDNA
44	1·476	23·1	p. 125	—	22	0·602
44	1·488	23·0	p. 105	—	22	0·595
66	1·365	44·0	p. 113	43	25	0·613
66	1·434	40·0	p. 105	46	22	0·588
66	1·425	37·5	p. 121	47	22	0·574
66	1·46	35·4	p. 235	49	22	0·581
66	1·47	34·5	p. 235			
75	1·40	45·0	p. 235	(44)	22	0·581
75	1·406	47·2	p. 235			
92	1·29	87·3	p. 235	—	22	0·581

0·55 according to recent unpublished measurements of Dr. G. Zubay (see also Kahler, 1948). If we assume that the difference of partial volumes of Li and Na is negligible, the estimated specific volume of LiDNA would be 0·58 which is the value found for solid LiDNA.

We wish to thank Professor J. T. Randall, F.R.S., and Drs. C. P. Rhoads,† J. Burchenal and C. C. Stock for encouragement; Drs. W. E. Seeds, A. R. Stokes, F. H. C. Crick, N. S. Simmons, G. L. Brown for discussion; Miss N. Chilson, Mr. R. Lerner and Mrs. Menegas for technical assistance with making DNA; Miss L. Verheyden and Mr. P. J. Cooper for analysis of DNA; and Mr. J. Hayward for making X-ray cameras.

The development of methods of making DNA was aided by the work of Dr. R. K. Barclay and the work as a whole was aided by the studies of our late colleague Dr. Rosalind E. Franklin and Dr. R. G. Gosling and by the work of Dr. H. W. Wyckoff. A few uncertainties in the X-ray data have been removed by comparing the data with the more extensive data obtained recently by Mr. D. A. Marvin.

One of us (H.R.W.) acknowledges award of a grant from the British Empire Cancer Campaign. Work at King's College was aided by a grant from The Rockefeller Foundation and that at the Sloan-Kettering Institute by a grant (to L.D.H.) from The Commonwealth Fund.

REFERENCES

Astbury, W. T. (1947). *Symp. Soc. Exp. Biol. I. Nucleic Acid*, p. 66. Cambridge: University Press.

Bessman, M. J., Lehman, I. R., Adler, J., Zimmerman, S. B., Simms, E. S. & Kornberg, A. (1958). *Proc. Nat. Acad. Sci., Wash.* **44**, 633.

Bradley, A. J. (1935). *Proc. Phys. Soc. Lond.* **47**, 879.

† Died 13 August, 1959.

Brown, D. M. & Todd, A. R. (1952). *J. Chem. Soc.* p. 52.
Caspersson, T. (1940). *Chromosoma*, **4**, 605.
Chargaff, E. (1950). *Experientia*, **6**, 201.
Chesley, G. F. (1947). *Rev. Sci. Instr.* **18**, 422.
Cochran, W., Crick, F. H. C. & Vand, V. (1952). *Acta Cryst.* **5**, 581.
Commission on Crystallographic Apparatus of the International Union of Crystallography, (1956). *Acta Cryst.* **9**, 520.
Crick, F. H. C. & Watson, J. D. (1954). *Proc. Roy. Soc.* A, **223**, 80.
Donohue, J. (1956). *Proc. Nat. Acad. Sci., Wash.* **42**, 60.
Ehrenberg, W. & Spear, W. E. (1951). *Proc. Phys. Soc. Lond.* B. **64**, 67.
Feughelman, M., Langridge, R., Seeds, W. E., Stokes, A. R., Wilson, H. R., Hooper, C. W., Wilkins, M. H. F., Barclay, R. K. & Hamilton, L. D. (1955). *Nature*, **175**, 834.
Franklin, R. E. & Gosling, R. G. (1953*a*). *Acta Cryst.* **6**, 673.
Franklin, R. E. & Gosling, R. G. (1953*b*). *Nature*, **172**, 156.
Franklin, R. E. & Gosling, R. G. (1953*c*). *Nature*, **171**, 740.
Franklin, R. E. & Gosling, R. G. (1953*d*). *Acta Cryst.* **6**, 678.
Franklin, R. E. & Gosling, R. G. (1955). *Acta Cryst.* **8**, 151.
Furberg, S. (1950). *Acta Cryst.* **3**, 325.
Gulland, J. M. (1947). *Cold. Spr. Harb. Symp. Quant. Biol. XII*, p. 95.
Gulland, J. M. & Jordan, D. O. (1947). *Symp. Soc. Exp. Biol. I. Nucleic Acid.* Cambridge: University Press.
Hooper, C. W. (1957). M.Sc. thesis. University of London.
Kahler, H. (1948). *J. Phys. Colloid Chem.* **52**, 676.
Kay, E. R. M., Simmons, N. S. & Dounce, A. L. (1952). *J. Amer. Chem. Soc.* **74**, 1724.
Langridge, R., Seeds, W. E., Wilson, H. R., Hooper, C. W., Wilkins, M. H. F. & Hamilton, L. D. (1957). *J. Biophys. Biochem. Cytol.* **3**, 767.
Levinthal, C. & Thomas, C. A. (1957). In *The Chemical Basis of Heredity*. Baltimore: Johns Hopkins Press.
Low, B. W. & Richards, F. M. (1952). *J. Amer. Chem. Soc.* **74**, 1660.
Marko, A. M. & Butler, G. C. (1951). *J. Biol. Chem.* **190**, 165.
Marvin, D. A., Spencer, M., Wilkins, M. H. F. & Hamilton, L. D. (1958). *Nature*, **182**, 387.
Meselson, M. & Stahl, F. W. (1958). *Proc. Nat. Acad. Sci., Wash.* **44**, 671.
Pauling, L. & Corey, R. B. (1953). *Proc. Nat. Acad. Sci., Wash.* **39**, 84.
Rich, A. & Davies, D. R. (1956). *J. Amer. Chem. Soc.* **78**, 3548.
Riley, D. P. & Oster, G. (1951). *Biochim. biophys. Acta*, **7**, 526.
Signer, R., Caspersson, T. & Hammersten, E. (1938). *Nature*, **141**, 122.
Signer, R. & Schwander, H. (1949). *Helv. chim. Acta*, **32**, 853.
Simmons, N. S., Chavos, S. & Orbach, H. K. (1952). *Fed. Proc.* **11**, 390.
Van Horn, M. H. (1951). *Rev. Sci. Instr.* **22**, 809.
Walker, P. M. B. (1955). *Exp. Cell Res.* **8**, 567.
Watson, J. D. & Crick, F. H. C. (1953). *Nature*, **171**, 964.
Wilkins, M. H. F., Gosling, R. G. & Seeds, W. E. (1951). *Nature*, **167**, 759.
Wilkins, M. H. F. & Randall, J. T. (1953). *Biochim. biophys. Acta*, **10**, 192.
Wilkins, M. H. F., Seeds, W. E., Stokes, A. R. & Wilson, H. R. (1953). *Nature*, **172**, 759.
Wilkins, M. H. F., Stokes, A. R. & Wilson, H. R. (1953). *Nature*, **171**, 737.
Wyatt, G. R. & Cohen, S. S. (1953). *Biochem. J.* **55**, 774.
Wyckoff, H. W. (1955). Ph.D. thesis, M.I.T., Cambridge, Mass.

J. Mol. Biol. (1960) **2**, 38-64

The Molecular Configuration of Deoxyribonucleic Acid

II. Molecular Models and their Fourier Transforms

R. Langridge, D. A. Marvin, W. E. Seeds and H. R. Wilson

Wheatstone Laboratory, King's College, London, England

C. W. Hooper and M. H. F. Wilkins

Medical Research Council Biophysics Research Unit, King's College, London, England

L. D. Hamilton

Sloan-Kettering Institute, New York, U.S.A.

(*Received 26 January 1960*)

The Watson-Crick molecular model of deoxyribonucleic acid (DNA) was built with the general dimensions derived from X-ray diffraction studies. The Fourier transform of the structure has been calculated, and comparison with the X-ray data described in Part I shows that the model needs modifying. Various models were built and adjusted until reasonable agreement was obtained between the Fourier transform, averaged by rotation about the helix axis, and the observed 2-dimensional intensity data. The space group in the microcrystalline fibres of DNA appears to be $P2_12_12_1$, and two orientations of the DNA molecules in the unit cell are possible. One orientation is compatible with the 3-dimensional intensity data; this confirms the correctness of the structure. The closest distances between neighbouring molecules are 2·7 Å between oxygen atoms. The structure is tightly packed; each nucleotide contains two distances of 2·9 Å between carbon and oxygen atoms. No bond angles differ more than 4° from those expected from study of crystal structures of the components of DNA and related compounds. The orientation of the phosphate groups agrees with that derived from measurements of the absorption by DNA of polarised infrared radiation. The deoxyribose ring is puckered, as one might expect, with the C_2 atom 0·3 Å out-of-plane. An approximate method for taking into account the scatter from water when calculating the diffraction from the structure is described.

1. Introduction

In this paper we describe the derivation of the molecular structure of DNA from the X-ray diffraction data described in Part I and from stereochemical considerations. The greatest limitation in deducing the structure of DNA from its X-ray diffraction photograph is that reflections are not observed for spacings much less than 3 Å.† Hence, although the separation of non-bonded pairs of atoms may be seen, much of the atomic detail, such as atoms covalently linked and about 1·5 Å apart, is not resolved. However, the problem of finding the coordinates of the atoms is not so hopeless as it might seem. An optical analogy is the viewing of a double slit through a

† Since this was written, spacings as small as 1·6 Å have been observed.

telescope that does not resolve the double structure, i.e. no minimum of intensity is visible in the centre of the diffraction pattern. If we *assume* that the object consists of two thin lines, their separation may be found by measuring the intensity distribution in the diffraction image; and the resolving power is then limited only by the reliability of the assumptions concerning the nature of the object and the accuracy of the intensity measurements. In the case of the X-ray analysis of DNA we make assumptions about the stereochemistry of DNA and about the scattering from water in the structure. Measurement of diffraction intensities then enables us to find the positions that the atoms should occupy. Similarly, it is usual, by assuming the form of atoms, to determine their positions in crystals to within 0·01 Å by measuring spacings no smaller than 0·7 Å.

It seems possible by our methods to find the position of many atoms in DNA, e.g. the phosphorus atom in each nucleotide, to within 0·5 Å. The procedure is as follows. Preliminary study of the X-ray data suggests that certain stereochemical assumptions, viz. those used in building the Watson-Crick model, are likely to be correct. Then with the aid of these assumptions, we build a molecular model and calculate intensities of diffraction for it, and adjust the model in an endeavour to make the calculated intensities agree with those observed. When agreement is reached we believe the structure is correct.

Because of lack of resolution we cannot check the correctness of our results, as is usual in X-ray structure determinations, by confirming that each atom has the correct shape and contains the right number of electrons. We must recognise that our procedure might not enable us to prove that there is no alternative stereochemical hypothesis that can be used in building some other kind of model that might also give calculated intensities which agree with those observed. When building a model of DNA there is considerable stereochemical freedom in arranging the components. There is, therefore, a slight possibility that, for any single type of diffraction pattern, agreement between observed and calculated intensities might be fortuitous. Fortunately, however, it is possible to obtain from DNA three different diffraction patterns that correspond to 3 distinct though related configurations (*A*, *B* and *C*) of the DNA molecule. In the present paper we describe a study of the *B* configuration only; but, using the same stereochemical assumptions, we have also been able to derive an *A* configuration that is in agreement with X-ray data. Moreover, by making a small alteration in the *B* structure, we can readily convert it into the *C* and account for the differences in the *B* and *C* diffraction patterns (Marvin, Spencer, Wilkins & Hamilton, 1958). We consider that these results taken together go a long way towards proving that our solution is unique. It should also be emphasised that we have adjusted our molecular model to correspond with 2-dimensional diffraction data only and we found subsequently that the model was consistent with diffraction data in three dimensions. The 3-dimensional data thus confirm the correctness of the model. Calculation of the distances of closest approach between neighbouring molecules provides, to some extent, further independent confirmation.

In determining the structure of DNA it is essential to decide how the water is arranged, since the total amplitude scattered from the water is, irrespective of phase, as much as half that from the DNA itself. In the earlier stages of our work we thought that scatter from the water might obscure the details of the DNA structure (Wilkins, 1956). We have found, however, that this is not so—the water scatters approximately as though it were a continuous medium filling the space between the DNA molecules, and we have devised a method for calculating this scatter.

2. Building the Molecular Model

(a) *Design of the molecular model*

The model built by Crick & Watson (1954) consists of two intertwined right-handed helical polynucleotide chains of 34 Å pitch and with ten nucleotides per turn of each chain. The chains are linked by hydrogen bonds between pairs of bases. The dimensions of the base-pairs are such that the position of the glycosidic bond is equivalent for all bases, and the arrangement of the deoxyribose and phosphate parts of each nucleotide in one chain is related to that of a nucleotide in the other chain by a dyad axis through the helix axis and perpendicular to it (Fig. 1). The model was designed

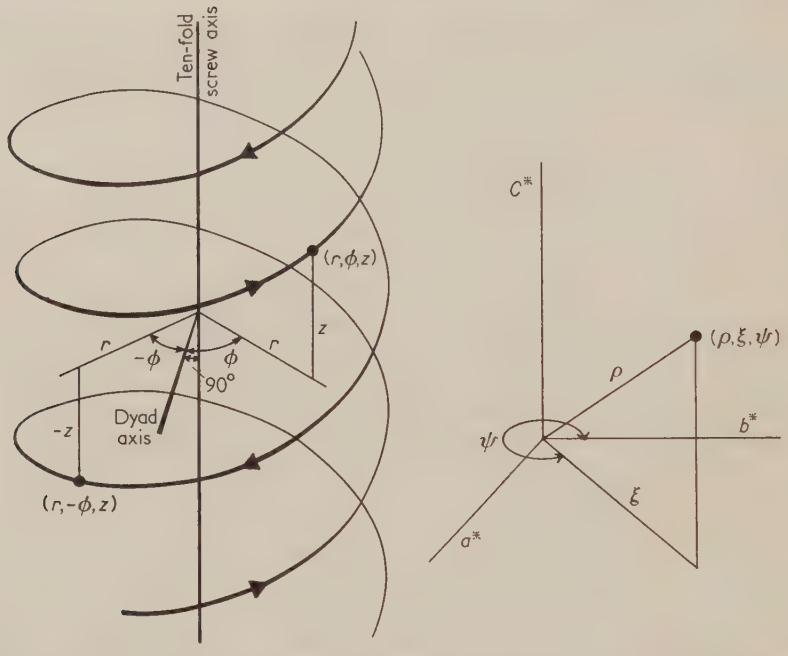

FIG. 1. *Left.* Basic geometry of the Watson-Crick structure. A line represents each polynucleotide chain and the sequence of atoms in a chain is indicated by an arrow. Also shown are the coordinates of an atom and the helix (or ten-fold screw) axis and dyad axis to which the coordinates are related. *Right.* Axes of the LiDNA crystal structure (see Part I) and coordinates of a point in reciprocal space.

to be compatible with the basic features of the X-ray diffraction pattern, but since few details of the X-ray data had been taken into account, it is not surprising that the model needed modification.

The square of the Fourier transform (T^2) of the model is shown in Fig. 2. There are large discrepancies between T^2 and the observed intensities of diffraction corrected to give values of f_m^2 the scattering factor of a DNA molecule (see Part I). The calculated central maximum on the equator is narrower than is indicated by the observed intensities. This shows that the diameter of the model is 10 to 20% too large. The transform on the equator and second layer line does not consist of one large maximum with adjacent subsidiary maxima of very low intensity as is indicated by the observed data; there are quite high peaks at $\xi = 0{\cdot}1$ Å^{-1} on the second layer line and at $\xi = 0{\cdot}07$ Å^{-1} on the equator. This means that the Watson-Crick model does not have the form, suggested by Wilkins, Stokes & Wilson (1953), in which a

nucleotide resembles a rod at right angles to the helix axis and passing through it. (See Part I.) A closer approximation to this form and a smaller diameter molecule can be achieved by moving the base-pairs nearer to the helix axis. We therefore built models of this modified type. Many models were built before a satisfactory solution was obtained. We will illustrate the main stages in the model building by describing three models only.

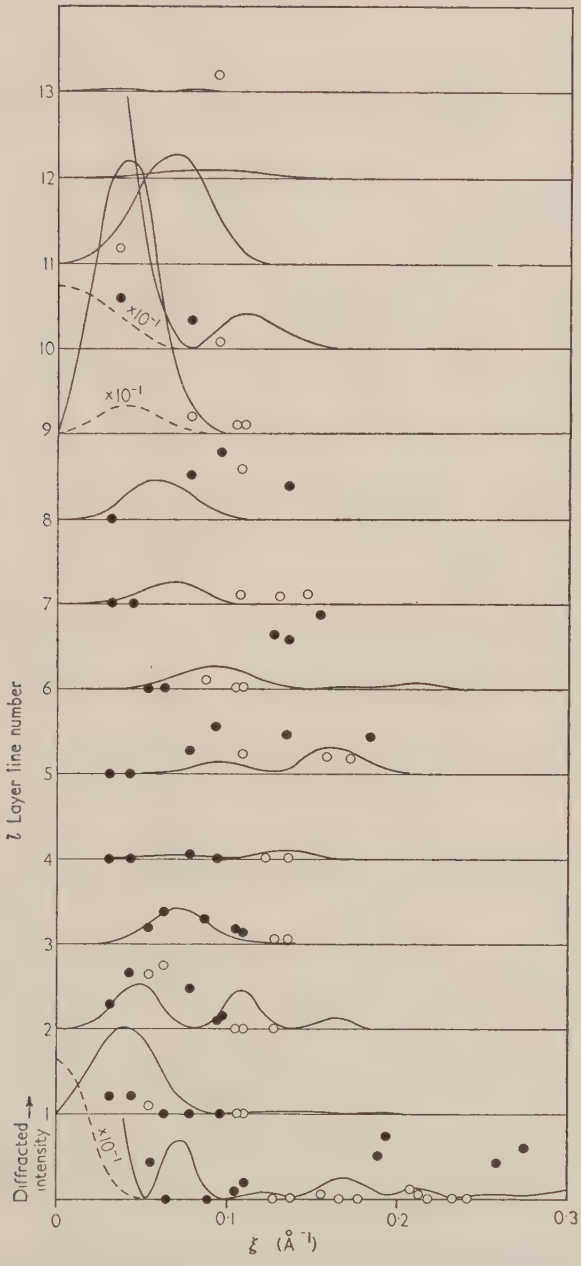

FIG. 2. Comparison of T^2, the square of the Fourier transform (averaged by rotation about the helix axis) of the Watson-Crick structure, with observed intensities of X-ray diffraction. In calculating the transform the atoms were regarded as points. The intensity values indicated ● are more reliable than those indicated ○.

(b) *Method of adjusting the model to give the desired transform*

There is considerable stereochemical freedom in building a model. The sugar ring may be moved relative to the base-pair by rotating it by as much as 90° about the glycosidic bond, and changes in the pucker of the sugar ring (Spencer, 1959) produce large changes in direction of the bonds joining sugar to phosphate. If the position of the sugar ring is

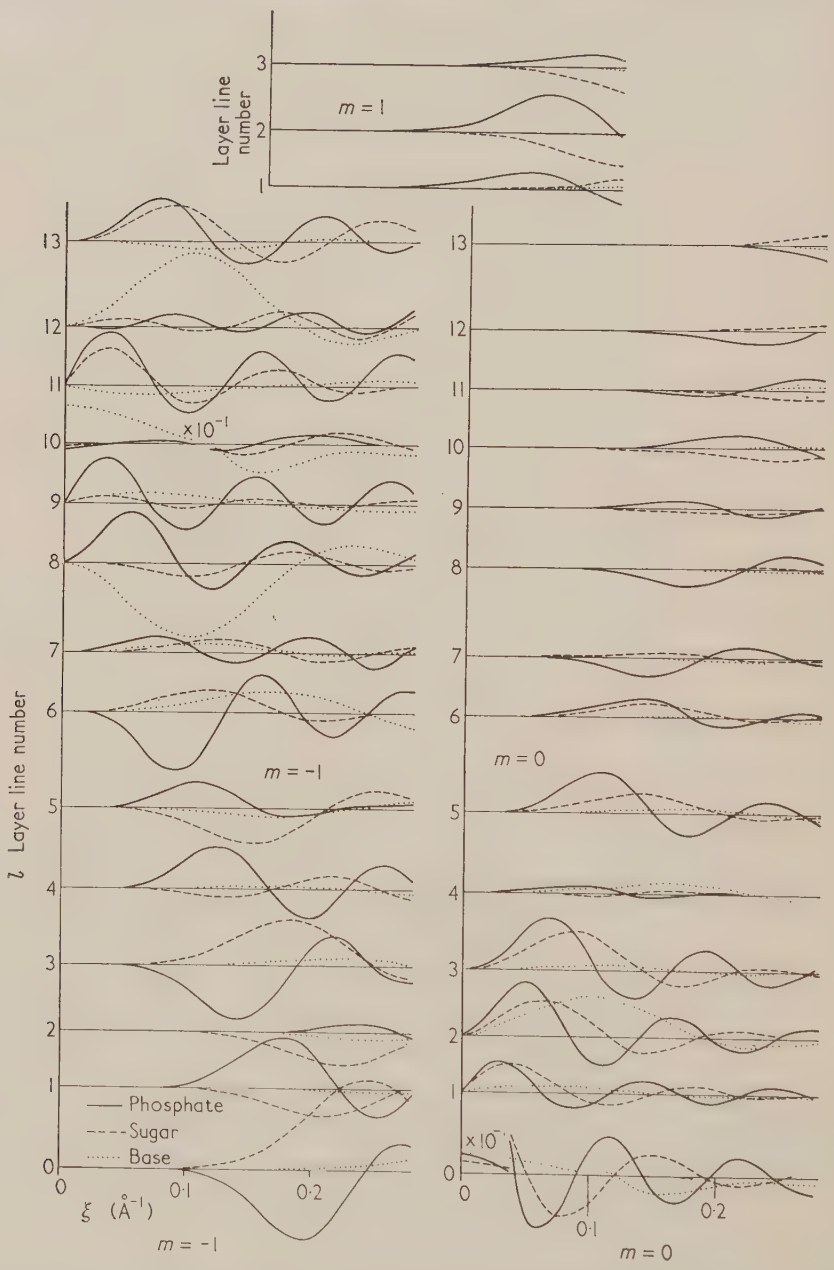

FIG. 3. Amplitudes of the $m = 0$, $m = 1$, and $m = -1$ terms in the Fourier transform of the base, sugar and phosphate parts of a DNA model (that described in Langridge *et al.*, 1957). On the zero layer line the $m = 1$ and $m = -1$ terms are equal and their sum is shown. In calculating the transform the atoms were regarded as points. To make the diagram compact, signs are reversed for $m = 0$, $l = 2$ and 3, and for $m = -1$, $l = 9$, 11, 12.

set, the phosphate group may often be placed in stereochemically possible positions covering a considerable range if bond angles are distorted slightly. This range can be extended if the sugar ring is rotated about the glycosidic bond, and if the pucker of the sugar ring is

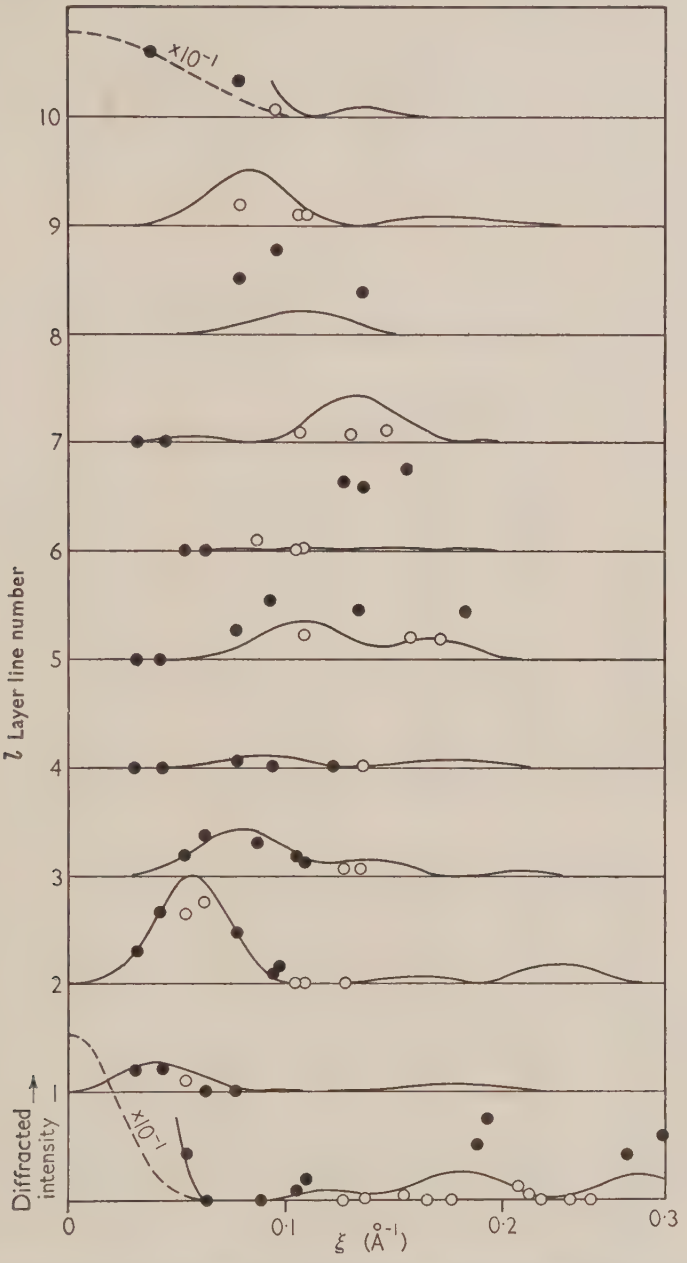

FIG. 4. Comparison of T^2, the square of the Fourier transform (averaged by rotation about the helix axis) of Model 1, with observed intensities of X-ray diffraction.

tered. Although the base, sugar, and phosphate groups may be moved considerably lative to each other, the geometry within each group itself is to a large extent fixed part from puckering of the sugar ring). It is convenient therefore to calculate the amitude produced by each group separately (Fig. 3) when estimating the effect on the ansform of an alteration in the model. For a rapid and rough estimate each group may be

represented by a point near its centre. It is also useful to project radially the group on to the surface of a cylinder coaxial with the helix. If we flatten the surface and draw on it straight lines that correspond to the loci of positions at which a diffracting point would produce maximum amplitude on the various layer lines, the effect of moving the groups may be estimated by eye. Part of this procedure resembles the method of radial projection described by Klug, Crick & Wyckoff (1958). It may be seen from plots such as those in Fig. 3 that some features of the diffraction pattern are determined largely by certain groups. For instance, the phosphate group makes large contributions in many parts of the pattern, e.g. at $\xi = 0{\cdot}2$ Å^{-1} on the equator, and is largely responsible for the relative intensities of the central parts of the first four layer lines. The contribution of the bases is dominant on layer lines near the 10th.

TABLE 1

Coordinates of molecular models of DNA. For definition of r, ϕ, Z see Fig. 1. The helix is right-handed, pitch is 33·6 Å and there are ten nucleotide pairs per turn

		Model 1			Model 2			Model 3		
Group	Atom	r (Å)	degrees	Z Å	r	ϕ	Z	r	ϕ	Z
phosphate	P	9·58	54·9	— 1·82	9·40	55	— 1·35	9·05	58·8	— 1·36
	O_1	8·85	62·7	— 2·39	9·10	65	— 1·63	8·88	62·9	0·04
	O_2	10·91	55·0	— 2·49	10·80	54	— 1·61	9·14	65·3	— 2·45
	O_3	9·68	54·1	— 0·27	9·00	53	0·00	10·33	54·2	— 1·18
	O_4	8·95	46·2	— 2·21	8·55	50	— 2·30	7·85	52·3	— 1·43
sugar	C_1	6·30	60·1	0·00	6·05	64	0·15	5·72	71·5	0·31
	C_2	6·72	58·5	— 1·37	6·65	65	— 1·18	6·95	74·1	— 0·56
	C_3	7·73	67·0	— 1·69	8·00	70	— 0·99	8·13	71·1	0·35
	C_4	8·30	70·4	— 0·35	8·20	70	0·50	7·58	70·4	1·80
	C_5	8·68	80·5	— 0·27	9·10	78	1·05	8·08	79·1	2·63
	O_5	7·72	67·7	0·63	6·90	70	1·13	6·13	70·0	1·70
purine	O_6, $(NH_2)_6$	0·76	123·2	0·00	1·18	150	0·00	2·40	155·0	— 0·14
	C_6	1·44	66·0	0·00	1·33	86	0·03	1·70	124·0	— 0·03
	C_5	2·84	71·8	0·00	2·70	82	0·07	2·90	104·0	0·02
	N_7	3·79	90·2	0·00	3·80	97	0·10	4·20	112·0	0·00
	C_8	4·93	81·5	0·00	4·87	87	0·13	4·95	98·0	0·10
	N_9	4·95	66·0	0·00	4·76	72	0·12	4·63	82·5	0·19
	C_4	3·83	56·3	0·00	3·57	63	0·09	3·30	79·0	0·16
	N_3	4·07	36·5	0·00	3·67	41	0·06	2·90	56·0	0·20
	C_2	3·20	20·8	0·00	2·73	24	0·02	1·70	40·0	0·14
	N_1	1·89	19·0	0·00	1·42	24	0·00	0·60	83·0	0·02
guanine	$(NH_2)_2$	4·03	4·1	0·00	3·55	4	0·00	2·25	0·80	0·20
pyrimidine	O_6, $(NH_2)_6$	2·37	119·2	0·00	2·51	128	0·05	3·20	140·0	— 0·14
	C_6	2·92	93·0	0·00	2·87	102	0·08	3·20	117·0	— 0·03
	N_1	2·60	64·5	0·00	2·35	73	0·06	2·40	96·0	0·05
	C_2	3·85	55·3	0·00	3·60	62	0·09	3·34	76·0	0·16
	O_2	4·35	39·0	0·00	3·98	43	0·07	3·40	55·0	0·23
	N_3	4·95	66·0	0·00	4·76	72	0·12	4·63	82·5	0·19
	C_4	5·07	82·0	0·00	5·11	88	0·13	5·17	97·0	0·10
	C_5	4·31	94·7	0·00	4·27	101	0·10	4·60	112·0	0·00
thymine	CH_3	5·20	110·0	0·00	5·20	110	0·12	5·33	121·0	— 0·09

(c) *Development of a suitable model*

In Model 1 the base-pairs are 4 Å nearer the helix axis than in the Watson-Crick model. Atomic coordinates are given in Table 1. A rather similar model was built by Wyckoff (1955). Having chosen the position of the bases, the remainder of the structure was obtained as follows. The relative intensities of the 1st, 2nd, 3rd and 4th layer

ines (for ξ between 0 and 0·1 Å^{-1}) change considerably when the separation, in the helix axis direction, of the two phosphate-ester chains is altered slightly. We esti-

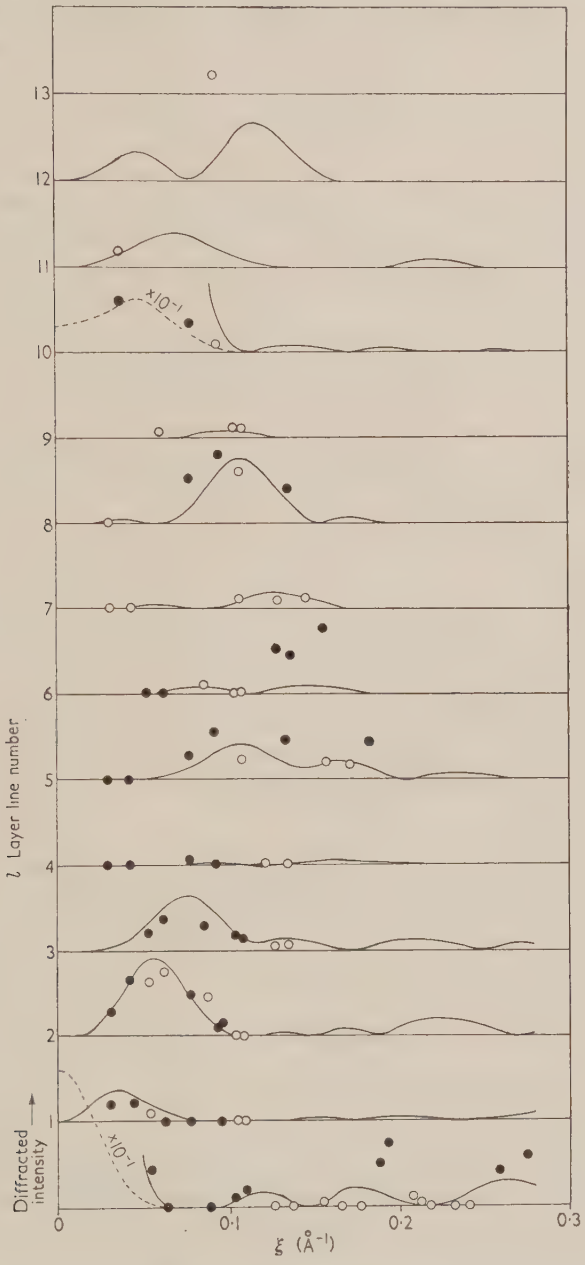

Fig. 5. Comparison of T^2, the square of the Fourier transform (averaged by rotation about the helix axis) of Model 2, with observed intensities of X-ray diffraction. In calculating the transform the atoms were regarded as points.

mated the separation that would give the observed intensities. We then found that only one configuration was stereochemically likely. The transform of Model 1 is shown in Fig. 4. It may be seen that the agreement between the Fourier transform

and the observed data is satisfactory on the equator for small ξ. There is good agreement in the central part of the pattern on all layer lines and, because this considerable overall improvement had been obtained by simple adjustment of the model, we felt that we were near a correct solution. There were, however, discrepancies in the

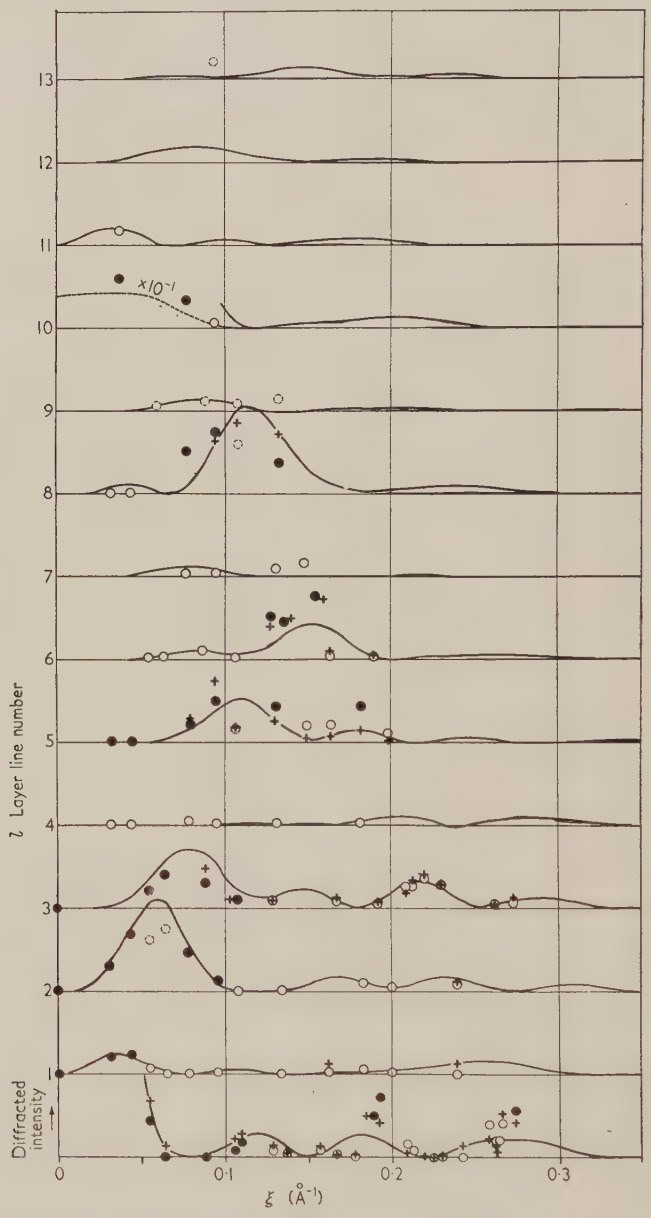

FIG. 6. Comparison of T^2, the square of the Fourier transform of Model 3, with observed intensities of X-ray diffraction (see Part I, Table 2). The values of T^2 averaged by rotation about the helix axis are shown as a continuous curve. When the value of T^2 for an individual reflection differs appreciably from the average T^2 the value for the reflection is indicated +. Observed intensities in order of decreasing reliability are indicated ●, ○, ◌. The observed intensities have been corrected by making the assumption (for simplicity) that d (see Part I) is 1/3; if d is taken as 0·328 the intensity values, e.g. those on the second layer line between $\xi = 0$ and 0·1 Å^{-1}, fall more nearly on a smooth curve.

outer parts of the pattern. At first we thought it might not be possible to avoid these discrepancies because water in the structure might be specially arranged and the pattern due to DNA might be obscured (Wilkins, 1956). However, it was noticed that the maxima on the 6th, 7th, 8th and 9th layer lines were in the correct positions and the disagreement between observed and calculated data was simple and consistent—weak peaks occurred where strong should be and *vice versa*. We thought a minor adjustment of the model might remove this discrepancy (Wilkins, 1957).

The contribution of the bases is dominant in the region of the discrepancies. We decided, therefore, to alter the position of the base-pair so that the amplitude due to the bases would be small on the 9th and 7th layer lines and large on the 8th. The required amplitudes would be produced if the plane of the bases were perpendicular to the helix axis and the base-pairs were central with respect to the axis. This would be so if the bases in Model 1 were moved towards the helix axis. Similar amplitude changes would be produced if the base-pairs were slightly tilted about the dyad axis. In Model 2 (Table 1) the bases were tilted 1·5° and moved 0·5 Å towards the helix axis. The desired intensities (Fig. 5) were obtained on the 7th, 8th and 9th layer lines but values were still low on the 6th layer line where they should be large, and the value at $\xi = 0{\cdot}05$ Å^{-1} on the first layer line had increased so that a discrepancy present in Model 1 was now greater. We had wished to avoid moving the base-pair closer to the helix axis, since this movement would reduce several non-bonded interatomic distances (e.g. C_2 (sugar)—C_4' (pyrimidine)) that were already small. However, since Model 2 was not satisfactory, we tested the effect of moving untilted bases closer to the axis. The model described by Langridge *et al.* (1957) was built and close contacts to a large extent avoided by adjusting bond angles. The required intensities were then obtained on the 6th, 7th, 8th and 9th layer lines and it was encouraging that no new discrepancies appeared. We believed the positions of the base, sugar and phosphate parts of the model were nearly correct, but for reasons stated later we were not satisfied with the stereochemistry of the model. We then moved the base-pair 0·2 Å closer to the helix axis and tilted the pair 2° so that diffraction from the bases on layer lines near the 10th was largely unaltered. As a result of this minor adjustment it was found possible to rearrange the configuration of the phosphate-ester chain without altering the position of the phosphate and sugar groups. This structure, Model 3 (Table 1), is to be preferred to the previous model for reasons given later. The transform is shown in Fig. 6.

(d) *Technique used in constructing and measuring molecular models*

Molecular models were made of straight wires that defined the chemical bonds and intersected at the centres of the atoms, and metal plates that represented the base-pairs. For preliminary study, a scale of 2 cm per Å and $\frac{1}{16}$ inch wire were used. Wire was "silver steel," hard-soldered to form a separate group for each atom. The wires were soldered while held at the correct angle in a jig. Afterwards the angles could be altered slightly by bending the soldered joint. A set of templates was used for measuring the angles. To join atoms together, the two wires forming a chemical bond were slipped into opposite ends of a hole drilled through a metal block and, with the ends of the wires touching, were clamped by screws with knurled heads.

Coordinates of atoms in the smaller models were obtained by measuring the shadow of the model in a beam of parallel light produced by reflection from a mirror and projected along the helix axis and along a dyad axis. About 7 nucleotides were joined in a chain, the coordinates of the 7 nucleotides were made roughly equivalent, and average coordinates were obtained. With the larger models only two sugar rings were built and these were made

almost exactly equivalent, and joined by a phosphate group. The model was mounted with the helix axis perpendicular to a drawing board and coordinates were measured directly, e.g. with ruler and set-square. Bond lengths and angles were calculated from the coordinates; slight adjustments of the coordinates were then made to give the best bond lengths and angles.

3. The Arrangement of Water in the DNA Crystals

(a) *General considerations*

In crystals of substances of low molecular weight, water molecules are held in definite positions by hydrogen bonds. In protein crystals the space occupied by water is larger and it appears that many water molecules do not occupy defined positions (Boyes-Watson, Davidson & Perutz, 1947; Bragg & Perutz, 1952). In crystals of vitamin B_{12} some water molecules alternate in position from one defined site to another (unpublished work of Dr. D. C. Hodgkin). We might expect that water is more likely to be arranged in a definite way between DNA molecules—with their high concentration of charged groups—than between the relatively less charged proteins.

In DNA crystals we may expect some water molecules to be arranged in a regular tenfold helical manner, e.g. a water molecule could form, by hydrogen bonds, a bridge between the oxygen atom of the sugar and the O-2 atom of a pyrimidine or the N-3 atom of a purine in the neighbouring nucleotide. Water molecules will be bound to the NH_2 groups of the bases and held in fairly well defined positions relative to the base. Hydrogen bonding to the oxygen or ring nitrogen atoms, although it will fix the distance of the water molecule from the atom, will not otherwise fix its position. Since the sequence of the bases in DNA is irregular, the arrangement of water molecules near the bases must to some extent be irregular. However, the bases, though irregular in sequence, have a helical arrangement and diffract as though they were a regular tenfold helical arrangement of an "average base-pair." Similarly, the water close to the bases may have on the average some degree of regular tenfold helical arrangement, e.g. the water molecules might tend to lie in the planes of the bases and form somewhat irregular layers hydrogen-bonded together like the layers 3·67 Å apart in ice (Megaw, 1934). Water would be bound strongly to the charged phosphate groups and Li ions. Here the positions of the water will be determined, not by binding to the phosphate groups of one DNA molecule alone, but largely by binding to the phosphate groups of two or three DNA molecules which are neighbours. Since the operation, on such a water molecule, of the tenfold screw axis through one DNA molecule will be opposed to that of the neighbouring DNA molecules, it is to be expected that the water will, to a large extent, be arranged not helically but in some more complicated way.

It seems likely that water will fill the space between the DNA molecules when the vapour pressure of water is fairly high (e.g. at 66% relative humidity) and that there will be no holes produced by evaporation. At that pressure, water will be extensively hydrogen bonded to DNA since the surface density of hydrogen-bonding sites on the DNA molecule is about the same as that on a surface of liquid water. Calculation using surface tension theory, which applies only roughly, shows that a 10 Å diameter hole in water will fill up if the relative humidity is greater than 10%. In the DNA crystals the holes cannot be as large as 10Å and the relative humidity is much greater. Hence we expect that there are no holes; and experimental data described later support this.

(b) *Dependence of the diffraction pattern on the arrangement of the water in the DNA crystals*

Probably the water molecules in the DNA crystals are arranged in rather the same way as in liquid water, which contains marked periodicities in the region of 3 Å but little periodicity above 4 Å. If this is so, the water will diffract, at angles corresponding to spacings greater than 4 Å, approximately as though it were a gas of uniform electron density. Its contribution in this manner to the diffraction pattern may be large.

Water molecules arranged in a regular or quasi-regular tenfold helical manner will contribute to the helical diffraction. For angles of diffraction corresponding to spacings greater than 5 Å, this contribution is taken into account by the method to be described: water is regarded as a gas of uniform electron density occupying a volume determined by the partial atomic volumes of the atoms in the DNA. The method, however, only takes into account the average closeness of approach of water molecules to the atoms in the DNA and therefore will not give a proper estimate of the diffraction, at angles corresponding to spacings of less than 5 Å, from water molecules in defined positions.

If some of the water molecules are arranged in a non-helical way and if the positions of these molecules, whether defined or on the average, are the same in each unit cell, then the diffraction from these water molecules will cause irregularity in the symmetrical 3-dimensional diffraction pattern from the tenfold DNA helix, and intensity may appear on the meridian of layer lines other than the 10th. It may be noted that unless the water is arranged in a helical manner, the diffraction from it is not likely to contribute much to the diffraction determined by the helical DNA, and averaged in two dimensions by rotation about the helix axis. This is because diffraction from the helix is concentrated at certain positions on the layer lines, whereas the diffraction from non-helical water is not. We expect that the fine structure within the volume of the water will have marked periodicities in the region of 3 Å. If the water molecules do not occupy fixed positions, or if the positions are fixed but are different in each unit cell (so that the positions differ by 0 to 1·5 Å from one unit cell to the next), there is no coherence between the amplitudes produced by the periodicity of the water in different unit cells. As a result, the periodicity produces diffuse scatter in the outer regions of the diffraction pattern and does not contribute to the intensity of the spots on layer lines. However the contribution of the average electron density of water to the diffraction pattern will not necessarily be affected by the periodicity of the water. The diffuse scatter from water and that due to the randomness of the sequence of the bases will be of low intensity compared with the well defined crystalline reflections and is therefore difficult to observe.

(c) *Experimental evidence concerning the arrangement of the water*

The *B* configuration of DNA occurs in several different forms in different preparations at 66% relative humidity. There are two crystalline forms of LiDNA and a partly-disordered form. LiDNA or NaDNA are sometimes observed in a form resembling that normally found at 92% humidity. In all cases the average distance apart of the molecules at 66% humidity is about the same, and no difference is apparent in the molecular structure factor f_m, averaged by rotation about the helix axis. We know that the DNA molecules are in contact at some points and that the thickness of the water layer between DNA molecules contains, on the average, a small number of water

molecules. Because the mutual arrangement of the DNA molecules is different in the various forms, we may expect differences in the arrangement of the water. Since no difference in the averaged structure factor is apparent, it appears either that the difference in the arrangement of the water in the various forms is small or that the details of the arrangement of the water are not contributing to the diffraction. The same holds for LiDNA in the *C* configuration (Marvin *et al.*, 1958) in two different semi-crystalline forms. Furthermore, the averaged structure factor of the *B* form does not alter when the separation of the molecules is increased by adding water (i.e. by increasing the relative humidity to 92%). Evidently, when we are considering the diffraction data in two dimensions (the average f_m), we are justified in regarding many of the water molecules in the structure as not having defined positions.

The observations we have described do not refer to the diffraction in three dimensions. However, when we examine the limited 3-dimensional data available (see Figs. 9 and 10), we find that the intensity distribution does not show much deviation from the symmetrical form given by a tenfold helix. Evidently any non-helical regularity that may exist in the arrangement of the water does not make a large contribution to the diffraction.

For the crystalline *A* configuration of the Na, K, and Rb salts of DNA at 75% relative humidity the outer parts of the diffraction patterns are almost identical, although the intensities in the central part differ considerably. Evidently the metal ions make little contribution to the diffraction at larger angles, and, if this is so for the ions, we may assume the same is true for at least many of the water molecules that are close to the ions. A similar effect has also been observed with a specimen of crystalline LiDNA that became contaminated with unidentified heavy ions.

The partial molecular volume of DNA (Part I, Table 3) is about the same in dilute solution and in the solid state at 40 to 92% relative humidity. This confirms our expectation that the space between the DNA molecules in the crystals is filled with water, and shows that water added above 40% relative humidity has unit density.

4. Calculation of the Fourier Transform of the Model

(a) *Diffraction from water in the structure*

The X-ray diffraction data show that periodicity in the water does not contribute much to the diffraction. Therefore it is a reasonable approximation (Wrinch, 1950) to regard the water as a uniform electron gas that fills the space between the DNA molecules. That is our procedure in the present work: later, when refining the structure, attempts will be made to find defined positions for some of the water molecules. We consider that the space occupied uniformly by the water is defined by the partial atomic volumes of the atoms in DNA. Since the volumes of charged atoms and of hydrogen-bonding atoms are smaller than those of hydrophobic atoms, account is taken of the closeness of binding of water to the various parts of the DNA molecule.

The partial molecular volume of a substance in solution is obtained by measuring the density of the solution and assuming that the solvent in the solution has the same density as pure solvent. The partial molecular volumes of bases, sugars and phosphates may be measured in solution, and, following the empirical procedure of Traube (e.g. see Smiles, 1910), the molecular volume of DNA is given by the sum of the volumes of the components minus covolumes. The value so obtained is close to that observed for DNA itself. We therefore have reason to believe that the volumes of the parts of DNA when combined in the molecule are not very different from those given by measurements of the parts separately in solution. Similar results are obtained for proteins (Cohn & Edsall, 1943). We therefore carry this approach further by taking the values for atomic volumes given by Traube as representing the distribution of volume between the atoms in the DNA molecule.

In earlier work (Feughelman *et al.*, 1955) we estimated the volume of water displaced by the bases, deoxyribose, and phosphate parts of DNA by measuring, by displacement, the volume of Courtauld models (Hartley & Robinson, 1952) of the parts. The size of the atoms in the models corresponded to van der Waals diameters, and the spaces between atoms were filled with Plasticine. This procedure gives about the same value as obtained above for the bases and phosphates, but a value too low for deoxyribose, presumably because it contains a large proportion of hydrophobic groups.

By Babinet's Principle the scattering due to the water between the DNA molecules has the same amplitude, but with opposite phase, as the scatter that would be produced by water if it filled the molecular volume of DNA. Hence the amplitude of scattering from DNA immersed in water is the amplitude from the DNA minus the amplitude from the molecular volume filled uniformly with electron density of water of unit density (0·33 electrons per Å^3). A water molecule in liquid water behaves, so far as size is concerned, like a sphere of 2·76 Å diameter (Wells, 1954); hence the atomic volumes coalesce in DNA to form a continuous molecular volume from which water is excluded.

There is in general no easy way of calculating the diffraction from the continuous molecular volume.† However, if we consider different parts of the molecular volume separately it can be seen that in all cases the diffraction from the volume is small in the outer parts of the DNA diffraction pattern.

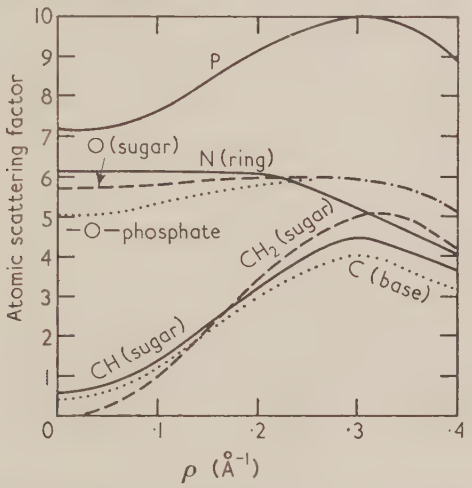

Fig. 7. Atomic scattering factors for atoms immersed in water. To avoid confusion some curves used in our calculations have been omitted; these may be obtained by interpolation from the curves shown and from the Z_e values in Table 2.

(1) Some atoms in DNA, e.g. the charged oxygen atoms of the phosphate group, are to a large extent surrounded by water and may be regarded approximately as isolated atoms. The atomic volume of an isolated atom surrounded by water may be taken as a sphere. The average volume of atoms (other than hydrogen) in DNA is equal to that of a sphere of 3 Å diameter. The scattering factor of a 3 Å sphere for $\rho = 0{\cdot}3$ Å^{-1} is one third its value for $\rho = 0$. Hence in the outer part of the diffraction pattern of DNA ($\rho = 0{\cdot}3$ Å^{-1}) the ratio of the amplitude of scattering from the displaced water to that from the atom is small compared with the ratio for $\rho = 0$. This is so simply because the electrons in the atom are concentrated in a volume smaller than that of the displaced water. (2) For a layer of atoms, e.g. a nitrogen base or sugar ring viewed edge-ways, the scattering factor of the molecular volume will resemble that of a plate 3 to 3·5 Å thick and will have a small value in the region of $\rho = 0{\cdot}3$ Å^{-1}. (3) Where a number of DNA atoms are close together and a large continuous molecular volume is formed, the scattering factors of the atomic volumes are not simply defined. However, the scattering from a large continuous volume decreases, as ρ increases, to a small fraction of that at $\rho = 0$.

† The development of the ideas in this section was greatly aided by discussion with Dr. A. R. Stokes.

These considerations indicate that we will not be greatly in error if we take the scattering factors of all the atomic volumes in DNA as being of the same form and resembling, for instance, that of a plate 3 Å thick. To obtain the scattering from DNA in water, we subtract such scattering factors from those of the atoms of DNA. At $\rho = 0$ the factors are equal to the product of the atomic volume and the electron density of water. The resulting atomic scattering factors, multiplied by a temperature factor $\exp\left(\frac{B}{4}\rho^2\right)$, with $B = 4$ Å^2, are shown in Fig. 7.

The approximate method we have described could be used to calculate the diffraction from macromolecules, other than DNA, when immersed in water. The method will be valid in the case of globular proteins, where water does not penetrate the bulk of the molecule, because the partial volume of the atoms are approximately the same whether an atom is surrounded by other protein atoms or by water molecules.

When calculating diffraction from Model 3 we used the scattering factors shown in Fig. 7. The data in Figs 2 to 5 were calculated earlier using the somewhat different method of Feughelman *et al.* (1955), Z_e the effective number of electrons scattering X-rays for

Table 2

The volumes (V) of the atoms in DNA and the effective atomic scattering factor (Z_e) at zero angle for the atoms immersed in water

Group	Atom	V (Å^3)	Z_e
phosphate	P	47	7·2
	—O—	9·1	5·0
	½–O	5	6·9
	Li	1·8	(0)
	ionisation	− 22·4	
sugar	C_1, C_3, C_4	19·5	0·6
	C_2, C_5	24·7	− 0·2 (0)
	—O—	7·1	5·7
bases	N (ring)	2·5	6·2
	NH_2	12·8	4·8
	C (no H)	16·4	0·6
	CH	21·6	− 0·1 (0)
	= O	9·1	5·0
	CH_3	32	− 1·6 (0)

atoms immersed in water being as follows: for base and sugar C = 3·2, N = 3·8, O = 4·3; for phosphate P = 9·6 and O = 5·4 (Langridge *et al.*, 1957). We regard the hydrogen atoms as being centred at the adjacent atoms. We ceased using the method of Feughelman *et al.* because it involved the use of different atomic scattering factors in the various Bessel function terms (see Appendix) of which T^2 is composed: this seemed unjustifiable. The transforms of a DNA model obtained by the new and old methods have the same general form but the ratio of the values of T^2 for large and small ρ is greater with the new method than for the old.

The partial atomic volumes used in deriving the scattering curves in Fig. 7 are given in Table 2. In estimating the atomic volumes in the phosphate group the negative volume associated with the ionisation of the group is distributed between all atoms in the group. The small negative scattering factors of hydrophobic groups are taken as zero. If the atomic volumes in Table 2 are used to calculate the specific volume of LiDNA containing equal properties of all four bases, a value of 0·56 is obtained. This is in reasonable agreement with the value for solid LiDNA (Part I, Table 3).

(b) *Diffraction from DNA*

The Fourier transform of the molecular model is calculated in terms of Bessel functions (see Appendix). The phosphate and sugar part of the molecule and the nitrogen atoms at the end of the glycosidic link are arranged helically in the model. The bases are planar and are all inclined to the helix axis at the same angle. The four bases in the model are present in equal proportions and the sequence of bases along a polynucleotide chain is random. Because the bases have random sequence, they diffract as though they were a regular helical arrangement of an average base, except that the randomness gives rise to diffuse diffraction. This diffuse scatter is not concentrated on the layer lines of the helical pattern and is ignored. Therefore, in the expression for diffraction from the model, we take the amplitude scattered from each atom in the phosphate and sugar and one quarter the amplitude from every atom in the four different bases.

(c) *Comparison of the observed diffraction with that calculated from Model* 3

Model 3 was designed so that the observed intensities of diffraction when plotted in two dimensions were in reasonably good agreement with T^2, the square of the Fourier transform of the model averaged by rotation about the helix axis. Many

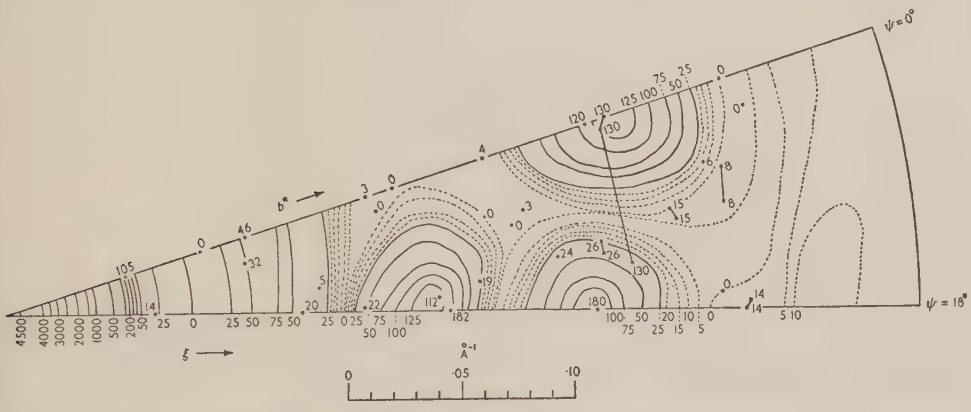

Fig. 8. Square of the Fourier transform of Model 3 on the equatorial layer plane. Observed intensities are obtained from the diffraction pattern shown in Part I, Plate IV; where reflections overlap, the corresponding reciprocal lattice points are joined by a line and the intensities are divided equally between the points. To show the tenfold symmetry of the intensity data, the layer plane has been divided into 18° sectors and these have been superimposed.

fibrous substances consist of non-crystalline aggregates of parallel molecules and give diffraction that corresponds to an averaged T^2, and the data cannot be analysed in three dimensions. Because DNA is crystalline it is possible to identify the directions of diffraction in three dimensions. This is a considerable advantage because one can test the correctness of the model by comparing observed and calculated intensities in three dimensions.

The X-ray data in Part I indicate that the DNA crystal lattice is orthorhombic and molecules m_1 and m_2 in the unit cell (Part I, Fig. 4) are oriented, about the c axis, in the same or very nearly the same direction. It follows that, if the DNA molecules have the symmetry shown in Fig. 1 and the space group is $P2_12_12_1$, a dyad axis through the molecule must lie close to or along a or b. The symmetry of packing then suggests that the dyad axis will lie exactly along a or b.

The transform of the DNA structure has, for small ξ, approximately circular symmetry about the helix axis and the 3-dimensional data have this form. For larger

ξ, the transform has a component with tenfold symmetry; for a given ξ, T^2 varies considerably as ψ varies. The observed intensities show this effect. By comparison of observed intensities with the transform, it is clear that a dyad in the DNA molecule is parallel to b. The 6th and equatorial layer planes show most clearly the tenfold symmetry; a comparison of the observed intensities and the transform is shown in Figs. 8 and 9. In these figures the data are plotted as follows: a layer plane is divided into sectors covering the range ψ from 0° to 18°, 18° to 36°, etc.; all the sectors are then superimposed. There is general agreement between calculated and observed data and no serious discrepancy. If the observed intensities correspond to diffraction from a tenfold helix, the values will lie on a continuous surface. They do so approximately, but there are small discrepancies, e.g. compare the intensities of the 406 and 136 reflections. These discrepancies may be due to scatter from water arranged in a special manner that is not that of a tenfold helix.

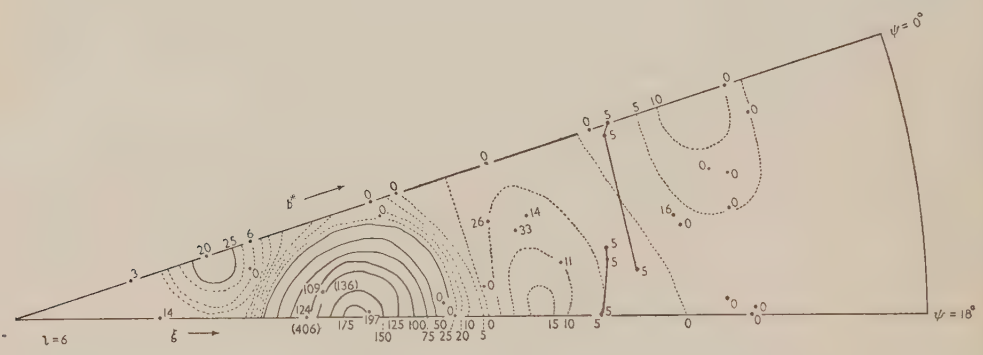

Fig. 9. The equivalent of Fig. 8 for the 6th layer plane.

If reciprocal lattice points on a given layer plane have the same value of ξ, the reflections overlap on the fibre diagram. When plotting the observed intensities of overlapping reflections we assume, in the absence of direct information, that the structure amplitude is the same for all ψ and we plot the average observed intensity per point. The calculated value is the sum of the intensities for the various points divided by the weighted number of reciprocal lattice points. The weighting takes into account interference between amplitudes scattered from the two molecules in the unit cell (see Part I).

(d) *The optical transform*

Optical transforms of two projections of the DNA structure were obtained to check our calculations of T^2. We used masks prepared by photographic reduction (Hooper, Seeds & Stokes, 1955). The areas of the holes in the mask were roughly proportional to the number of electrons in the atoms. Where the atomic positions in the projection were so close that the holes in the mask would overlap slightly, the atomic positions were displaced (but not more than 0·2 Å) so that overlap of holes was avoided. Where atomic positions almost coincided, one large hole was used to correspond to the scattering of the atoms.

The optical transform was, as described by Hooper (Finch, Green, Holmes & North, 1958), similar in its main features to the calculated transform. This result was not affected by the fact that the atomic positions used for the optical transform were slightly different from those of Model 3. The difference of the transform (Plate I) for

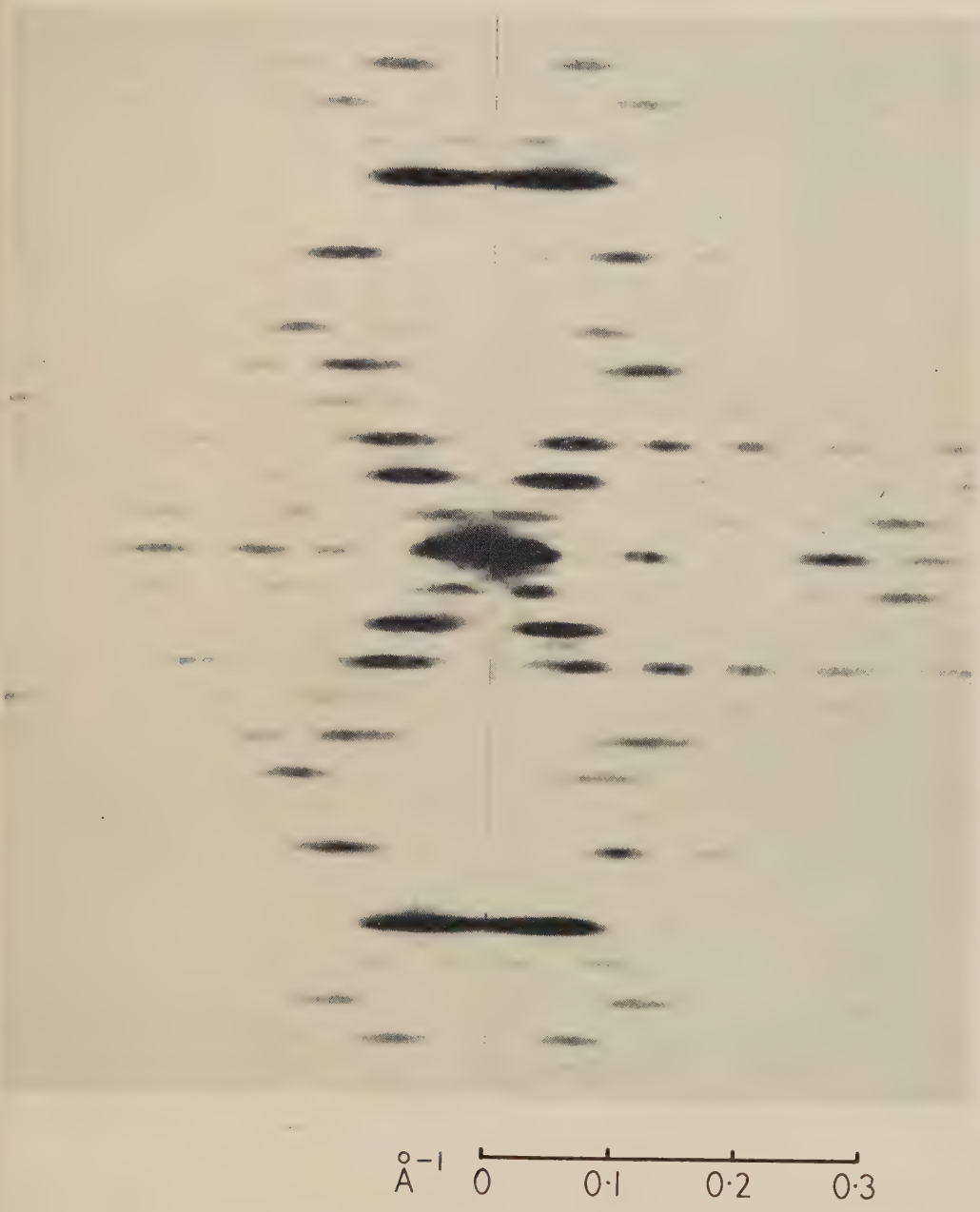

PLATE I. Optical transform of two projections of a DNA structure resembling Model 3. On the left the structure is projected down a dyad axis, i.e. parallel to b and $\psi = 18°$; on the right the projection is along a or $\psi = 0°$.

[*To face page* 54

two projections of the DNA molecule was similar to that calculated. This may be seen by comparing densitometer curves of the diffractograms (Fig. 10) with the plots of T^2 in Figs 8 and 9.

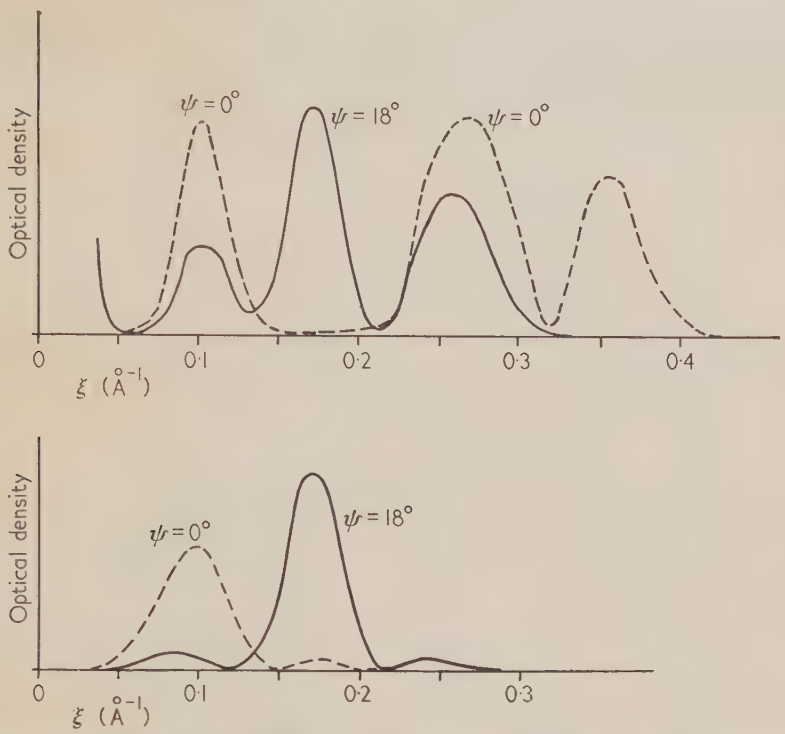

Fig. 10. Densitometer traces along the equator (top) and 6th layer line (bottom) of the optical diffraction pattern in Plate I.

5. Discussion of the Structure

(a) *Stereochemistry of Model 3*

The stereochemical basis for building molecular models of macromolecules is not as precise as one would wish. We consider that our model is fairly close to the actual structure of DNA and is satisfactory within the limits of present stereochemical knowledge but is likely to be improved, e.g. bond angle distortions may be reduced, as further X-ray and stereochemical data become available and are utilised.

The dimensions of the base-pairs were derived from data on structure of purines, pyrimidines and analogous compounds (Spencer, 1959); they were not very different from those used earlier (Langridge *et al.*, 1957). To increase the distance between a base and the C_2 atom of the sugar of the neighbouring nucleotide, the base pairs were twisted 5° about an axis passing through the helix axis and perpendicular to it and the dyad axis. The twist causes the hydrogen bonds between bases to be deflected through 8°. Distances between atoms in a base and in another lying on it are greater than 3·36 Å except where a purine on one polynucleotide chain overlaps a purine on the other. In these regions twisting of the base-pair causes distances to be smaller, e.g. 3·13 Å between N_2 of guanine and C_2 of an adjacent purine, 3·12 Å between one N_2 of guanine and another N_2, and 3·13 Å between N_6 or O_6 of a purine and another

N_6 or O_6. These distances are small, and it is clear that the twist cannot be made much greater than 5° if the structure is to be regular.

In various nucleotides and nucleosides (Furberg, 1950; Huber, 1957; Alver & Furberg, 1959) the orientations of the sugar ring relative to the base are different, presumably because the sugar can be rotated about the single bond that forms the glycosidic link. This rotation is restricted by repulsion between the C_2 and O_5 atoms

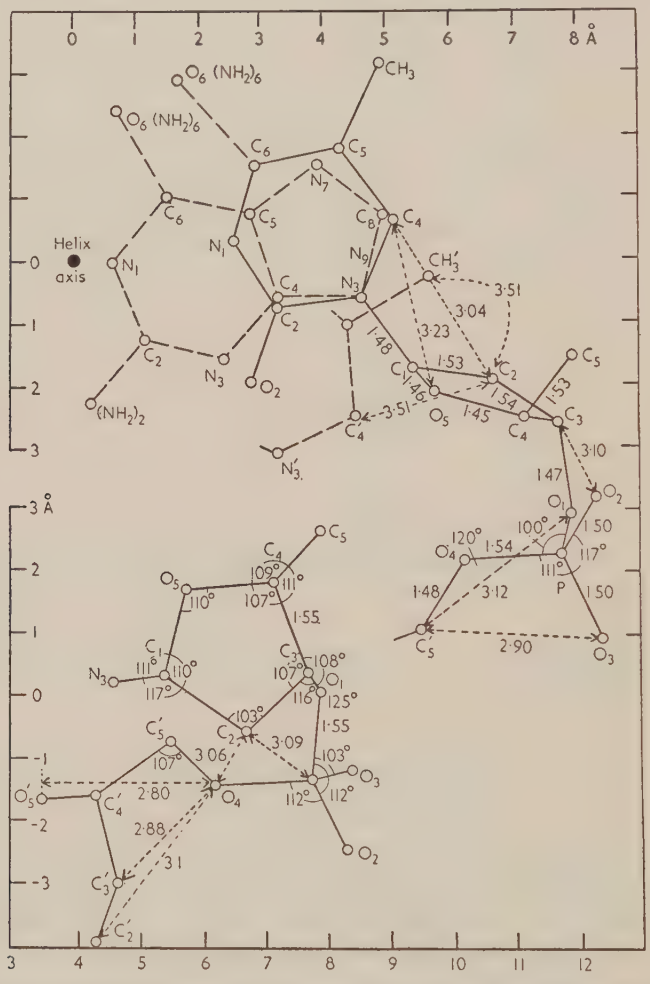

Fig. 11. Model 3 showing projections of a nucleotide on planes perpendicular to the helix axis and to the dyad axis. Bond lengths and angles and short interatomic distances are shown.

of the sugar and the C_4 atom of pyrimidines. In our model the C_2 and C_4 atoms are slightly closer (less than 0·05 Å) than in the roughly determined structure of bromodeoxythymidine (Huber, 1957). If we suppose (Westheimer, 1956) that the forces between the atoms are similar to those between neon atoms (Zucker, 1956), 60 and 150 cal/mole will be required to move a pair of atoms respectively 0·3 and 0·4 Å closer than the equilibrium van der Waals distance. On this basis we estimate that the difference of energy between the suggested configuration and that of lowest energy is not more than 100 cal/mole. In purine nucleotides this difference is probably negligible because the purine C_8 atom is 0·2 Å further from the C_2 atom of the sugar. A difficulty in making

estimates of repulsive energy between non-bonded atoms is that the van der Waals radius of an atom is probably not fixed but varies with the angle between the direction in which it is measured and the direction of the bonds to the atom (Pauling, 1948).

It is expected (Spencer, 1959) that the sugar ring will be puckered with either C_2 or C_3 about 0·5 Å out of the plane in which, approximately, the other atoms lie. In our model the configuration is as expected; though the amount by which the C_2

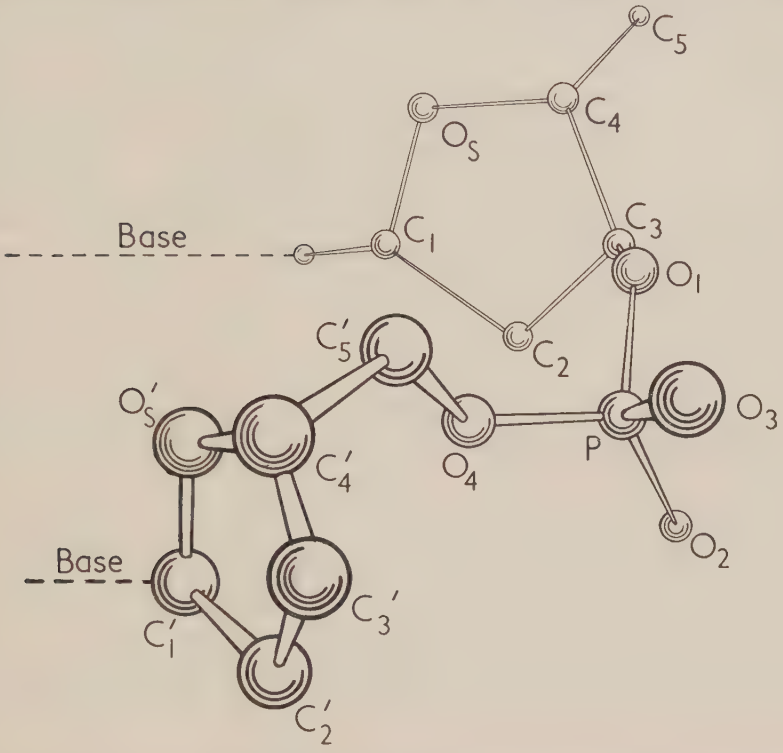

Fig. 12. Part of a polynucleotide chain in Model 3. The view is along a dyad axis (as in Fig. 11) and atoms nearer to the viewer are drawn larger.

atom is out-of-plane (0·3 Å) is rather small. In calcium thymidylate (Horn, Luzzati & Trueblood, private communication) the C_3 atom is 0·5 Å out-of-plane. Analogy with *cyclo*pentane (Pitzer, 1945) suggests that the energy required to flatten the ring may be about 5 kcal. In building a previous model (Langridge *et al.*, 1957) we had been unable to avoid a planar ring; clearly the present model is much to be preferred so far as sugar configuration is concerned. The hydrogen atoms attached to C_5 are staggered in relation to the bonds about C_4 (Dauben & Pitzer, 1956).

The phosphate group resembles that in dibenzyl phosphate (Dunitz & Rollett, 1956). The angle between the C_3O_1P and C_5O_4P planes is about 100°: Dunitz & Rollett suggested a value of about 90° is to be expected. The O_1PO_4 and C_3O_1P angles are 100° and 125° respectively; values in dibenzyl phosphate are 104° and 122°; comparable angles in sodium triphosphate are 98° and 121° (Davies & Corbridge, 1958). The position of the phosphate group is little different from that in our previous model (Langridge *et al.*, 1957). The orientation, however, is different and is in agreement with deductions from the infrared absorption of DNA. The correctness of the interpretation

of the infrared data is not firmly established but it seems very likely that the absence, in oriented specimens of DNA, of dichroism in the region of 1230 cm^{-1} means that the O_2O_3 direction and the bisector of the O_2PO_3 angle both lie at 54·5 $\pm$ 10° to the helix axis (Fraser & Fraser, 1951; Sutherland & Tsuboi, 1957; Wilkinson, Price & Bradbury, 1959). In our present model these angles are 60° and 57° respectively. In the previous model they were 13° and 81° and, if this were so in DNA, one might expect considerable dichroism.

Some bond angles in the structure (Fig. 11) differ by 4° from values (Spencer, 1959) one might expect from consideration of the structure in crystals of the components of DNA and related compounds. We would prefer these differences to be smaller but they are, in fact, no greater than has been recently observed in calcium thymidylate (Horn, Luzzati & Trueblood, private communication). In some crystals packing of the parts of the molecules can cause fairly considerable distortion of some bond angles, e.g. in a di- and a tri-peptide (Leung & Marsh, 1958) an angle between bonds in a tetrahedral carbon atom is respectively 115° and 118° instead of 109·5°. While it is very desirable when building models of large molecules to seek a structure without distorted bonds, it is reasonable to make, when necessary, distortions of about 3° in angles. The energy required to distort a bond angle is proportional to the square of the distortion, and for 3° is about 200 cal/mole for single bonds at carbon atoms (Westheimer, 1956). When comparing the bond angles observed in a crystal of a component of DNA with those in DNA it must be remembered that the angles in a chemical group may be distorted in the crystal in a different or opposite direction to that in DNA.

The structure is tightly packed, and several distances between non-bonded atoms (Fig. 11) are less than the sum of the van der Waals radii. However, none of the distances seems very objectionable—the shortest is 2·88 Å between phosphate O_4 and sugar C_3'. If the sum of the van der Waals radii of carbon and oxygen is 3·1 Å, the energy of repulsion between the atoms is probably not more than 0·1 kcal per pair. The distance between the hydrogen atom attached to C_2 of the sugar and O_4 is about 2·5 Å. This distance might be short if there were a weak CHO hydrogen bond.

(b) *Molecular packing in the unit cell*

There is correlation between molecular packing and the configuration of the DNA molecule. Since we deduced the configuration without reference to packing, this correlation helps to confirm the correctness of the configuration.

To a large extent, packing is determined by the positions of the O_2 and O_3 atoms of the phosphate groups. These atoms are the most projecting parts of the molecules and, since each O_2 O_3 pair carries charge $-e$, they repel each other. Molecules m_2 (Part I, Fig. 4), at the same height in the unit cell, are 22·7 Å apart and cannot come much closer together because the chain of phosphate groups on one molecule is almost in contact with the chain on the neighbouring molecule. Molecules m_1 and m_2 are only 19·3 Å apart: they can approach this closely because their relative displacement dc in the helix axis direction enables phosphate chains on m_1 to fit between the chains on m_2. The observed value of d may be accounted for as follows.

First let us represent the chains of O_2 and O_3 atoms by continuous helices (A, B, etc., Fig. 13) drawn through points midway between the O_2 and O_3 atoms. If the width of the two grooves on the double helical molecule were equal, i.e. if the separation of A and B and A' and B on m_2 were equal, C and D on m_1 could penetrate

furthest between the chains on m_2 if $d = 0{\cdot}25$. In our model of DNA A and B are separated in the helix axis direction by 14·8 Å and A' and B by 18·8 Å. Chain C can penetrate less between A and B than D can between A' and B. If C lies halfway between A and B the molecules can approach as close as is possible; d is then 0·28.

In semi-crystalline LiDNA at relative humidity above 75% (see Part I, Table 1), the structure resembles the crystalline structure at 66% relative humidity except that the molecules are further apart and the structure is disordered. Regarded as continuous helices, the molecules are related in position to each other, but there is no special relation between the position of phosphate groups on different molecules. In

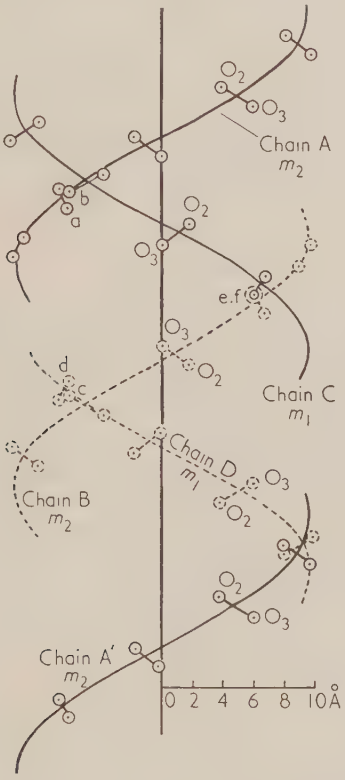

Fig. 13. Diagram showing the relative arrangement of molecules m_1 and m_2 in the unit cell. The contiguous parts of m_1 and m_2 are projected parallel to a line in the ab plane and passing through the centres of m_1 and m_2. Each phosphate-ester chain is represented by a line and the O_2 and O_3 atoms are shown.

other words (Klug & Franklin, 1958) the structure has screw disorder. Since the molecules behave like continuous helices, as we expect, the observed value of d is about 0·25 (Marvin, 1958). In the semi-crystalline hexagonal structure of NaDNA at 92% relative humidity (Feughelman *et al.*, 1955), neighbouring molecules are displaced $c/3$ and $c/6$ relative to each other: the average value of d is 0·25.

In the crystalline structure of LiDNA the arrangement of the phosphate groups along the polynucleotide chains has an important influence on the packing and causes d to differ somewhat from the value expected for continuous chains. The observed arrangement of m_1 and m_2 is shown in Figs. 13 and 14. The value of d is 0·33. There is no obvious reason why d should have this value precisely. While it is true that increase of d from 0·28 to 0·33 causes the distance between the juxtaposed phosphate groups on

chains B and C and on D and C to increase, increase of d above 0·33 causes the distance to increase further—in particular the separation of O_3 atoms a and b, c and d, which are in contact, increases. However, change of d does not have a marked effect on their separation and they cannot come closer than 2·5 Å because they are that distance apart in projection on the ab plane. Because of this, and because the interaction of m_1 and m_2 as a whole will determine d, we do not expect that we can account precisely

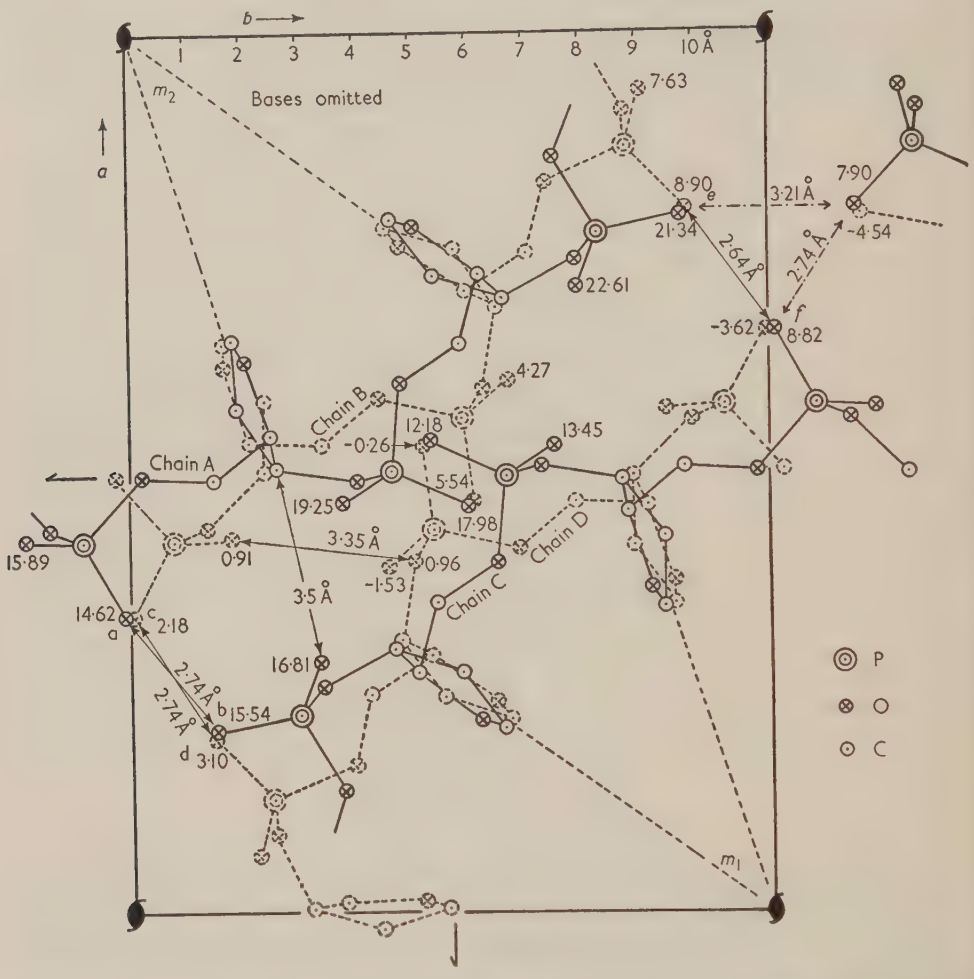

Fig. 14. Projection down the c axis of a quarter unit cell of LiDNA showing short intermolecular distances and the c coordinates of O_2 and O_3 atoms relative to a dyad axis through m_2 and parallel to b. The nomenclature a, b, etc. for atoms and A, B, etc. for phosphate-ester chains is the same as in Fig. 13.

for the value of d observed. In fact, the lack of marked molecular interlocking, which could fix the value of d, is consistent with the difficulty of obtaining good crystalline specimens of LiDNA (see Part I).

Distances of close approach between atoms of neighbouring molecules are shown in Fig. 14. Between m_1 or m_2 the smallest distance is 3·2 Å between O_3 atoms. In each pair of m_1 and m_2 molecules there are, per helix turn, one 2·64 Å and two 2·74 Å distances between O_3 atoms. We might not expect these atoms to be so close together—in fact at roughly the van der Waals equilibrium distance—because, in the absence of

applied field, we may expect each atom to have half an electronic charge and they will repel each other. However, when two O_3 atoms are close together, charge will move from O_3 to O_2 atoms and repulsion between the O_3 atoms will be reduced. Moreover, there is little reason to suppose that the molecules are exactly helical: local distortion would permit the O_3 atoms to move apart.

Consideration of packing confirms that the arrangement of the molecules in the unit cell, deduced from 3-dimensional diffraction data, is correct. If the molecules are rotated 90° into the alternative position compatible with the space group but not with 3-dimensional diffraction data, there are between m_1 and m_2, per turn of the helix, two distances of 2·18 Å between O_3 and O_1 atoms and two distances of 2·34 Å between O_3 and C_5 atoms. Also the number, per unit cell, of interatomic distances less than 3·5 Å is increased 6 times. Clearly this arrangement of molecules is not to be preferred.

It is likely that most phosphate groups are linked by hydrogen bonds through water molecules and that the Li ions are surrounded by water molecules. We have not yet attempted to determine this part of the structure.

6. Conclusion

There are good reasons for believing that Model 3 is essentially correct in spite of the limited resolution of the diffraction data and the approximations used for taking into account the water in the structure. Preliminary examination of 3-dimensional data clearly confirms the correctness of the structure. It is also significant that a minor adjustment of the model previously described (Langridge *et al.*, 1957) gave rise to Model 3 which was superior in several important respects: (1) stereochemistry generally; (2) pucker of the sugar ring; (3) correlation of the orientation of the phosphate group with infrared absorption data.

It is not suggested that Model 3 is more than approximately correct. More detailed 3-dimensional diffraction data now becoming available should make it worthwhile to use 3-dimensional Fourier synthesis. In this way it may be possible to refine the DNA configuration and more adequately treat the water in the structure.

We wish to thank Professor J. T. Randall, F.R.S. and Drs. C. P. Rhoads,† J. Burchenal and C. C. Stock for encouragement; Drs. A. R. Stokes, M. Spencer, G. Zubay, F. H. C. Crick, H. W. Wyckoff, J. S. Rollett, D. C. Hodgkin, J. Iball and Mr. G. R. Wilkinson for discussion; Mr. W. Fuller for recalculating various data; I.B.M. United Kingdom Ltd. and I.B.M. World Trade Corporation for free computer time and the University of London Computer Unit for computing facilities.

Two of us (W.E.S. and H.R.W.) acknowledge award of grants from the British Empire Cancer Campaign and one of us (D.A.M.) acknowledges award of a National Science Foundation Predoctoral Fellowship. The work at King's College was aided by a grant from The Rockefeller Foundation and that at Sloan-Kettering Research Institute by a grant from the Commonwealth Fund.

REFERENCES

Alver, E. & Furberg, S. (1959). *Acta. Chem. Scand.* **13**, 910.
Boyes-Watson, J., Davidson, E. & Perutz, M. F. (1947). *Proc. Roy. Soc.* A. **191**, 83.
Bragg, W. L. & Perutz, M. F. (1952). *Acta Cryst.* **5**, 277.
Cohn, E. J. & Edsall, J. T. (1943). In *Proteins, Amino acids and Peptides*, Chapter 7. New York: Reinhold.

† Died 13 August, 1959.

Crick, F. H. C. & Watson, J. D. (1954). *Proc. Roy. Soc.* A, **223**, 80.
Dauben, W. G. & Pitzer, K. S. (1956). *In Steric Effects in Organic Chemistry*, Chapter 1, ed. by M. S. Newman. New York: Wiley.
Davies, D. R. & Corbridge, D. E. C. (1958). *Acta Cryst.* **11**, 315.
Dunitz, J. D. & Rollett, J. S. (1956). *Acta Cryst.* **9**, 327.
Feughelman, M., Langridge, R., Seeds, W. E., Stokes, A. R., Wilson, H. R., Hooper, C. W., Wilkins, M. H. F., Barclay, R. K. & Hamilton, L. D. (1955). *Nature*, **175**, 834.
Finch, J., Green, D. W., Holmes, K. C. & North, A. C. T. (1958). *Brit. J. Appl. Phys.* **9**, 1.
Fraser, M. J. & Fraser, R. D. B. (1951). *Nature*, **167**, 759.
Furberg, S. (1950). *Acta Cryst.* **3**, 825.
Hartley, G. S. & Robinson, C. (1952). *Trans. Faraday Soc.* **48**, 847.
Hooper, C. W., Seeds, W. E. & Stokes, A. R. (1955). *Nature*, **175**, 679.
Huber, M. (1957). *Acta Cryst.* **10**, 129.
Klug, A., Crick, F. H. C. & Wyckoff, H. W. (1958). *Acta Cryst.* **11**, 199.
Klug, A. & Franklin, R. E. (1958). *Disc. Faraday Soc.* **25**, 104.
Langridge, R., Seeds, W. E., Wilson, H. R., Hooper, C. W., Wilkins, M. H. F. & Hamilton, L. D. (1957). *J. Biophys. Biochem. Cytol.* **3**, 767.
Leung, Y. C. & Marsh, R. E. (1958). *Acta. Cryst.* **11**, 17.
Marvin, D. A. (1958). *Disc. Faraday Soc.* **25**, 203.
Marvin, D. A., Spencer, M., Wilkins, M. H. F. & Hamilton, L. D. (1958). *Nature*, **182**, 387.
Megaw, H. D. (1934). *Nature*, **134**, 900.
Pauling, L. (1948). *The Nature of the Chemical Bond*, 2nd Edition, p. 192. Ithaca: Cornell University Press.
Pitzer, K. S. (1945). *Science*, **101**, 672.
Smiles, S. (1910). In *The Relation between Chemical Constitution and some Physical Properties*. London: Longman & Green.
Spencer, M. (1959). *Acta Cryst.* **12**, 60.
Sutherland, G. B. B. M. & Tsuboi, M. (1957). *Proc. Roy. Soc.* A, **239**, 446.
Wells, A. F. (1954). *Quart. Rev. Chem. Soc.* **VIII**, No. 4, 380.
Westheimer, F. H. (1956). In *Steric Effects in Organic Chemistry*, Chapter 12, ed. by M. S. Newman. New York: Wiley.
Wilkins, M. H. F. (1956). *Cold Spr. Harb. Symp. Quant. Biol.* **21**, 75.
Wilkins, M. H. F. (1957). In *Special Publications of the New York Academy of Sciences*, **V**, 180.
Wilkinson, G. R., Price, W. C. & Bradbury, E. M. (1959). *Spectrochemica Acta*, **14**, 284.
Wrinch, D. (1950). *Acta Cryst.* **3**, 475.
Wyckoff, H. W. (1955). Ph.D. Thesis, M.I.T., Cambridge, Mass., U.S.A.
Zucker, I. J. (1956). *J. Chem. Phys.* **25**, 915.

APPENDIX

Calculation of the Fourier Transform of a Helical Molecule

R. Langridge

Wheatstone Laboratory, King's College, London, England

AND

M. P. Barnett and A. F. Mann

I.B.M. United Kingdom Ltd., London, England

The unit cell of LiDNA contains about 840 atoms apart from hydrogen and water. The calculation of structure factors by the usual methods would take a long time. However, the symmetry of the helical DNA molecule is such that a simplified expression for the structure factors may be derived.

If there are j atoms in the repeating unit of a helical molecule the structure factors can be written (Cochran, Crick & Vand, 1952; and Stokes (unpublished)).

$$F(l, \psi, \xi) = \sum_n \sum_j f_j J_n (2\pi R_j \xi) \exp i\left\{n\left(\psi - \phi_j + \frac{\pi}{2}\right) + \frac{2\pi l z_j}{c}\right\} \tag{1}$$

where l = layer line number
ψ = angular co-ordinate of a lattice point in reciprocal space
ξ = radial co-ordinate of a lattice point in reciprocal space
R_j, ϕ_j, Z_j = real space cylindrical co-ordinates of the j^{th} atom in the repeating unit
f_j = scattering factor of the j^{th} atom
c = length of the unit cell c axis
J_n = Bessel function of the first kind of order n
n is defined as the integral solutions of

$$\frac{n}{P} = \frac{l}{c} - \frac{m}{p}$$

where P = pitch of the helix
p = axial separation of the repeating units
and m can take any integral value.

$\frac{c}{P}$ and $\frac{c}{p}$ must be integral, because c is the crystallographic repeat, but $\frac{P}{p}$ is not necessarily integral; so if we write $\frac{c}{P} = K$ and $\frac{c}{p} = \mathrm{N}$ we have

$$n = \frac{l - mN}{K} \tag{2}$$

The expression in this form is more suitable for use on a digital computer.

If the azimuthal orientation of the molecule in the unit cell is unknown, ψ cannot be determined, and a more useful function in this case is the Fourier transform of a single molecule calculated for each value of n

$$G(l, n, \xi) = \sum_j f_j J_n (2\pi R_j \xi) \exp i\left(\frac{2\pi l Z_j}{c} - n\phi_j\right) \tag{3}$$

Having calculated G, the values of ψ can be found which give the best fit of the calculated structure factors to the observed values from

$$F(l, \psi, \xi) = \sum_n G(l, n, \xi) \exp i\, n(\psi + \pi/2) \tag{4}$$

The transform of DNA is a special case of (3) as there is a dyad in each helical repeat perpendicular to the helix axis. For every atom at (R_j, ϕ_j, Z_j) there is an equivalent atom at $(R_j, -\phi_j, -Z_j)$ so that the expression for G only involves the real (cosine) part of the imaginary exponential. Specially computed scattering factors are also required to allow for the high water content of the molecule.

Equation (3) was programmed for calculation by the IBM 650 Electronic Data Processing Machine.

The computer is provided with the limits of l and m; the range and increments of ξ; c^2 and $1/c^2$; N and K. Each atom is represented by a card carrying its co-ordinates (R, ϕ, Z) and the atoms are arranged in groups having similar scattering factors. Each group is preceded by a table of scattering factors appropriate to that group. These are read into machine storage in one-to-one correspondence with a series of values of $\left(\frac{2 \sin \theta}{\lambda}\right)^2$ (θ = Bragg angle, λ = wavelength of the radiation). Now $\left(\frac{2 \sin \theta}{\lambda}\right)^2 = \frac{l^2}{c^2} + \xi^2$ so that for each (l, ξ), $\left(\frac{2 \sin \theta}{\lambda}\right)^2$ is computed and the appropriate scattering factor selected by a table-look-up operation. Integral solutions of equation (2) are found by the machine, and for these the transform over the required range one atom at a time is computed, the partial sum being stored until all the atoms have been used. Then the results are punched or printed on the form: m, l, n, ξ, (cos), (sin), G, where (cos) and (sin) denote the real and imaginary parts of G.

The Bessel functions J_0 and J_1 are computed to 9 decimal places by the use of Chebychev polynomials derived by Hitchcock (1957). The Bessel functions of higher order are found by repeated application of the recurrence relation,

$$J_{n+1}(x) = \frac{2n}{x} J_n(x) - J_{n-1}(x)$$

Although significant figures are lost by using this technique, the percentage error becomes large only for values of $J_n(x)$ so small that they can be neglected.

As an example of computer running times, with 450 points on the transform (10 layer lines, 15 points along each layer line, $m = 0$ and ± 1), the programme takes 30 min for the 30 atoms of the DNA helical repeating unit; the output time being 4·5 min. The general programme (including the real and imaginary parts) is slightly slower. This speed compares favourably with approximately 2 weeks of hand calculation required, using previously prepared tables of Bessel functions.

REFERENCES

Cochran, W., Crick, F. H. C. & Vand, V. (1952). *Acta Cryst.* **5**, 581.

Hitchcook, A. J. M. (1952). *Mathematical Tables and other Aids to Computation*, Volume XI, No. 58, p. 86.

J. Mol. Biol. (1960) **2**, 65-68

A Strongly Antigenic Synthetic Polypeptide

Thomas J. Gill III† and Paul Doty

Department of Chemistry, Harvard University, Cambridge, Massachusetts, U.S.A.

(*Received 7 February 1960*)

A linear polypeptide of L-glutamic acid, L-lysine and L-tyrosine in the proportions of 2·8 : 2·6 : 1·0 has been synthesised and found to behave as a strong antigen giving precipitin, agar diffusion and ring tests comparable to typical proteins. The polypeptide has a molecular weight of 49,000 (370 residues) and appears to have no significant helical structure at pH 10·7 where the immunological tests were made. The bands in the gel diffusion tubes and the precipitin curve showed several maxima suggesting the presence of several different antibodies.

We wish to report the synthesis of a linear polypeptide that is strongly antigenic, giving precipitin, agar diffusion, and ring tests comparable to typical proteins.

Previous work in this direction has been of two kinds. In one approach synthetic polypeptides have been used directly with the result that antibody formation did not occur or was very weak, exhibiting itself not in precipitin or ring tests with antisera but rather by the more sensitive passive cutaneous anaphylaxis test (Maurer, Subrahmanyam, Katchalski & Blout, 1959). In some cases precipitin reactions were found if the polypeptide was linked to a protein carrier (Stahmann, Tsuyuki, Weinke, Lapresle & Grabar, 1955; Maurer, 1957; Stahmann, Lapresle, Buchanan-Davidson & Grabar, 1959; Buchanan-Davidson, Dellert, Kornguth & Stahmann, 1959; Buchanan-Davidson, Stahmann, Lapresle & Grabar, 1959; Buchanan-Davidson, Stahmann & Dellert, 1959). In another approach gelatin, a protein of very low antigenicity, was coupled with various aromatic groups and tested as an antigen (Landsteiner, 1919; Hooker & Boyd, 1933). When short poly-L-tyrosine chains were coupled to gelatin resulting in a branched structure having a tyrosine content of 16%, intra-abdominal injection of this material sensitized guinea pigs against intracardiac injection of the same substance; similar treatment with gelatin produced no sensitization (Sela, Katchalski & Olitzki, 1956). More recently, Sela & Arnon (in the press) have shown that polytyrosyl gelatins act as strong antigens in rabbits and induce specific antibody formation.

In order to search for the minimal requirements for antigenicity we have prepared a synthetic polypeptide containing tyrosine and two other amino acids whose copolymer is known to be only weakly antigenic (Maurer *et al.*, 1959). The polymer prepared was a linear polypeptide of L-glutamic acid, L-lysine and L-tyrosine in the mole ratio of 2.8 : 2.6 : 1.0. It was made by polymerizing the mixture of the corresponding N-carboxy-anhydrides in benzene at a total concentration of 4% using sodium methoxide as initiator at an anhydride : initiator ratio of 400. The polymerization proceded for 28 min and was then stopped by bubbling HBr into the reaction mixture. The amino acid content was determined after acid hydrolysis by ion exchange chromatography using the Spinco amino acid analyzer. Infrared spectra showed an absence of any band

† Junior Fellow of the Society of Fellows, Harvard University.

in the 1740 cm^{-1} region, thereby demonstrating that the removal of the carbobenzoxy protecting groups was complete. The polypeptide was water-soluble but in 0·15 M-NaCl a pH greater than 10 was required for solubility.

Albino rabbits weighing 2 to 2·5 kg were immunized in two ways. Each of the nine rabbits in one group was injected in the ear vein with 7 mg of the polypeptide in 0·15 M-NaCl solution, adjusted to pH 10·4, 3 times per week for a period of 3 weeks. After a week's rest they were bled by cardiac puncture. Seven of the nine rabbits survived the 4 week course. Each of the seven rabbits in the other group was injected subcutaneously with the polypeptide mixed with Freund's adjuvant. The adjuvant solution was prepared by mixing Difco † complete adjuvant, to which had been added additional killed tubercle bacilli, and an equal volume of a saline solution of the polypeptide to give a final concentration of 9 mg polypeptide and 3 mg killed tubercle bacilli per ml. of adjuvant solution. The rabbits received 0·2 ml. of adjuvant solution into alternate hind-footpads on each of 3 succeeding weeks, then 0·3 ml. in the back of the neck on the fourth week; the total amount of the polypeptide given was 8 mg per animal. The animals were rested 1 month, then given 7 mg of the polypeptide solution intravenously, and bled by cardiac puncture following one week's rest. Five of the seven rabbits survived the 9 week course.

The sera of these rabbits together with normal controls were tested by ring formation, agar diffusion and the precipitin reaction. In each case the serum was adjusted to pH 9·0 and the polypeptide, at 0·7 mg/ml. concentration in 0·15 M-NaCl, was adjusted to pH 10·3 to meet its solubility requirements. The agar for the diffusion studies was made up to a final concentration of 0·15% in 0·15 M-NaCl at pH 9·0.

All the sera were tested in duplicate several times by (1) ring tests, (2) single diffusion in agar according to the method of Oudin (1952) and (3) double diffusion in agar according to the method of Preer (1956). All of these gave the same results: three of the five in the adjuvant group gave strong precipitations, two of the seven in the intravenous group gave strong precipitations and one other in this group gave a weak reaction. Seven normal sera run in duplicate as controls gave no precipitation in any of the tests. In Plate I is shown a photograph of the double diffusion tubes after 6 days with the bands of specific precipitate clearly evident.

A quantitative precipitin reaction was carried out using the antiserum from one of the adjuvant immunized rabbits. The amount of precipitate was determined by direct weighing on fine fritted-disc glass funnels using a micro-balance. The precipitin curves obtained showed several peaks which apparently resulted from precipitates due to different antigenic determinants in the polymer and their corresponding antibodies. Approximately 5 mg/ml. serum of antibody was found; this is quite comparable to the maximum amount that Heidelberger & Kendall obtained by immunizing rabbits with ovalbumin (Heidelberger & Kendall, 1935).

The molecular weight of the antigenic polypeptide was determined by measuring the sedimentation coefficient and intrinsic viscosity in 0·15 M-NaCl at pH 10·6 and using these values in the Scheraga-Mandelkern equation (Scheraga & Mandelkern, 1953) with a value of 2.5×10^6 for β. The measured values were $S^\circ_{20,w} = 1{\cdot}96$ s and $[\eta] = 0{\cdot}47$. Using a value of 0·722 for $\bar{v}$, the partial specific volume, which was obtained from the $\bar{v}$ for the individual amino acid residues, the molecular weight was found to be 49,000; this corresponds to 370 residues.

The configuration of the polypeptide was explored by use of rotatory dispersion measurements. By using the results found for the 1 : 1 copolymer of L-lysine and L-glutamic acid (Doty, Imahori & Klemperer, 1958) and poly-L-tyrosine (Coombes, Katchalski & Doty, in the press), and assuming additive relationships, one can predict

† Difco Laboratories Inc., Detroit, Michigan.

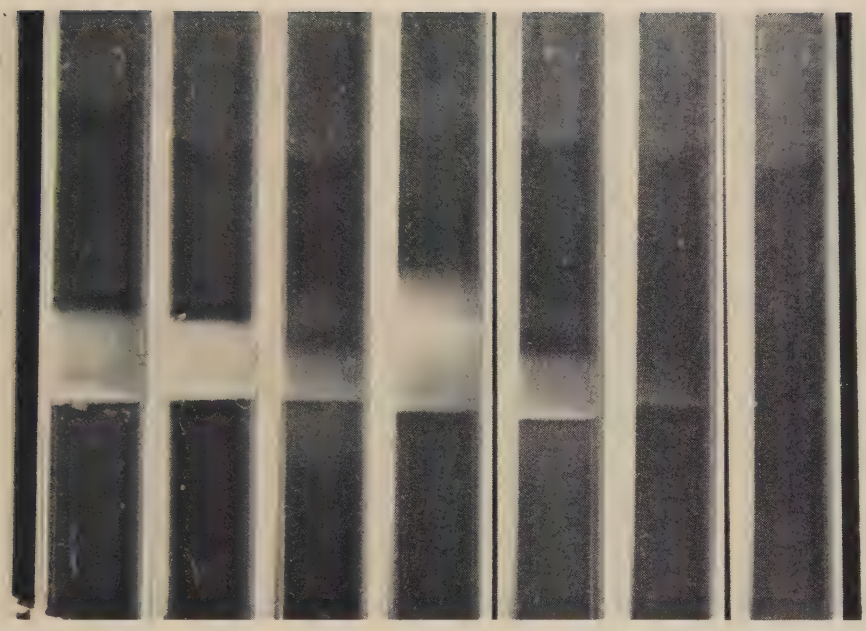

PLATE I. Double diffusion in gel showing the zones of precipitation of the polypeptide and its homologous rabbit antiserum. From left to right: (a) tubes 1 to 3 are from the adjuvant immunized group; (b) tubes 4 to 6 are from the intravenously immunized group; and (c) tube 7 is a typical control tube.

[*To face page* 66

that the complete helix would have an $[\alpha]_D$ value of + 33° and the random coil a value of − 84°. In 2-chloroethanol (with 5 mol% water added) the $[\alpha]_D$ value was found to be 42°, agreeing fairly well with the prediction for the helix. In 8 M-urea and in 0·15 M-NaCl at pH 12·3 the $[\alpha]_D$ value was − 80°. Since there is no anomalous dispersion ($b_0 = 0$) in the last two solvents and since the neglect of the effects of interaction of tyrosine residues with lysine and particularly glutamic acid residues in the coil form gives some leeway in the above estimate it appears that the configuration in this case is that of the structureless coil.

Under the conditions used in the immunological tests (0·15 M-NaCl and pH 10·7) the $[\alpha]_D$ was − 61°. Using the above values of $[\alpha]_D$ to define a scale this value is seen to correspond to that of about 15% of the residues being in the helical configuration (Doty, Imahori & Klemperer, 1958). However, no corresponding appearance of anomalous dispersion was found, i.e. $b_0 = 0$. Since the specific rotation in the coil form is subject to substantial variation due to solvent and segmental interaction effects and since b_0 values are not generally subject to such effects, we tentatively conclude that in alkaline saline solution the configuration of the polypeptide is that of a disordered coil essentially devoid of helical regions.

Thus, a synthetic straight-chain polypeptide of glutamic acid, lysine, and tyrosine has been found to be antigenic in rabbits with the most effective method of immunization being the adjuvant method of Freund. Since a copolymer of glutamic acid and lysine is weakly antigenic at best (Maurer *et al.*, 1959) it appears that the presence of tyrosine is the factor which determines antigenicity in the synthetic polypeptide. The bands in the gel diffusion tubes and the several peaks in the precipitin curve suggest the presence of several different antibodies. Since the antigen appears to be devoid of secondary or tertiary structure the multiple antibody response may simply be the result of doublet or triplet sequences involving tyrosine serving as the major antigenic determinant.

In any event, the demonstration that synthetic polypeptides containing only three amino acids are strongly antigenic makes possible through structural variations under synthetic control a new approach to the study of the structural requirements of antigenicity *within* the protein structure itself. For example, it appears that the number of adjacent tyrosine groups required for the antigenic determinant can be found by the study of cross reactions between the above antisera and polypeptides of the same composition but containing predominantly single, or double, or triple tyrosine sequences. The role of the amino acid residues adjacent to the tyrosine can be similarly explored. Prior studies directed toward elucidating the nature of the region eliciting specific antibody formation involved adding groups to proteins or modifying groups already present. However, such an approach does not allow the clear delineation between the factors involved in the determination of specificity and those involved in the determination of antigenicity. The approach suggested here eliminates such complications by involving only three peptide-linked amino acid residues, two of which alone are essentially non-antigenic, and avoiding structures, such as unnatural amino acids and branching of the polypeptide chain, that are foreign to proteins.

We wish to thank Dr. Brian Harrap, Professor A. M. Pappenheimer, Jr., Professor G. J. Dammin, Mr. Edward Freidman, Dr. Marvin Winkler and Dr. J. D. Coombes for their helpful advice. This work was supported in part by the National Science Foundation (G-7487).

Note added in proof.—Three further observations have been made on the antisera described above. (1) Reversed passive anaphylaxis was elicited in each of 5 guinea pigs tested. This occurred when the polypeptide was injected intravenously 24 hours after the antiserum had been similarly administered. (2) L-tyrosine had a marked retarding effect on the development of precipitate. L-tyrosine in concentrations of 0·05 to 0·5 M delayed the onset of the precipitin reaction from 1 to 44 hours respectively. A comparable effect was not observed with L-glutamic acid, L-lysine, L-phenylalanine, or L-leucine in approximately 0·07 M concentrations. (3) A strong cross-reaction occurred on mixing the antisera with a polypeptide of L-glutamic acid, L-lysine and L-phenylalanine (6·1 : 5·4 : 1·0) of molecular weight 47,000 (provided by Mr. E. Friedman) and with a polypeptide of L-glutamic acid, L-lysine, and L-tyrosine (14·4 : 9·8 : 1·0) which was soluble in the physiological pH range.

REFERENCES

Buchanan-Davidson, D. J., Dellert, E. E., Kornguth, S. E. & Stahmann, M. A. (1959). *J. Immunol.* **83**, 543.

Buchanan-Davidson, D. J., Stahmann, M. A. & Dellert, E. E. (1959). *J. Immunol.* **83**, 561.

Buchanan-Davidson, D. J., Stahmann, M. A., Lapresle, C. & Grabar, P. (1959). *J. Immunol.* **83**, 552.

Doty, P., Imahori, K. & Klemperer, E. (1958). *Proc. Nat. Acad. Sci., Wash.* **44**, 424.

Heidelberger, M. & Kendall, F. E. (1935). *J. Expt. Med.* **62**, 697.

Hooker, S. B. & Boyd, W. C. (1933). *J. Immunol.* **24**, 141.

Landsteiner, K. (1919). *Biochem. Z.* **93**, 106.

Maurer, P. H. (1957). *Proc. Soc. Expt. Biol. Med.* **96**, 394.

Maurer, P. H., Subrahmanyam, D., Katchalski, E. & Blout, E. R. (1959). *J. Immunol.* **83**, 193.

Oudin, J. (1952). *Methods in Medical Research*, **5**, 335. Chicago: Yearbook Publishers Inc.

Preer, J. R. (1956). *J. Immunol.* **77**, 52.

Scheraga, H. A. & Mandelkern, L. (1953). *J. Amer. Chem. Soc.* **75**, 179.

Sela, M., Katchalski, E. & Olitzki, A. L. (1956). *Science*, **123**, 1129.

Stahmann, M. A., Lapresle, C., Buchanan-Davidson, D. J. & Grabar, P. (1959). *J. Immunol.* **83**, 534.

Stahmann, M. A., Tsuyuki, H., Weinke, K., Lapresle, C. & Grabar, P. (1955). *C.R. Soc. Biol., Paris*, **241**, 1528.

J. Mol. Biol. (1960) **2**, 69-71

Letters to the Editor

Über den Einbau von 5-Nitrouracil, 5-Aminouracil und 2-Thiothymin in die Bakterien-Desoxyribonukleinsäure

Studies of the metabolism of [2-^{14}C]-5-nitrouracil, [2-^{14}C]-5-aminouracil and [2-^{14}C]-2-thiothymine indicate that these pyrimidine analogues cannot be directly incorporated into the bacterial DNA, with the exception of [2-^{14}C]-5-aminouracil, which is directly used in very small amount for DNA synthesis.

The incorporation of 5-nitrouracil, 5-aminouracil and 2-thiothymine by *Enterococcus* are reduced in the presence of thymine or 5-bromouracil.

5-Bromuracil hebt bei Bakterien nicht nur die 5-Nitrouracil-Hemmung auf (Hitchings, Elion & VanderWerff, 1948; Weygand & Wacker, 1952), sondern auch die des 5-Aminouracils (Wacker, unveröffentlichte Ergebnisse). Mit ^{14}C-markiertem 5-Nitrouracil und 5-Aminouracil wurde die Aufnahme und der Stoffwechsel dieser Verbindungen, sowie der Mechanismus der kompetitiven Enthemmung näher untersucht. 2-Thiothymin beeinflußt in gleicher Weise wie 5-Aminouracil den Stoffwechsel der Desoxyribonukleinsäure (DNS) bei bestimmten Bakterien. In Anwesenheit dieser beiden Pyrimidin-analogen Verbindungen findet man in der DNS zusätzlich 6-Methyl-adenin (Dunn & Smith, 1955). Im Rahmen der vorliegenden Arbeit über 5-Aminouracil-[2-^{14}C] haben wir uns ebenfalls mit der Aufnahme und dem Stoffwechsel von 2-Thiothymin-[2-^{14}C] beschäftigt.

Die Synthese von 2-Thiothymin-[2-^{14}C] erfolgte nach Bennett (1952), die Synthesen von 5-Nitrouracil-[2-^{14}C] und 5-Aminouracil-[2-^{14}C] sind beschrieben (Weinblum, 1959). Alle verwendeten radioaktiven Verbindungen, einschließlich Thymin-[2-^{14}C], hatten eine spezifische Aktivität von 1 mc/mMol. Die Kultivierung der Bakterienstämme *Enterococcus* Stei, *Streptococcus faecalis* R, *Escherichia coli* B und *E. coli* 1883 Co, sowie die Zusammensetzung des Nährmediums ist beschrieben (Wacker, Ebert & Kolm, 1958). Die Isolierung der Desoxyriboside erfolgte wie früher angegeben (Wacker, Kirschfeld & Träger, 1959). Bei den Versuchen mit 2-Thiothymin-[2-^{14}C] wurde die mit 10%iger NaCl-Lösung extrahierte DNS entweder enzymatisch oder mit 100%iger Ameisensäure gespalten. Lösungsmittelsysteme und die quantitative Bestimmung der Radioaktivität als $^{14}CO_2$ siehe nachherige Mitteilung (Wacker, Kirschfeld & Weinblum, 1960).

Wie aus Tabelle 1 hervorgeht, nehmen alle untersuchten Stämme 5-Nitrouracil, 5-Aminouracil und 2-Thiothymin aus dem Nährmedium auf. Auffällig ist, daß die beiden *E. coli*-Stämme im Vergleich zu *Enterococcus* Stei und *Streptococcus faecalis* R weniger 5-Aminouracil und 2-Thiothymin aufnehmen. Bei 5-Nitrouracil ist die unterschiedliche Aufnahme nicht so ausgeprägt.

Wächst *Enterococcus* Stei entweder mit 5-Nitrouracil-[2-^{14}C], 5-Aminouracil-[2-^{14}C] oder 2-Thiothymin-[2-^{14}C], so verringert sich die Radioaktivität der Bakterienzellen, wenn gleichzeitig Thymin oder 5-Bromuracil vorhanden ist. 10 μg Thymin erniedrigen die Aufnahme von 10 μg 5-Nitrouracil um mehr als 80%, 10 μg 5-Bromuracil um etwa 70%. Bei 5-Aminouracil-[2-^{14}C] und 2-Thiothymin-[2-^{14}C] ist Thymin im Vergleich zu 5-Bromuracil wirksamer bei der Verdrängung der unnatürlichen Pyrimidine.

Umgekehrt wird die Aufnahme radioaktiven Thymins nur durch 5-Bromuracil verringert, nicht aber durch 5-Nitrouracil, 5-Aminouracil oder 2-Thiothymin.

Untersucht man in den mit 5-Nitrouracil-[2-^{14}C] gewachsenen Bakterien die Verteilung der Radioaktivitat, so zeigt sich, daß mehr als 90% der Radioaktivität nicht in der DNS enthalten ist. Nach Spaltung der DNS mit $HClO_4$ findet man auf den Papierchromatogrammen deutlich nur eine radioaktive Substanz, die in den Lösungsmittelsystemen I, II und III die R_F-Werte 0,13; 0,1 und 0,33 besitzt. Infolge des

Tabelle 1

Aufnahme verschiedener Pyrimidine durch Enterococcus Stei, Streptococcus faecalis R, E. coli B und E. coli 1883 Co nach 36 Stunden Wachstum; Zahlenangaben: µg.

Im Nährmedium vorhanden 10 µg/ml.	Einbau der radioaktiven Verbindung in a) 100 mg Bakterien b) 100 mg DNS				
	Enterococcus Stei		*Streptococcus faecalis* R	*E. coli* B	*E. coli* 1883 Co
	a	b	a	a	a
5-Nitrouracil-[2-^{14}C]	9	10	6	6	5
5-Aminouracil-[2-^{14}C]	10	40	12,5	2	2
2-Thiothymin-[2-^{14}C]	40	750	30	2	2

äußerst geringen Vorkommens der radioaktiven Verbindung in der DNS konnte vorerst nur durch einen Vergleich der R_F-Werte des 5-Nitrouracils und seiner biochemisch möglichen Umwandlungsprodukte auf die Struktur der radioaktiven Verbindung geschlossen werden. *Danach ist die aus der DNS isolierte radioaktive Substanz mit 5-Nitrouracil nicht identisch.* (In 100 mg DNS von *Enterococcus* Stei werden 10 µg 5-Nitrouracil nach vorhergehender Umwandlung aufgenommen.)

Wächst *Enterococcus* Stei mit 10 µg 5-Aminouracil-[2-^{14}C] pro ml. Nährmedium, so nehmen 100 mg Bakterien etwa 10 µg 5-Aminouracil auf. Nur etwa 20% der aufgenommenen Radioaktivität sind in der DNS enthalten. Spaltet man die DNS mit $HClO_4$, so findet man papierchromatographisch in verschiedenen Lösungsmittelsystemen 4 radioaktive Flecke, von denen 3 mit 5-Aminouracil, Cytosin und Thymin identisch sind. Die 4. radioaktive Substanz (Verbindung X), deren Struktur wir noch nicht aufgeklärt haben, hat in den Lösungsmittelsystemen I, II und III die R_F-Werte 0,13; 0,10 und 0,33. In 100 mg DNS findet man von den aufgenommenen 40 µg 5-Aminouracil-[2-^{14}C] nur 1 µg als 5-Aminouracil, 18 µg als Cytosin, 14 µg als Thymin und 7 µg als Verbindung X wieder. Spaltet man die gesamten Bakterien mit $HClO_4$, so findet man noch zusätzlich radioaktives Uracil und eine weitere radioaktive, unbekannte Verbindung (Verbindung Y).

Enterococcus Stei nimmt gegenüber 5-Aminouracil etwa die 4-fache Menge 2-Thiothymin auf. Da bei der $HClO_4$-Spaltung 2-Thiothymin in Thymin umgewandelt wird, war es nicht möglich, auf diese Weise die Struktur der radioaktiven Verbindung in den Bakterien aufzuklären. Es wurden daher aus den mit radioaktivem 2-Thiothymin gewachsenen Zellen einmal die Desoxyriboside aus der DNS nach enzymati-

scher Spaltung isoliert, zum anderen die mit NaCl isolierte DNS mit Ameisensäure gespalten. In beiden Fällen findet man nur eine radioaktive Substanz, die mit Thymindesoxyribosid bzw. Thymin identisch ist. (In 100 mg DNS werden 750 μg 2-Thiothymin nach vorhergehender Umwandlung aufgenommen.) Nach Perchlorsäurespaltung der gesamten Bakterien findet man ebenfalls keine andere radioaktive Base außer Thymin.

Wie die Versuche zeigten, werden 5-Nitrouracil, 5-Aminouracil und 2-Thiothymin von den Bakterien nur sehr wenig aufgenommen. Im Gegensatz zu 5-Bromuracil, das Thymin in der DNS weitgehend ersetzen kann, wird 5-Aminouracil nur zu etwa 0,1% an Stelle von Thymin in die DNS eingebaut. 5-Nitrouracil und 2-Thiothymin werden als solche nicht in die DNS aufgenommen. Das äußerst geringe Vorkommen von 5-Aminouracil in der Bakterien-DNS und die vollständige Umwandlung von 5-Nitrouracil und 2-Thiothymin in andere Pyrimidinbasen erklären auch die bisher in der Literatur mitgeteilten negativen Befunde über die Aufnahme und den Einbau dieser unnatürlichen Pyrimidine (Dunn & Smith, 1955; Zamenhof, de Giovannii & Rich, 1958; Zamenhof, Reiner, de Giovannii & Rich, 1956).

Wir danken der Deutschen Forschungsgemeinschaft und dem Verband der Chemischen Industrie—Fonds der Chemie—für die Unterstützung dieser Arbeit.

Organisch-chemisches Institut
der Technischen Universität Berlin
Berlin-Charlottenburg 2, Germany

Adolf Wacker
Sigrid Kirschfeld
Dieter Hartmann
Dieter Weinblum

Received 17 November 1959

REFERENCES

Bennett, L. L., Jr. (1952). *J. Amer. Chem. Soc.* **74**, 2432.
Dunn, B. D. & Smith, J. D. (1955). *Nature*, **175**, 336.
Hitchings, G. H., Elion, Gertrude B. & VanderWerff, H. (1948). *J. Biol. Chem.* **174**, 1037.
Simon, H., Daniel, H. & Klebe, J. F. (1959). *Angew. Chem.* **9**, 303.
Wacker, A., Ebert, M. & Kolm, H. (1958). *Z. Naturf.* **13**b, 141.
Wacker, A., Kirschfeld, S. & Träger, L. (1959). *Z. Naturf.* **14**b, 145.
Wacker, A., Kirschfeld, S. & Weinblum, D. (1960). *J. Mol. Biol.* **2**, 72.
Weinblum, D. (1959). Diplomarbeit, Technische Universität, Berlin.
Weygand, F. & Wacker, A. (1952). *Z. Naturf.* **7**b, 26.
Zamenhof, S., Rich, K. & de Giovannii, R. (1958). *J. Biol. Chem.* **232**, 651.
Zamenhof, S., Reiner, B., de Giovannii, R. & Rich, K. (1956). *J. Biol. Chem.* **219**, 165.

J. Mol. Biol. (1960) **2**, 72-74

Über den Einbau von 5-Bromcytosin und 5-Bromuracil in die Bakterien-Desoxyribonukleinsäure

A study has been made of the uptake and conversion of [2-^{14}C]thymine, [2-^{14}C]-uracil and [2-^{14}C]cytosine by *E. coli* B and *Enterococcus*. [2-^{14}C]-5-bromocytosine was not incorporated by the bacterial cell; on the other hand [2-^{14}C]-5-bromouracil was in part incorporated unchanged and in part incorporated as [2-^{14}C]uracil, [2-^{14}C]cytosine and [2-^{14}C]thymine.

Kürzlich berichteten Bessman *et al.* (1958) über die enzymatische Synthese einer Desoxyribonukleinsäure (DNS), die an Stelle von Cytosin 5-Bromcytosin enthielt. Bei Arbeiten über den Stoffwechsel radioaktiv-markierter Pyrimidine und Pyrimidin-analoger Verbindungen (Weygand, Wacker & Dellweg, 1952; Weygand & Wacker, 1952; Wacker, Trebst, Jacherts & Weygand, 1954; Weygand, Wacker, Trebst & Swoboda, 1957) untersuchten wir ebenfalls die Aufnahme von 5-Bromcytosin-[^{82}Br] und 5-Bromcytosin-[2-^{14}C] in die DNS verschiedener Bakterien. Vergleichsweise dazu untersuchten wir die Aufnahme und Umwandlung von 5-Bromuracil-[2-^{14}C], Thymin-[2-^{14}C], Uracil-[2-^{14}C] und Cytosin-[2-^{14}C].

Die synthetisierten radioaktiven Verbindungen hatten eine spezifische Aktivität von 1 mc/mMol. Die Synthesen von Cytosin-[2-^{14}C], 5-Bromcytosin-[2-^{14}C] und 5-Bromcytosin-[^{82}Br] sind beschrieben (Weinblum, 1959). Die Synthesen der übrigen Verbindungen erfolgten nach früheren Angaben (Weygand, Wacker, Trebst & Swoboda, 1954). Die Kultivierung der Bakterien *Enterococcus* Stei und *Escherichia coli* B und die Zusammensetzung des Nährmediums ist ebenso wie die Spaltung der Bakterien mit Perchlorsäure und die papierchromatographische Trennung der Purin- und Pyrimidinbasen schon mitgeteilt worden (Weygand *et al.*, 1954). Lösungsmittelsysteme: I. *n*-Butanol/H_2O (86 : 14); II. *n*-Butanol/H_2O/NH_3 (86 : 13 : 1); III. *Iso*propanol/konz. HCl/H_2O (680 : 176 : 144) (Dunn & Smith, 1958). Für die Bestimmung der Radioaktivität wurde ein Glockenzählrohr (1,2 mg/cm^2 Glimmer), ein Methandurchflußzähler oder ein Gaszählrohr (Simon, Daniel & Klebe, 1959) verwendet.

Enthält das Nährmedium pro ml 10 μg Thymin-[2-^{14}C], so nehmen 100 mg Bakterien von *Enterococcus* Stei 200 μg Thymin auf und von *E. coli* B 15 μg (quantitative Bestimmung der Radioaktivität mittels Gaszählrohr; 100 mg getrocknete Bakterien von *Enterococcus* Stei enthalten 5,2 mg DNS, von *E. coli* B 4,6 mg). Spaltet man beide Bakterienstämme mit Perchlorsäure und bestimmt nach papierchromatographischer Trennung die Radioaktivität der Pyrimidinbasen, so ist nur Thymin radioaktiv, Uracil und Cytosin sind inaktiv. Im Vergleich zu Thymin nimmt *Enterococcus* Stei unter den gleichen Bedingungen 1250 μg Uracil-[2-^{14}C]/100 mg Bakterien auf und *E. coli* B 750 μg. Wie die Perchlorsäurespaltung der mit Uracil-[2-^{14}C] gewachsenen Bakterien zeigt, wird das aufgenommene Uracil von *Enterococcus* Stei zu 40% und von *E. coli* B zu 60% in Cytosin umgewandelt; beide Stämme überführen das aufgenommene Uracil zu 25% in Thymin.

Im Gegensatz zu *E. coli* B nimmt *Enterococcus* Stei nur wenig Cytosin auf. Nach Wachstum mit 10 μg Cytosin-[2-^{14}C] hat *Enterococcus* Stei 95 μg/100 mg Bakterien

aufgenommen, *E. coli* B 1050 μg. Beide Stämme wandeln das aufgenommene Cytosin zu 10% in Uracil und *Enterococcus* Stei zu 70%, *E. coli* B zu 30% in Thymin um.

Aus früheren Untersuchungen mit 5-Bromuracil-[^{82}Br] war bekannt, daß *Enterococcus* Stei und *E. coli* (Weygand, 1951; Weygand *et al.*, 1952; Dunn & Smith, 1954; Zamenhof & Griboff, 1954) diesen unnatürlichen Baustein an Stelle von Thymin in ihre DNS einbauen. Nach 36 Stdn. Wachstum mit 10 μg 5-Bromuracil-[2-^{14}C] hat *Enterococcus* Stei 470 μg/100 mg Bakterien aufgenommen, und *E. coli* B 85 μg. Spaltet man beide mit 5-Bromuracil-[2-^{14}C] gewachsenen Bakterienstämme mit Perchlorsäure und isoliert papierchromatographisch die Pyrimidinbasen, so stellt man fest, daß alle Basen radioaktiv geworden sind. Von dem aufgenommenen 5-Bromuracil wandelt *Enterococcus* Stei 20% in Uracil, 5% in Cytosin und 5% in Thymin um. *E. coli* B dehalogeniert wesentlich mehr 5-Bromuracil und überführt 20% des aufgenommenen 5-Bromuracils in Uracil, 15% in Cytosin und 35% in Thymin.

Im Gegensatz zu 5-Bromuracil-[2-^{14}C] nehmen sowohl *Enterococcus* Stei als auch *E. coli* B keine nachweisbaren Mengen 5-Bromcytosin auf. Nach Wachstum beider Stämme mit 10 μg 5-Bromcytosin-[^{82}Br] oder 5-Bromcytosin-[2-^{14}C], spezifische Aktivität beider Verbindungen 1 mc/mMol, zeigen die Bakterien im Methandurchflußzähler eine Radioaktivität, die nur wenige Impulse über dem Nullwert liegt.

Die Versuche mit 5-Bromcytosin-[^{82}Br] und 5-Bromcytosin-[2-^{14}C] zeigen deutlich, daß 5-Bromcytosin weder Cytosin noch Thymin bei *Enterococcus* Stei und *E. coli* B ersetzen kann. Der Grund hierfür liegt in dem Fehlen des Enzyms, das 5-Bromcytosin-desoxyribosid-5-phosphat in das Triphosphat umwandelt (vergl. Bessman *et al.*, 1958). Die Tatsache, daß bestimmte Phagen an Stelle von Cytosin 5-Hydroxymethylcytosin (Cohen, 1953; Kornberg, Zimmerman, Kornberg & Josse, 1959) enthalten, hängt mit deren enzymatischer, struktureller und genetischer Sonderstellung zusammen.

Während Uracil und Cytosin gegenseitig ineinander umgewandelt werden, ist die Bildung des Thymins bei den von uns untersuchten Bakterien ein irreversibler Vorgang (Weygand *et al.*, 1954). Um so merkwürdiger ist es, daß 5-Bromuracil, das Thymin bei *Enterococcus* Stei und auch bei anderen Bakterien in so hohem Maße ersetzen kann, in Uracil, Cytosin und damit letztlich auch in Thymin umgewandelt wird. Auffällig ist der Befund, daß die beiden Bakterienstämme mehr 5-Bromuracil aufnehmen als Thymin (dies gilt für alle bisher untersuchten Bakterienstämme; unveröffentlichte Ergebnisse). Die Abspaltung des Bromatoms in 5-Stellung des Uracil-Moleküls ist aber nicht allein auf Bakterien beschränkt. Wie Untersuchungen bei Säugetieren und am Menschen (Barrett & West, 1958; Pahl, Gordon & Ellison, 1959) gezeigt haben, können verschieden substituierte Pyrimidine *in vivo* dehalogeniert werden.

Die vorliegende Arbeit wurde mit Unterstützung der Deutschen Forschungsgemeinschaft und dem Verband der Chemischen Industrie—Fonds der Chemie—durchgeführt.

Organisch-chemisches Institut
der Technischen Universität Berlin
Berlin-Charlottenburg 2, Germany

Adolf Wacker
Sigrid Kirschfeld
Dieter Weinblum

Received 17 November 1959

REFERENCES

Barrett, H. W. & West, R. A. (1956). *J. Amer. Chem. Soc.* **78**, 1612.
Bessman, M., Lehman, J. R., Adler, J., Zimmerman, S. B., Simms, E. S. & Kornberg, A. (1958). *Proc. Nat. Acad. Sci., Wash.* **44**, 633.
Cohen, S. S. (1953). *Cold Spr. Harb. Symp. Quant. Biol.* **18**, 221.
Dunn, D. B. & Smith, J. D. (1954). *Nature*, **174**, 305.
Dunn, D. B. & Smith, J. D. (1958). *Biochem. J.* **68**, 627.
Kornberg, A., Zimmerman, S. B., Kornberg, S. R. & Josse, J. (1959). *Proc. Nat. Acad. Sci., Wash.* **45**, 772.
Pahl, H. P., Gordon, M. P. & Ellison, R. R. (1959). *Arch. Biochem. Biophys.* **79**, 245.
Simon, H., Daniel, H. & Klebe, J. F. (1959). *Angew. Chem.* **71**, 303.
Wacker, A., Trebst, A., Jacherts, D. & Weygand, F. (1954). *Z. Naturf.* **9**b, 616.
Weinblum, D. (1959). Diplomarbeit, Technische Universität, Berlin.
Weygand, F. (1951). *Proc. Radioisotope Techniques Conf.*, Oxford, **1**, 287.
Weygand, F., Wacker, A. & Dellweg, H. (1952). *Z. Naturf.* **7**b, 19.
Weygand, F. & Wacker, A. (1952). *Z. Naturf.* **7**b, 26.
Weygand, F., Wacker, A., Trebst, A. & Swoboda, O. P. (1954). *Z. Naturf.* **9**b, 764.
Weygand, F., Wacker, A., Trebst, A. & Swoboda, O. P. (1957). *Z. Naturf.* **12**b, 184.
Zamenhof, S. & Griboff, G. (1954). *Nature*, **174**, 305.

J. Mol. Biol. (1960) **2**, 75-77

A Helical Structure in Mumps, Newcastle Disease and Sendai Viruses

The structure of tobacco mosaic virus (TMV) has been investigated extensively by both X-ray diffraction and electron microscopy. From evidence obtained by X-ray diffraction studies TMV rods have been shown to consist of protein subunits arranged in the form of a helical array (Franklin, Klug & Holmes, 1956). Further studies have also suggested that there is a hollow central region along the rod axis with a radius of 20 Å, and that the nucleic acid forming the axial core is located at a radius of 40 Å (Franklin, 1956). The nucleic acid is therefore deeply embedded in the outer protein component, and its structural arrangement and chain direction are closely related to the protein helical array. Electron micrographs have confirmed the existence of a hollow central hole of approximately 40 Å diameter along the rod axis (Huxley, 1957; Brenner & Horne, 1959). More recently Nixon & Woods (1959) have obtained high resolution electron micrographs from preparations of reaggregated protein from TMV, revealing the subunit arrangement along the rod axis. Particles viewed along the axis show evidence of radial symmetry.

This short communication is concerned with the structure of components forming the internal region found in particles of mumps, Newcastle Disease (NDV) and Sendai viruses. The Enders strain of mumps virus and strains of NDV and Sendai virus obtained from the National Institute for Medical Research, Mill Hill, were used. Mumps virus was grown in 8-day embryonated eggs, and concentrated from allantoic fluid (harvested after 5 days' incubation) by differential centrifugation. NDV and Sendai virus were similarly prepared by concentration after 2 days' incubation in 11-day eggs.

Preparations of NDV, mumps and Sendai viruses have been examined in the electron microscope using the negative staining technique of Brenner & Horne (1959). The complete virus particles are of variable size (1000 to 6000 Å) and spherical shape. They have no regularly arranged subunits on the surface corresponding to the structures seen in preparations of adenovirus and poliovirus (Horne, Brenner, Waterson & Wildy, 1959; Horne & Nagington, 1959), but Crick & Watson (1956) have suggested that the related influenza virus might consist of a regularly arranged inner component enclosed in an outer coat made partly from host cell material. More recently Schäfer & Rott (1959) have shown by electron microscopy that flexible cylindrical structures can be obtained from both NDV and mumps virus by ether treatment. These structures have been estimated to have an RNA content of 5·7% and 9·6% respectively. In their metal shadowed preparations it was not possible to resolve fine details of these components, except that in the case of mumps virus there was some evidence of a repeating periodic arrangement along the axis of the strands. These separated flexible components were observed to have the same diameter as TMV rods.

NDV, mumps and Sendai viruses prepared for electron microscopy by the negative staining technique had in each case some partially disintegrated particles. The structure forming the inner component can be seen in Plate I, where it has been released from a partially disrupted mumps virus particle. It has a diameter of 170 Å and a regular periodic structure along the axis. In some areas small lengths suitably

orientated reveal the existence of a central hole with a diameter of 40 Å. At higher magnification the structural arrangement can be seen in more detail, and has a regular periodicity of 50 Å (Plate II). Similar structures have been observed in preparations of disrupted Sendai virus particles (Plate IV), where strands up to one micron in length have been seen. Plate V(a) shows part of a strand from Sendai virus at high magnification revealing regions where the periodic structure extends across the axis of the strand. The electron micrographs suggest that this periodicity is due to a helical arrangement within the strand, and in the case of Sendai virus the structure may have a double helical array when the angles at which the periodic structure crosses the axis are considered (Plate V(b)). The symmetry arrangements in fibrous molecules have been described by Klug, Crick & Wyckoff (1958), and for a structure of this type there would appear to be two-fold symmetry parallel with the strand axis. The existence of a double helical structure with separate RNA chains could offer a possible basis for explaining heterozygosis and diploidy in myxoviruses (Gotlieb & Hirst, 1954; Granoff & Hirst, 1954). Further evidence for interpreting the structures as helices in the case of mumps virus is suggested from regions showing the strands unwinding (Plate III) or connected by threadlike structures connecting partially broken pieces (Plate II). In areas containing large concentrations of strands, the structures are often looped or coiled in a way which would be considered unlikely if they were made up of a series of hollow discs (Plate VI).

Particles of NDV have been seen in which the outer coat has been partly or almost completely lost. This also reveals an inner structure, of dimensions similar to that seen in the particles of mumps and Sendai viruses. The arrangement within the particle differs in that the helix is more tightly packed in the particle of NDV, and it is possible that the subunits of neighbouring strands interlock with each other.

The striking resemblance of this inner component to the particles of TMV suggests that this RNA-bearing structure is built from a number of subunits arranged in helical array, but forming a flexible structure similar to the filaments observed in sugar beet yellows virus (Horne, Russell & Trim, 1959).

Luria (1959) has defined as an essential attribute of viruses the ability to direct the synthesis of apparatus for transfer from one susceptible cell to another and survival in between. It appears that these three animal viruses contain within such a protective outer coat a structure which fulfils that other attribute of viruses, the construction of the particle by the use of multiple similar protein subunits.

Electron Microscopy Section,
Cavendish Laboratory, Cambridge, England — R. W. Horne

Department of Pathology,
University of Cambridge, England — A. P. Waterson

Received 25 November 1959

REFERENCES

Brenner, S. & Horne, R. W. (1959). *Biochim. biophys. Acta*, **34**, 103.

Crick, F. H. C. & Watson, J. D. (1957). In *The Nature of Viruses*, ed. by G. E. W. Wolstenholme & E. C. P. Millar, p. 5. London: Churchill.

Franklin, R. E. (1956). *Nature*, **177**, 929.

Franklin, R. E., Klug, A. & Holmes, K. C. (1956). In *The Nature of Viruses*, ed. by G. E. W. Wolstenholme & E. C. P. Millar, p. 3. London: Churchill.

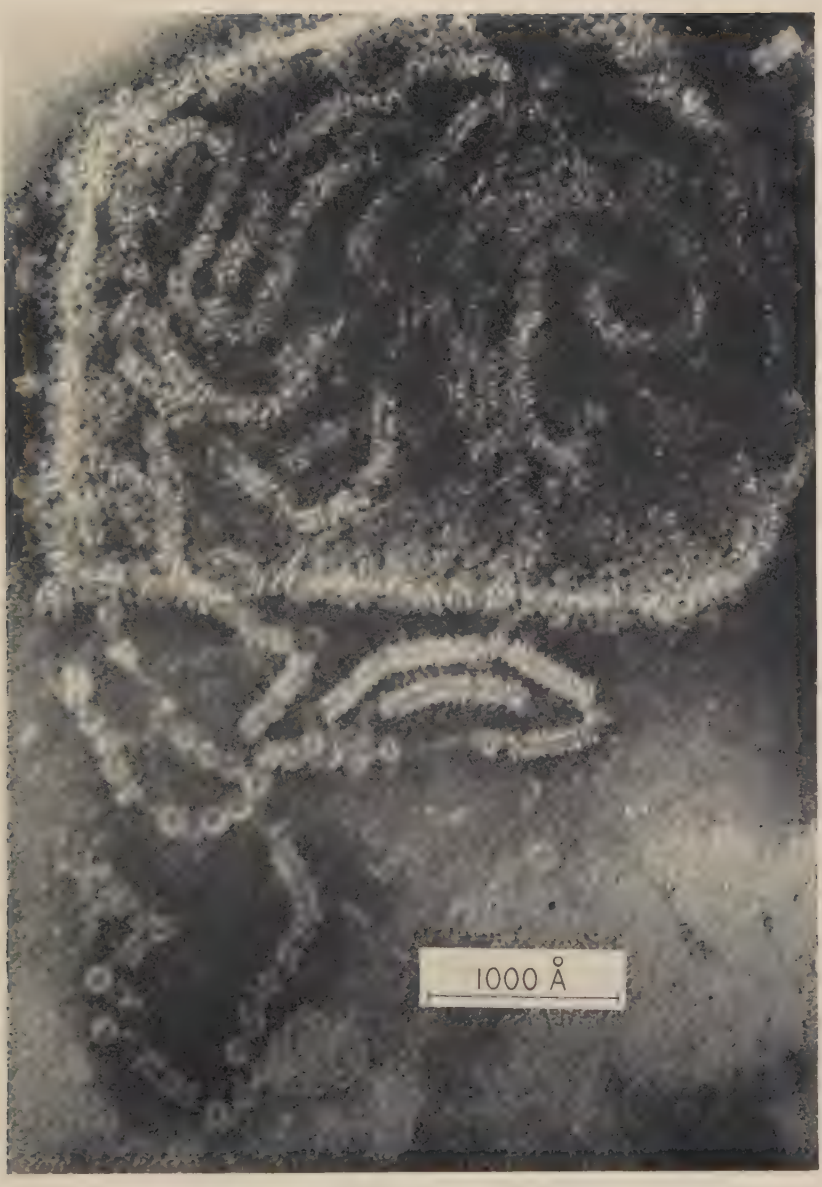

PLATE I. Partially disrupted mumps virus particle showing hollow strands forming the internal component. A number of broken strands have been released revealing periodic structures along the axis. (× 250,000.)

[*To face page* 76

PLATE II. Strands from mumps virus particles at high magnification. Fine threads connecting separated pieces are visible at "A" and partial unwinding of the structure can be seen at "B." (× 410,000.)

PLATE III. Strands of mumps virus showing evidence of the structure unwinding at areas marked "C" and "D." (× 520,000.)

PLATE IV. Strand from Sendai virus with structural details similar to those of mumps virus. (× 350,000.)

PLATE V. (a) High magnification electron micrograph of Sendai virus strand suggesting a double helical array. (× 750,000.)

(b) Diagram illustrating the possible arrangement of the periodic structure extending across the axis.

PLATE VI. Large concentration of helix from mumps virus embedded in phosphotungstate, showing the flexibility of the structure and formation of "loops." (× 160,000.)

Gotlieb, T. & Hirst, G. K. (1954). *Virology*, **2**, 235.
Granoff, A. & Hirst, G. K. (1954). *Proc. Soc. Exp. Biol., N.Y.* **86**, 84.
Horne, R. W., Brenner, S., Waterson, A. P. & Wildy, P. (1959). *J. Mol. Biol.* **1**, 84.
Horne, R. W. & Nagington, J. (1959). *J. Mol. Biol.* **1**, 333.
Horne, R. W., Russell, G. E. & Trim, A. R. (1959). *J. Mol. Biol.* **1**, 234.
Huxley, H. E. (1956). *First European Conference on Electron Microscopy, Stockholm.* p. 260. Stockholm: Almqvist & Wiksell.
Klug, A., Crick, F. H. C. & Wyckoff, H. W. (1958). *Acta Cryst.* **11**, 199.
Luria, S. (1959). In *Virus Growth and Variation.* London: Cambridge University Press.
Nixon, H. L. & Woods, R. D. (1959). *Virology*, in the press.
Schäfer, W. & Rott, R. (1959). *Z. Naturf.* **14b**, 629.

J. Mol. Biol. (1960) **2,** 78-80

Multiplicity Reactivation of Heat-disrupted T2 Phage

Recently, Spizizen (1957) and Fraser, Mahler, Shug & Thomas (1957) have shown that disrupted T2 phage could infect *E. coli* spheroplasts which were resistant to infection by intact phage. In these cases, the infection of disrupted phage was inhibited by trypsin digestion (Spizizen, 1957; Sekiguchi, 1958; Mahler & Fraser, 1959). The mechanism of this loss of infectivity was unknown, but the presence of protein seemed to be essential in some way for the infection of spheroplasts. In this connection, it is interesting that the presence of protein, which is different from phage coat protein, has been shown in T2 osmotic shockates by chemical (Hershey, 1957) and immunological (Levine, Barlow & Van Vunakis, 1958) methods.

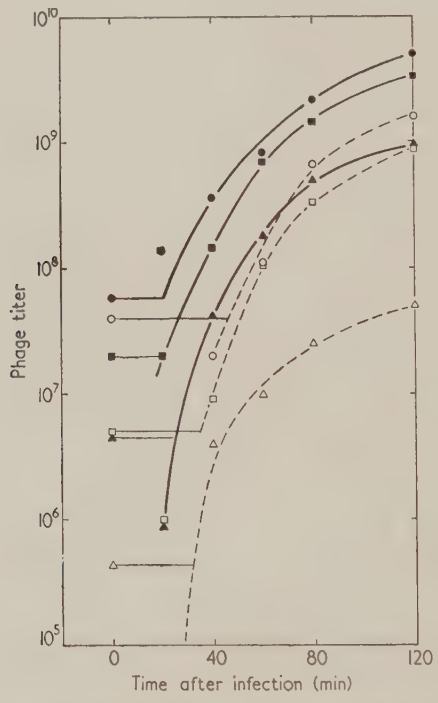

FIG. 1. *Intraspheroplast T2 multiplication in* E. coli *spheroplasts, infected with heat-disrupted T2 and its trypsin digest.* Solid lines: infected with heated T2; dashed lines: infected with trypsin digest of heated T2. T2 was heated for 15 min at 70°C (●, ○), at 71°C (■, □), and at 74°C (▲, △). Spheroplasts (2×10^8/ml.) were infected with these heated T2 (2×10^{11} T2 equivalents/ml.). Intraspheroplast phage was measured by assaying the samples after 50-fold dilution with water, at the times indicated on the abscissa.

We found that heat-disrupted T2, without osmotic shocking, could infect *E. coli* spheroplasts. Although the chemical characterization of this heated T2 has not yet been investigated, the infectivity of this preparation was also sensitive to trypsin digestion. Upon infection of spheroplasts with this trypsin-digested preparation, we obtained evidence to indicate that some initial reaction (Watanabe & Kiho, 1957) could take place, to the same degree as the control with heated T2, although the

multiplication of T2 phage was suppressed (Kiho, Haruna & Watanabe, 1959). Such studies show that the trypsin-sensitive protein may be required for the synthesis of phage constituent protein and/or DNA. We propose the hypothesis that the trypsin-sensitive protein may be required for the construction of a complete set of phage chromosomes, by the study of the multiplicity reactivation (MR) of these heat-disrupted T2 preparations.

E. coli spheroplasts were prepared according to the method of Fraser *et al.* (1957). Heating of T2 phage was performed at 70°C for 15 min. When trypsin digestion was

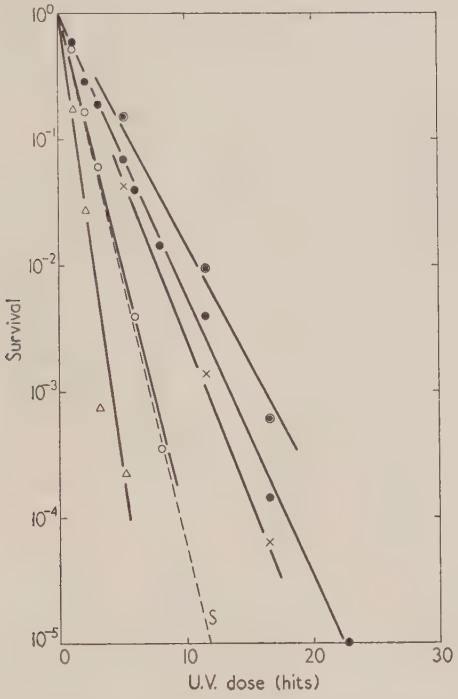

FIG. 2. *Multiplicity reactivation of heat-disrupted T2.* T2 phage which had been irradiated with various doses of u.v. was heated at 70°C for 15 min. Trypsin digestion was carried out at 37°C for 60 min with 10 μg/ml. trypsin. *E. coli* spheroplasts (1×10^{8}/ml.) were infected with these heated T2 preparations, at the following input ratios:

		input (T2 equivalents per spheroplast)
○	heated T2	160
×	heated T2	800
●	heated T2	1600
⊙	heated T2	3200
△	trypsin-treated heated T2	160 ~ 3200
S	T2, singly infected.	

After adsorption onto spheroplasts, infective centers were assayed.

performed, this heated T2 was incubated with 10 μg/ml. trypsin at 37°C for 60 min. As shown in Fig. 1, trypsin digestion was observed to increase the eclipse period of T2 multiplication in this system, whereas the number of infective centers after adsorption was not affected so much. This fact shows that the trypsin-treated preparations seem to be qualitatively different from the untreated control. However, it was also observed that trypsin digestion had the effect of decreasing the number of

infective centers when the T2 preparation was treated at higher temperatures such as 74°C. In further experiments, we used those trypsin-digested preparations which, after adsorption onto spheroplasts, reduced the number of infective centers least. (T2 phage was heated at 70 to 71°C for 15 min.) Ultraviolet light irradiation was carried out in dim light with a 15 watt "germicidal lamp" at a distance of 80 cm. After u.v. irradiation, T2 phage was heated and then, when necessary, trypsin digestion was carried out as described above.

The result of a typical experiment is presented in Fig. 2, in which the survivals of infective centers after adsorption have been plotted against the u.v. dose. It is shown that MR can take place in spheroplasts infected with heated T2 but not with trypsin digests of heated T2. In addition, the trypsin digested preparation is more sensitive to u.v. irradiation than intact phage. It can be concluded from these results that some protein is required for MR.

To explain MR, Luria has proposed the recombination theory (Luria, 1947; Luria & Dulbecco, 1949). This theory is not sufficient to explain MR, but recently, Baricelli (1956) introduced some generalization into the original concept of the recombination theory by the consideration of vulnerable centers as well as ordinary genes. From these results it may be inferred that some protein is required for the construction of phage chromosome.

Studies on this point are now in progress and will be published with the details of the present investigation.

Institute for Virus Research,
Kyoto University, Kyoto, Japan

YUKIO KIHO
ITARU WATANABE

Received 29 December 1959

REFERENCES

Baricelli, N. A. (1956). *Acta biotheor. Leiden*, **11**, 107.
Fraser, D., Mahler, H. R., Shug, A. L. & Thomas, C. A., Jr. (1957). *Proc. Nat. Acad. Sci., Wash.* **43**, 939.
Hershey, A. D. (1957). *Virology*, **4**, 237.
Kiho, Y., Haruna, I. & Watanabe, I. (1959). *Progr. in Virus Res.* (Japan), **2**, 55 (in Japanese).
Levine, L., Barlow, J. L. & Van Vunakis, H. (1958). *Virology*, **6**, 702.
Luria, S. E. (1947). *Proc. Nat. Acad. Sci., Wash.* **9**, 253.
Luria, S. E. & Dulbecco, R. (1949). *Genetics*, **34**, 93.
Mahler, H. R. & Fraser, D. (1959). *Virology*, **8**, 425.
Sekiguchi, M. (1958). *Virology*, **6**, 777.
Spizizen, J. (1957). *Proc. Nat. Acad. Sci., Wash.* **43**, 694.
Watanabe, I. & Kiho, Y. (1957). *Int. Symp. Enz. Chem.*, Tokyo and Kyoto, 418.

[*To face page* 81

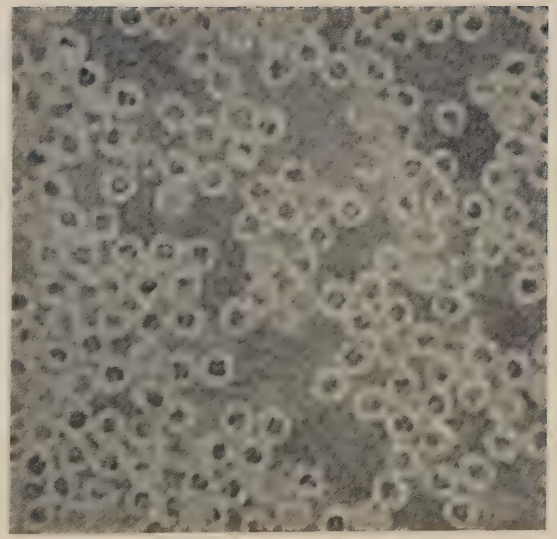

PLATE I. Electron micrograph of ferritin molecules. (× 400,000.)

PLATE I(a)

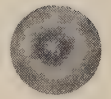

PLATE I(b)

PLATE I(c)

PLATE I(d)

Different appearances of micelle substructure in ferritin molecules. (× 800,000.)

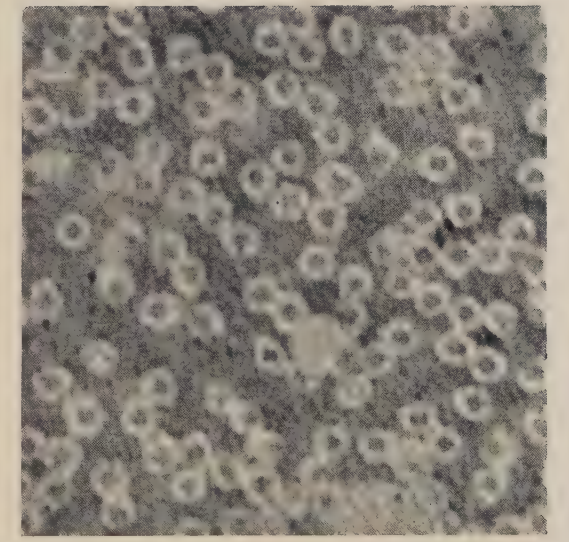

PLATE II. Apoferritin molecules. (× 400,000.)

J. Mol. Biol. (1960) **2**, 81-82

Electron Micrographs of Ferritin and Apoferritin Molecules †

Ferritin is a protein containing a large proportion of iron (about 20% of its dry weight) in the form of a "ferric hydroxide" micelle of composition $(FeO.OH)_8(FeO.OPO_3H_2)$, (Granick & Hahn, 1944). Apoferritin is obtained when the iron is removed from ferritin by the action of reducing agents.

The structure of these proteins has been studied by electron microscopy (Farrant, 1954; Valentine, 1959; and others) and by X-ray diffraction (Harrison, 1959). The electron micrographs strongly suggest that a ferritin molecule consists of the iron hydroxide micelle surrounded by an approximately spherical shell of apoferritin. In both protein shell and central core subunits are observed, and the different appearances of the micelles on the micrographs were stated to be compatible with a square planar arrangement of four subunits. The X-ray photographs of apoferritin and ferritin crystals seem to indicate a cubic 432 symmetry of the protein shell and a cubic 432, $\bar{4}3m$ or $m3m$ symmetry of the micelle. As possible forms for the micelle a tetrahedron or a cube were suggested. It is possible, however, that the high symmetry of the molecules is produced statistically by different orientations of molecules of lower symmetry in the crystal. It is also conceivable that the protein has full cubic symmetry, while the high cubic symmetry of the micelle is simulated by micelles of lower symmetry being differently orientated with respect to the protein shell.

On our electron micrographs, which were made by the negative staining technique of Brenner & Horne (1959), the cores of ferritin molecules have various shapes (Plate I). Some typical examples are given in Plates I(a) to I(d). They include: the square arrangement of four subunits reported previously; three subunits arranged in an equilateral triangle; two parallel rods, each probably consisting of three subunits; and less regular patterns resembling a horse-shoe.

These different appearances may correspond either to different species of molecule or to different projections of identical molecules. In the latter case none of the three models proposed for the micelle seems to fit our observations very well. A square arrangement of four subunits does not account for the observed triangles and horse-shoes, a tetrahedron does not fit the parallel rods and the horse-shoes, and a cube is not compatible with the observed triangles and horse-shoes.

A simple model which seems to account for all observed projections is one consisting of six subunits, situated at the corners of a trilateral prism (point group symmetry $\bar{6}$). The low symmetry of this model, however, would make it necessary to assume some kind of statistical orientation of the micelles in ferritin crystals.

Our electron micrographs of apoferritin (Plate II) show protein shells similar to those of ferritin molecules. The centres of the apoferritin molecules appear in most cases as homogeneous disks of about the same intensity as the background. This is probably due to phosphotungstate having penetrated the central regions of the molecules which are, in apoferritin, presumably filled with water. In some cases the

† The editors have drawn our attention to a recent paper by Richter, G. W. (1959). *J. Biophys. Biochem. Cytol.* **6**, 531 on "Internal Structure of Apoferritin as Revealed by the 'Negative Staining Technique'". Our results seem to be in agreement with the work described in this paper. (Note added in proof.)

central regions in apoferritin show structures similar to those observed in ferritin, although less pronounced. We cannot decide at this stage whether this is a significant effect, possibly due to the structure of the interior of the protein shell, or whether it is an artifact.

Experimental

Ferritin was isolated from horse spleen (Granick, 1942). Apoferritin was prepared by the method of Granick & Michaelis (1943).

Both proteins were studied with the negative staining technique of Brenner & Horne (1959). One droplet of a solution, containing 2% of protein and 2% of ammonium acetate (pH 7·0), was mixed with 1 ml. of a 2% phosphotungstate solution (pH 7·2). The mixture was sprayed immediately on a carbon film of a thickness of about 200 Å. The carbon film was made on a glass slide in a shadow-casting unit, which was evacuated by means of a mercury diffusion pump with liquid air trap. The photographs were taken with a Siemens Elmiskop-I electron microscope; the double condenser lens and a 20 μ spot on the specimen were used.

We thank Mr. R. W. Horne (Cambridge University) for taking the photographs published in this paper and for his help and interest in this work, which was made possible by a grant to one of us (E.F.J.v.B.) from the Netherlands Organization for the Advancement of Pure Research (Z.W.O.).

Laboratory of Inorganic
and Physical Chemistry,

E. F. J. van Bruggen
E. H. Wiebenga

Laboratory of Biochemistry,
University of Groningen,
10 Bloemsingel, Groningen,
The Netherlands

M. Gruber

Received 13 February 1960

REFERENCES

Brenner, S. & Horne, R. W. (1959). *Biochim. biophys. Acta*, **34**, 103.
Farrant, J. L. (1954). *Biochim. biophys. Acta*, **13**, 569.
Granick, S. (1942). *J. Biol. Chem.* **146**, 451.
Granick, S. & Hahn, P. F. (1944). *J. Biol. Chem.* **155**, 661.
Granick, S. & Michaelis, L. (1943). *J. Biol. Chem.* **147**, 91.
Harrison, Pauline, M. (1959). *J. Mol. Biol.* **1**, 69.
Valentine, R. C. (1959). *Nature*, **184**, 1838.

INSTRUCTIONS TO AUTHORS

1. The *Journal of Molecular Biology* will publish papers on the nature, production and replication of biological structure at the molecular level, and its relation to function. Suitable subjects are sub-cellular organization: molecular genetics: structure and replication of viruses: molecular structure of muscle, nerve and other tissues: structure of proteins, nucleic acids, carbohydrates, lipids, etc., and their synthetic analogues, as investigated by X-rays, light absorption and other methods: problems of inter- and intra-molecular energy transfer.

2. The Journal will also publish Letters to the Editor (averaging 1000 words), and occasional review articles dealing with a more restricted or immediately topical field than those in review journals. (The Editor should be consulted in advance by anyone who considers submitting such a review.)

3. Communications will often describe results obtained by specialized techniques (for example, those of X-ray crystallography and of genetics), and it is most important that technical terms should be avoided or be clearly defined; in any event the actual results obtained and their implications should be described in a way which does not demand from the reader specialized knowledge of a particular technique.

Papers should contain the maximum density of information compatible with clarity, and every sentence should be scrutinized to ensure that its presence is essential. Authors should include enough experimental details to enable others to repeat the work (these may be printed in small type). Careful preparation of manuscript will aid prompt publication; carelessness will cause delay.

4. *Submission of Manuscripts.* Manuscripts should be sent to Dr. J. C. Kendrew, Peterhouse, Cambridge, England, or to any member of the Editorial Board. The submission of manuscript will be taken to imply that the material is original, and that no similar paper has been or will be submitted for publication elsewhere.

Papers will normally be published in English. Manuscripts in French or German will also be accepted, though the use of these languages may cause delay in publication.

5. *Copy.* Papers should be typewritten in double spacing *throughout* (including tables, legends and footnotes), on one side of quarto paper, with a margin of 1 inch all round. The position of tables and illustrations should be indicated in the text; tables and legends for illustrations should be typed separately at the end of the manuscript. All pages should be numbered serially and securely fastened together. Two copies of each manuscript should be submitted, together with three copies of the summary (see § 6) and four copies of the abstract (see § 9).

A short running title of not more than 40 characters (including spaces), suitable for page headings, should be indicated if the full title is longer than this.

The name of the laboratory where the work has been done should be indicated on the title page. All typescript (including the references) should be carefully checked for errors.

6. *Summary.* A summary will be printed at the head of all papers (excluding Letters to the Editor); this should generally not exceed 300 words, and should be intelligible to the general reader without reference to the main text. Abbreviations should be avoided. Summaries of papers to be printed in French or German will be in English, and should be longer (up to 1000 words) for the benefit of readers not familiar with these languages.

7. *Conventions.* The conventions used in current issues of the Journal for headings, references, etc., should be followed in preparing manuscripts. References should be listed alphabetically at the end of the paper, and abbreviated according to the *World List of Scientific Periodicals*, except that for periodicals with English names capital initial letters should be used throughout. Citations in the text should read thus: Smith, Brown & Robinson (1957), or (Smith, Brown & Robinson, 1957). When a citation has more than two authors, the names of all of them should be given at the first citation (except for more than five authors), and on subsequent citations thus: (Smith *et al.*, 1957). The conventions (Brown, 1957*a*), (Brown, 1957*b*) should be used where more than one paper by the same author(s) has appeared in one year. Volume number should be indicated in the typescript thus: **35.**

Footnotes should be avoided whenever possible. Essential footnotes should be indicated by superscript figures in the text and collected on a single page placed at the end of the manuscript.

Customary abbreviations will be used; authors may refer to *Chemical Abstracts*, to the *Biochemical Journal*, **66**, 8 (1957), and to *Notes on the preparation of papers to be communicated to the Royal Society* (1951). Certain non-standard abbreviations of chemical substances are convenient, and those listed in the *Journal of Biological Chemistry* may be used without further definition (e.g. DNA, ATP). Any other abbreviations of this kind should be used sparingly, and must be defined in a footnote at the point in each manuscript where the first such abbreviation occurs.

8. *Illustrations.* It is often convenient to make a *drawing* two or three times larger than it will appear in the Journal, but very large drawings should be avoided and it will be helpful if drawings and illustrations are submitted on quarto (or 8½ by 11 inch) sheets. Drawings should be made in

Indian ink on tracing linen, Bristol board, or faintly blue-lined graph paper; the originals should always be submitted with the manuscript, since photo-prints of drawings often cannot be reproduced satisfactorily. Explanations should, as far as possible, be placed in the legend; the drawing itself should contain a minimum of lettering, and this should be inserted lightly in *blue pencil*, in lower case except for proper names, when a capital should be used. It should be remembered that drawings will be reduced to a size not exceeding 8 by 5 inches, and that the final thickness of the lines should be 0·25 to 0·3 mm. If a curve is given merely for illustrative purposes no cross-lines are needed, but the axes should be graduated at intervals, and the diagram should be boxed in. Where possible, related diagrams should be grouped to form a single figure, and should be prepared uniformly and *on the same scale*. Where appropriate and possible a scale should be included in the illustration itself; the magnification may be noted in the legend and adjusted after reduction by the blockmaker.

Whenever possible *photographs* should be supplied the same size as they are to appear in the Journal. The page area available for a plate is 5 by 7 inches or, at the most, 6 by 8 inches.

Line drawings will be referred to as Figure 1, Figure 2, etc., and half-tone blocks as Plate I, Plate II, etc. The name(s) of the author(s) and the number should be written on all illustrations, together with the indication "Top" if necessary. Besides the original illustrations *one* duplicate set must accompany the second copy of the manuscript; these may be photo-prints, and need not be of the same quality as the originals but must be clear and legible. If *oversize* original drawings are submitted (bigger than 8½ by 11 inches) they must be accompanied by *two* sets of small photo-prints.

9. *Abstracts*. Authors should send with their manuscripts *four copies* (typewritten in double spacing) of an abstract, in about 100 words, suitable for inclusion in biological abstracting journals. This abstract will not appear in the *Journal of Molecular Biology* but will be scrutinized by the Editors before being passed for publication. The abstract should outline as briefly as possible the results and definitive conclusions of the work. Details of methods are generally not required.

The abstract should be headed as follows: title of paper; name(s) of author(s); *J. Mol. Biol.*, followed by space for the year, volume and page references; abbreviated postal address (including country of origin) to which applications for reprints may be sent. For example: The isolation and properties of deoxyribonucleoprotein particles containing single nucleic acid molecules. G. Zubay & P. Doty. J. Mol. Biol. . . . . (Dept. of Chem., Harvard Univ., Cambridge, Mass., U.S.A.). —text of abstract follows.

10. *Reprints*. Fifty reprints of each paper will be supplied free of charge; additional copies may be purchased.

FILED IN STACKS

29Aug1960R

29Mar 63

CONTENTS

LONGUET-HIGGINS, H. C. and ZIMM, BRUNO H., Calculation of the Rate of Uncoiling of the DNA Molecule 1

THOMAS, C. A., Jr. and MATHESON, A. T., The Intrinsic Viscosity of ^{32}P Labelled Phage DNA 5

HUXLEY, H. E. and ZUBAY, G., Electron Microscope Observations on the Structure of Microsomal Particles from *Escherichia coli* 10

LANGRIDGE, R., WILSON, H. R., HOOPER, C. W., WILKINS, M. H. F. and HAMILTON, L. D., The Molecular Configuration of Deoxyribonucleic Acid. I. X-ray Diffraction Study of a Crystalline Form of the Lithium Salt 19

LANGRIDGE, R., MARVIN, D. A., SEEDS, W. E., WILSON, H. R., HOOPER, C. W., WILKINS, M. H. F. and HAMILTON, L. D., The Molecular Configuration of Deoxyribonucleic Acid. II: Molecular Models and their Fourier Transforms 38

Appendix—Calculation of the Fourier Transform of a Helical Molecule. By R. LANGRIDGE, M. P. BARNETT and A. F. MANN . . . 63

GILL, THOMAS J., III and DOTY, PAUL, A Strongly Antigenic Synthetic Polypeptide 65

Letters to the Editor—

Über den Einbau von 5-Nitrouracil, 5-Aminouracil und 2-Thiothymin in die Bakterien-Desoxyribonukleinsäure, ADOLF WACKER, SIGRID KIRSCHFELD, DIETER HARTMANN and DIETER WEINBLUM 69

Über den Einbau von 5-Bromcytosin und 5-Bromuracil in die Bakterien-Desoxyribonukleinsäure, ADOLF WACKER, SIGRID KIRSCHFELD and DIETER WEINBLUM 72

A Helical Structure in Mumps, Newcastle Disease and Sendai Viruses, R. W. HORNE and A. P. WATERSON 75

Multiplicity Reactivation of Heat-disrupted T2 Phage, YUKIO KIHO and ITARU WATANABE 78

Electron Micrographs of Ferritin and Apoferritin Molecules, E. F. J. VAN BRUGGEN, E. H. WIEBENGA and M. GRUBER . . 81

Printed in Great Britain at the Aberdeen University Press